COMPUTER MODELLING
AND
NEW TECHNOLOGIES

Computer Modelling and New Technologies

2016 Volume 20 No 4

Journal topics:	Publisher	Supporting Organizations
- mathematical and computer modelling - computer and information technologies - natural and engineering sciences - operation research and decision making - nanoscience and nanotechnologies - innovative education	Latvian Transport Development and Education Association	Latvian Academy of Sciences Latvian Operations Research Society Fraunhofer Institute for Factory Operation and Automation IFF, Germany

Articles should be submitted in **English**. All articles are reviewed

Editors' Remarks

****

A Moments Indulgence

by Rabindranath Tagore

Day after day, O lord of my life,
shall I stand before thee face to face.

With folded hands, O lord of all worlds,
shall I stand before thee face to face.

Under thy great sky in solitude and silence,
with humble heart shall I stand before thee
face to face.

In this laborious world of thine,
tumultuous with toil and with struggle,
among hurrying crowds
shall I stand before thee face to face.
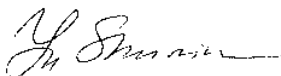
And when my work shall be done in this
world,
O King of kings, alone and speechless
shall I stand before thee face to face.

Rabindranath Tagore (1861-1941)♣

****

This 20th volume No.4 includes research papers on **Nanoscience and Nanotechnology, Information and Computer Technologies** and **Mathematical and Computer Modelling**.

Our journal policy is directed to fundamental and applied scientific researches, innovative technologies and industry, which is the fundamentals of the full-scale multi-disciplinary modelling and simulation. This edition is the continuation of our publishing activities. We hope our journal will be of interest for research community and professionals. We are open for collaboration both in the research field and publishing. We hope that the journal's contributors will consider collaboration with the Editorial Board as useful and constructive.

EDITORS

Yuri Shunin

Igor Kabashkin

♣ **Rabindranath Tagore (7 May 1861 – 7 August 1941),** was a Bengali poet, novelist, musician, painter and playwright who reshaped Bengali literature and music. As author of Gitanjali with its "profoundly sensitive, fresh and beautiful verse", he was the first non-European and the only Indian to be awarded the Nobel Prize for Literature in 1913. His poetry in translation was viewed as spiritual, and this together with his mesmerizing persona gave him a prophet-like aura in the west. His "elegant prose and magical poetry" still remain largely unknown outside the confines of Bengal.

CONTENT

Shunin Yu, Fink D, Kiv A, Alfonta L, Mansharipova A,
Muhamediyev R, Zhukovskii Yu, Lobanova-Shunina T,
Burlutskaya N, Gopeyenko V, Bellucci S

Theory and modelling of real-time physical and bio- nanosensor systems

Yu Shunin[1, 2*], D Fink[2], A Kiv[3], L Alfonta[3], A Mansharipova[4], R Muhamediyev[4], Yu Zhukovskii[1], T Lobanova-Shunina[5], N Burlutskaya[6], V Gopeyenko[6], S Bellucci[7]

[1]*Institute of Solid State Physics, University of Latvia, Kengaraga Str. 8, LV-1063 Riga, Latvia*
[2]*Departamento de Fisica, Universidad Autónoma Metropolitana-Iztapalapa, PO Box 55-534, 09340 México, D.F., México*
[3]*Ben-Gurion University, PO Box 653, Beer-Sheva 84105, Israel*
[4]*Almaty University, Kazakhstan*
[5]*Riga Technical University, Faculty of Mechanical Engineering, Transport and Aeronautics, Latvia*
[6]*ISMA University, 1 Lomonosova Str., Bld 6, LV-1019, Riga, Latvia*
[7]*INFN-Laboratori Nazionali di Frascati, Via Enrico Fermi 40, I-00044, Frascati-Rome, Italy*

*Corresponding author: yu_shunin@inbox.lv

Abstract

Our research pursues two important directions of real-time control nanosystems addressed to ecological monitoring and medical applications. We develop physical nanosensors (pressure and temperature) based on functionalized CNTs and GNRs nanostructures. The model of nanocomposite materials based on carbon nanocluster suspension in dielectric polymer environments (epoxy resins) is regarded as a disordered system of fragments of nanocarbon inclusions with different morphologies. Using the effective media cluster approach, disordered systems theory and conductivity mechanisms analysis we have formulated the approach of conductivity calculations for carbon-based polymer nanocomposites and obtained the calibration dependences. We also develop bio-nanosensors based on polymer nanotracks with various enzymes, which provide the corresponding biocatalytic reactions and give reliably controlled ion currents. Particularly, we describe a glucose biosensor based on the enzyme glucose oxidase (GOx) covalently linked to nanopores of etched nuclear track membranes. Using simulation of chemical kinetics glucose oxidation with GOx, we have obtained theoretical calibration dependences. Our objective is to demonstrate the implementation of advanced simulation models providing a proper description of electric responses in nanosensing systems suitable for real time control nanosystems. Comparisons with experimental calibration dependences are discussed. Prospective ways of developing the proposed physical and bio- nanosensor models and prototypes are considered.

1 Introduction

Nanosensor systems constitute an essential functional part of any modern devices that provide information processing for information systems, engineering interfaces, healthcare and many others. The talk is about nanosensor systems for various aspects of ecological monitoring and security. The fundamental electron devices are FET-transistors able to provide high sensitivity to various external influences of different nature. Conventional schemes of nanosensing systems are based on nano-FET-types devices, particularly:

a) unperturbed field-effect transistors based on CNT- or GNR- based FETs are mainly composed of the corresponding semiconducting carbon materials suspended over two electrodes;
b) physical nanosensors: a conducting threshold can be altered when the tube or graphene ribbon is bent;
c) chemical nanosensors: the same threshold can be altered when the amount of free charges on the tube

of graphene ribbon surface is increased or decreased by the presence of donor or acceptor molecules of specific gases or composites;
d) biological nanosensors: ensure monitoring of biomolecular processes such as antibody/antigen interactions, DNA interactions, enzymatic interactions or cellular communication processes, etc. [1, 2].

Another way to design nanosensing systems is the use of polymer nanoporous structures [3, 4]. In particular, ion tracks are suitable for biosensing applications because they have true nanometric dimensions. Ion tracks can confine chemical reactions in well-defined, pre-determined locations ensuring that their reaction products are highly enriched locally. If the membranes containing such etched tracks are put on the path of ion currents flowing through a vessel, all the ions are subsequently forced to pass through the nanopores, electrically sensing any confined chemical reaction occurring there via the changes of electrical resistance in the pores.

Shunin Yu, Fink D, Kiv A, Alfonta L, Mansharipova A,
Muhamediyev R, Zhukovskii Yu, Lobanova-Shunina T,
Burlutskaya N, Gopeyenko V, Bellucci S

We focus our research on two important directions of real-time control nanosystems addressed to ecological monitoring and medical applications, both of which provide environmental security of human society and every individual. Ecological monitoring has been widely presented at NATO Workshop 2011 Nanodevices and Nanomaterials for Ecological Security June20-24, Riga-Jurmala, Latvia [5].

For individual application, it is necessary to develop nanodevices controlling various functions of the human body, particularly, providing control over the *parameters of human health, the enhancement of human abilities, and the functioning of implants and prosthetics*. Another course in the development of nanosensors, nanoactuators, nanotransducers, etc - is the creation of artificial systems such as artificial intelligence or artificial individual. The main objective of the current study is to demonstrate the implementation of advanced simulation models ensuring a proper description of electric responses in nanosensing systems [2, 4, 5].

Initially, we consider physical nanosensors (pressure and temperature) based on functionalized CNTs and GNRs nanostructures. The model of nanocomposite materials based on carbon nanocluster suspension (CNTs and GNRs) in dielectric polymer environments (e.g., epoxy resins) is regarded as a disordered system of fragments of nanocarbon inclusions with different morphologies (chirality and geometry) in relation to a high electrical conductivity in a continuous dielectric environment. The electrical conductivity of a nanocomposite material depends on the concentration of nanocarbon inclusions (in fact, carbon macromolecules).

We should evaluate the role of particular conductivity mechanisms using the cluster approach based on the multiple scattering theory formalism, realistic analytical and coherent potentials, as well as effective medium approximation (EMA-CPA) which we have effectively used for modeling of nanosized systems, especially for various conductivity problems [6,7].

We have extensive experience in modelling conductivity calculations in CNT-Metal and GNR-Metal interconnects, where the conductivity mechanism is very sensitive to local morphological disordering [8-10].

Further on, we pay attention to the development of bio-nanosensors based on polymer nanoporous structures (nanotracks) with various enzymes, which provide the corresponding biocatalytic reactions and give reliably controlled ion currents [3, 4, 11].

In particular, we describe a concept for a glucose biosensor based on the enzyme glucose oxidase (GOx) covalently linked to nanopores of etched nuclear track membranes [12, 13]. The main objective of the current study is to demonstrate the implementation of advanced simulation models providing a proper description of electric responses in nanosensoring systems for creation of real-time detection nanodevices.

2 Models CNTs- and GNRs-based nanocomposites

2.1 DC-CONDUCTIVITY MECHANISMS OVERVIEW

Talking about conductivity mechanisms in a medium with practically essential conductivity, it is useful to consider the phenomenon through the contributions of scattering effects that can take place in nanocomposite

materails. We focus our attention on the four possible ways (see Figure 1) trying to find the best description, in particular, for functionalized nanocomposites.
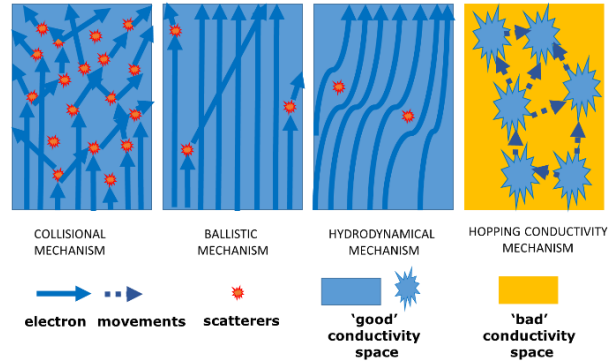
FIGURE 1 Review of general mechanisms of electron DC-conductivity

The key parameter for the analysis is the mean scattering length ℓ_{e-gen} of an electron in the conductive matter. In general, ℓ_{e-gen} includes various contributions in accordance with the well-known Matthiessen's Rule, chapeau stating:

$$\frac{1}{\ell_{e-gen}} = \frac{1}{\ell_{e-e}} + \frac{1}{\ell_{e-a/phon}} + \frac{1}{\ell_{e-o/phon}} +$$
$$+ \frac{1}{\ell_{e-o/phot}} + \frac{1}{\ell_{e-impurity}} + \frac{1}{\ell_{e-defect}} + \frac{1}{l_{e-boundary}} + ... \qquad (1)$$

where ℓ_{e-e} is the electron-electron scattering length, $\ell_{e-a/phon}$ is the acoustic phonon (emission and absorption) scattering length, $\ell_{e-o/phon}$ is the optical phonon emission scattering length, $\ell_{e-o/phot}$ is the optical phonon absorption scattering length, $\ell_{e-impurity}$ is the electron-impurity scattering length, $\ell_{e-defect}$ is the electron-defect scattering length, $\ell_{e-boundary}$ is the electron scattering length with the boundary.

Hydrodynamical character of electric conductivity is the fundamental property of certain metals at low temperatures [14, 15]. This quality can be observed for such cases, when the length of electron mean free path is the order of the sample character size, namely, $\ell_{e-boundary} \propto L$ and $l_{e-e} << L$.

The last relation should be precised in cases of collisional and non-collisional electronic plasma with concentrations less than $10^{17} cm^{-3}$. Hydrodynamical behavior of electron liquid is possible to observe in some critical spaces of graphene-based electronic devices [16].

Collisional mechanism is a more expanded conductivity mechanism and takes place in most cases of typical normal conditions, e.g. for metals and semiconductors. In this case $\ell_{e-phon} \propto a << L$, where a is the character distance between 'scatterers'- atoms. This mechanism for DC-conductivity is described by the classical Drude model [17, 18]:

Shunin Yu, Fink D, Kiv A, Alfonta L, Mansharipova A,
Muhamediyev R, Zhukovskii Yu, Lobanova-Shunina T,
Burlutskaya N, Gopeyenko V, Bellucci S

$$\sigma = \frac{ne^2\tau_{e-a/phon}}{m*},$$

where n is the electron concentration, e is the electron charge, τ_{e-phon} is the time electron-phonon scattering, $m*$ is the effective mass of electron.

Ballistic character of conductivity is characterized by transport of electrons in a medium having negligible electrical resistivity caused by scattering. Moreover, the scattering character is essentially elastic and the medium should be considered ideally regular. The time of electron-phonon interaction is negligible. This mechanism is observed, for example, in GNRs and CNTs included in FET-type devices. The most popular description of ballistic mechanism was given by Rolf Landauer and is known now as Landauer-Büttiker formalism [19]. Landauer formula:

$$G(\mu) = G_0 \sum_n T_n(\mu),$$

where G is the electrical conductance, $G_0 = e^2/(\pi h) \approx 7.75 \cdot 10^{-5} Ohm$ is the transmission eigenvalues of the channels, and the sum runs over all transport channels in the conductor. The conductance can be calculated as the sum of all the transmission possibilities that an electron has when propagating with an energy E equal to the chemical potential μ. In fact, the phenomenon is similar to optical thin films effect, when the transparency is achieved due to the quantization of the wave length. However, it is impossible to realize the remarkable conductivity property of GNRs and CNTs without any contacts. Appropriate nanocarbon-metal interconnects are characterized as disordered regions with essentially scattering mechanism of conductivity.

Hopping conductivity mechanism was proposed for disordered condensed systems (eg, for composite amorphous semiconductors and dielectrics) for the explanation of the metal-insulator transition [20]. The talk is about the existence of the electron hopping between the conductive clusters in the dielectric, or between the impurity centres of localization. In this model, the medium (insulator-metal) is represented by the following pattern: there is a random distribution of the nodal points related to each other by 'conductivities' exponentially dependent on the interstitial distances. The hopping conductivity model with a variable 'jump' length can be considered the most general one: $\ell_{e-impurity} \propto a$:

$$\sigma = A\exp(-\frac{4}{3}\left(\frac{4\alpha r_s}{a}\right)^{3/4}\left(\frac{W}{\kappa T}\right)^{1/4}, \qquad (2)$$

where a is the characrteristic 'borous radius' of the considered 'doping' centre, r_s is the characteristic radius of the doping centre or conductive region, W is the characteristic potential barrier for electon tunnelling, k is the Boltzmann constant, T is the sample temperature, $\alpha \approx 0.70$ is the empirical constant which can be evaluated only using Monte-Carlo numerical simulations [21].

2.2 NANOCARBON-BASED POLYMER COMPOSITE MODEL

We develop a set of prospective models of nanocarbon-based nanomaterials and nanodevices having various interconnects and interfaces. In particular, nanoporous and nanocomposite systems are considered as complicated ensembles of basic nanocarbon interconnected elements (e.g., CNTs or GNRs with possible defects and dangling boundary bonds) within the effective media type environment. Interconnects are essentially local quantum objects and are evaluated in the framework of the developed cluster approach based on the multiple scattering theory formalism as well as effective medium approximation [8, 22, 23].

In cases when nanocarbon clusters are embedded in high resistance media (instead of vacuum) we come to a nanocomposite material. The utilization of polymeric composite materials (e.g., epoxy resins) supplemented with various morphological nanocarbon groups of carbon nanotube-type (CNTs) and graphene nanoribbons (GNRs) allows us to create effective pressure and temperature sensors. Application of such nanocomposites as coatings can provide continuous monitoring of the mechanical strains in piping systems (for example, in aircraft or automotive applications), when the critical pressure values can indicate malfunctions of the engine. The analysis of possible medical instruments for real-time measuring human body temperature and blood pressure can also be realized.

The interest in CNTs and GNRs-based polymer nanocomposites as prospective pressure and temperature nanosensor materials is based on the observed electric percolation phenomena via the nanocarbon inclusions concentration. In particular, the electrical conductivity of a nanocomposite increases with the increasing CNT loading up to a critical filler concentration, where a dramatic increase in conductivity is observed. This critical filler concentration is called electrical percolation threshold concentration. At percolation threshold concentration, a filler forms a three-dimensional conductive network within the matrix, hence electron can tunnel from one filler to another and, in doing so, it overcomes the high resistance offered by insulating polymer matrix.

Consider the model of composite material with carbon nanocluster inclusions of CNTs- and GNRs- types.
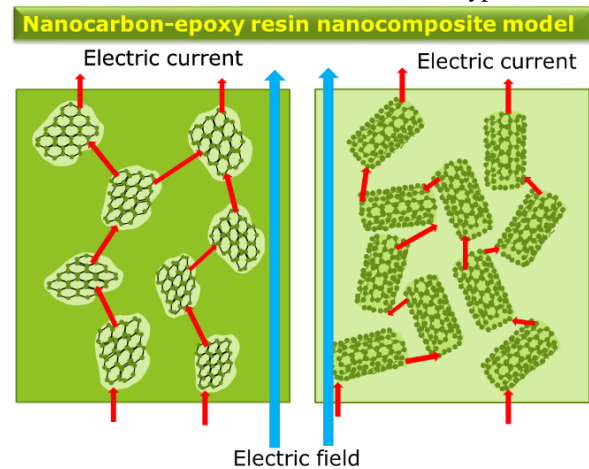

FIGURE 2 Model of composite polymer material with carbon nanocluster inclusions of GNRs- and CNTs- types.

Shunin Yu, Fink D, Kiv A, Alfonta L, Mansharipova A,
Muhamediyev R, Zhukovskii Yu, Lobanova-Shunina T,
Burlutskaya N, Gopeyenko V, Bellucci S

The host material – is a flexible dielectric medium of epoxy resin- type with high resistance [24]. However, a low concentration of nanocarbon inclusions cannot change the mechanical properties of the host material. At the same time, high electrical conductivity of CNTs- and GNRs incurporated in the host material can significantly affect the total conductivity of the nanocomposite material. According to our model, the mechanism of these changes is related to the effects of percolation through the **_hopping conductivity_** (see. Figure 2). This is the only mechanism that takes into account the compliance with our analysis induced morphological changes in the whole nanocomposite matrix. This is a single mechanism, which takes into account accordance with our analysis induced morphological changes in the whole nanocomposite matrix.

Thus, the model of nanocomposite materials based on carbon nanocluster suspension (CNTs and GNRs) in dielectric polymer environments (e.g., epoxy resins) is considered as a disordered system of fragments of nanocarbon inclusions with different morphology (chirality and geometry) in relation to a high electrical conductivity in a continuous dielectric environment. Presumably, the electrical conductivity of a nanocomposite material will depend on the concentration of nanocarbon inclusions (in fact, carbon macromolecules). Isolated nanocarbon inclusions will provide conductivity due to the hopping conductivity mechanism through dangling bonds up to the percolation threshold, when at high concentrations (some mass %) a sustainable ballistic regime appears, which is characteristic of pure carbon systems. The hopping mechanism is regulated by the electron hopping between 'nanocarbon macromolecules' (see (1) and [20, 22, 23]):

$$\sigma = A\sigma_0 \exp(-\frac{4}{3}\left(\frac{4\alpha r_{tun}}{a}\right)^{3/4}\left(\frac{W_0}{\kappa T}\right)^{1/4}, \qquad (3)$$

where r_{tun} is the length of the tunnel 'jump' of the electron equal to the distance between 'nanocarbon' clusters, σ_0 is the normalization constant, which means the conductivity of monolithic dielectric medium.
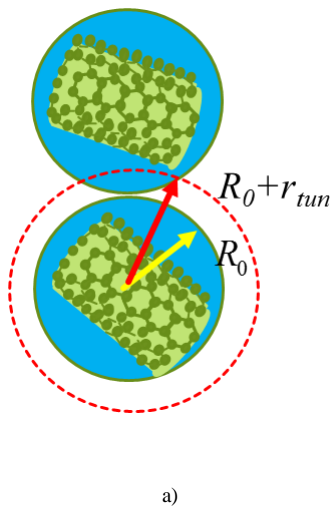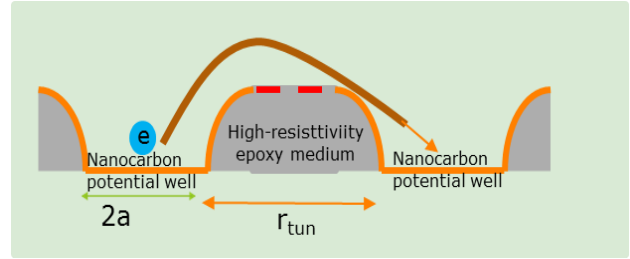
FIGURE 3 Potential wells model for hopping in polymer nanocomposistes, where *2a* is the characteristic size of nanocarbon inclusion, r_{tun} is the length of the tunnel 'jump' of the electron.

Added to this is the effect of intrinsic nanocarbon cluster conductivity, which is dependent on its morphology. The electric conductivity will also depend on the spatial orientation of nanocarbon inclusions. It will be greater for the longitudinal electric field orientations and lower for the transverse ones. Of course, any spatial orientations are technologically possible. If we introduce the volume part as an indicator of the nanocarbon inclusions concentration:

$$\eta = \left(\frac{R_0}{R_0 + r_{tun}}\right)^3,$$

where R_0 is the average nanocarbon macromolecule radius, r_{tun} is, as earlier, the statistically averaged width of the potential barrier between the nearest nanoclusters, which is responsible for percolation ability of the model nanocomposite. We should also diminish the hopping phenolmena and percolation probability taking into account the nanocarbon macromolecule orientation within a hypothetical sphere embedded into high resistance dielectric medium. Based on this definition, we can obtain a contribution of potential nanocarbon clusters to nanocomposite conductivity as follows (see also Figures 2, 3):

$$\ln\left(\frac{\sigma}{\sigma_0}\right) = -\frac{4}{3}(\frac{4\alpha}{3}R_0(\eta^{-1/3}-1))^{3/4}\left(\frac{W_0}{\kappa T}\right)^{1/4}. \qquad (4)$$

a)
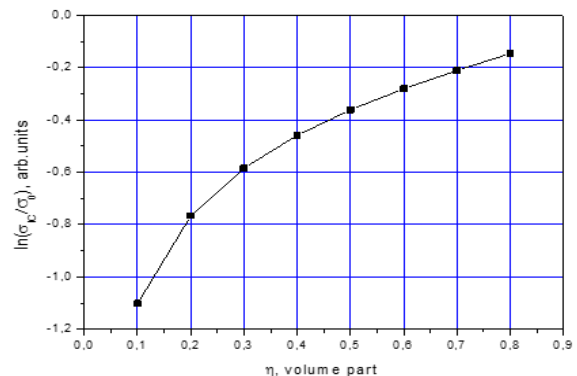
b)

FIGURE 4 Typical statistically averaged morphology of CNT-polymer nanocomposite: a) structural model; b) The hopping conductivity correlation via the average nanocarbon macromolecules volume part within continuous dielectric medium

Shunin Yu, Fink D, Kiv A, Alfonta L, Mansharipova A,
Muhamediyev R, Zhukovskii Yu, Lobanova-Shunina T,
Burlutskaya N, Gopeyenko V, Bellucci S

3 Simulation of stress- and temperature-induced resistance of carbon-based nanocomposite sensors: models and experiment

The overall conductance of nanocomposite material is evaluated using equivalent electric scheme [23]:

$$\Sigma \approx \Sigma_D + \Sigma_{NC},$$

$$\Sigma_{NC} = \sum_{i=1}^{N}(R_i)^{-1}, \qquad (5)$$

$$R_i = A\sum_{k=1}^{N_i}(\sigma_{nano,ik}^{-1} + \sum_{k=0}^{N_i}(N_{eff,ik\sigma}\sigma_{jump,ik})^{-1})$$

where N - is the number of conductivity channels, N_i – is the number of nanocarbon clusters in the conductivity channel, N_{eff} is the number of effective tunneling bonds

including the contact region, $\Sigma_D = (R_D)^{-1}$ is the conductance of dielectric medium, σ_{nano} is the conductivity nanocluster, σ_{jump} - is the hopping conductivity of the effective bond, which creates interconnect for large nanocarbon inclusion concentrations.
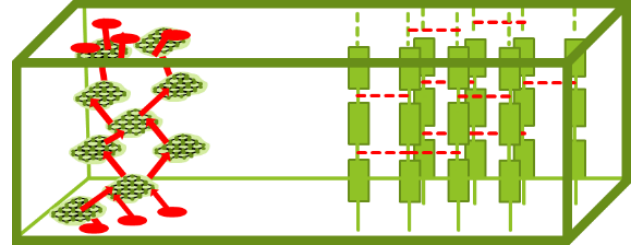
FIGURE 5 Principle equivalent scheme of nanocomposite model for resistance calculation

Basic nanocomposite models for simulation are presented in Figure 6.

FIGURE 6 Models of nanocarbon-based functionalized polymer nanocomposites: CNT configuration 1, CNT configuration 2 , GNR configuration 1, GNR configuration 2, ▮ - electric field direction

3.1 SIMULATION RESULTS

The basic dimensions of nanocarbon clusters (CNTs and GNRs) are as follows: the diameter of the CNT - 5 nm, the height - 10 nm, the width of the expanded CNT, i.e., the width of the GNR = $\pi \cdot 5 \approx 15,6$ nm.

The average statistical distance between nanocarbon clusters is - 5 nm. This is the key distance for the mechanism of hopping conductivity. Nanocarbon cluster is considered as a potential well with a typical size *2a*. Neighboring potential wells are separated by a distance r_{tun}. These two parameters are ultimately determine the morphology of the nanocomposite material. For modeling it also necessary to recalculate a microscopical parameter of relativive jumpimg length to macroscopic strain parameter $\varepsilon = \Delta L / L$ in Hook's law $\sigma = E\varepsilon$, where L is the total sample length. In cases of longitudinal orientation of CNTs (configuration CNT 1) the recalculation looks as:

$$\varepsilon = \frac{\Delta L}{L} \approx \frac{\Delta r}{r} \cdot \frac{1}{1 + \dfrac{1}{1 + (1/n)} \cdot \dfrac{l}{r}},$$

where *l* is the CNT length (close to *2a*) and n is the number of CNT inclusion along the line (current direction). For transversal CNTs orientations (configuration CNT 2) the similar recalculation looks as:

$$\varepsilon = \frac{\Delta L}{L} \approx \frac{\Delta r}{r} \cdot \frac{1}{1 + \dfrac{1}{1 + (1/n)} \cdot \dfrac{d}{r}},$$

where *d* is the diameter of the CNT. The proposed model of hopping conductivity for current percolation in carbon-based epoxy-resin nanocomposite takes into account basically the percolations along the nanocluster sets which are located along the stress direction. Interactions between the neighbouring sets are not considered for a low general concentration of nanocarbon inclusions.

Figure 7 demonstrates resistance correlations via static stresses for ideal morphologies of a nanocomposite when CNTs and GNRs are oriented pure longitudinally, pure transversely. Configurations CNT 2(min) and CNT 4(max) correspond to the minimal and maximal tunnelling (jumping) distances due to the angle deviation of CNTs relatively longitudinal orientation.

Shunin Yu, Fink D, Kiv A, Alfonta L, Mansharipova A,
Muhamediyev R, Zhukovskii Yu, Lobanova-Shunina T,
Burlutskaya N, Gopeyenko V, Bellucci S

a)   b)
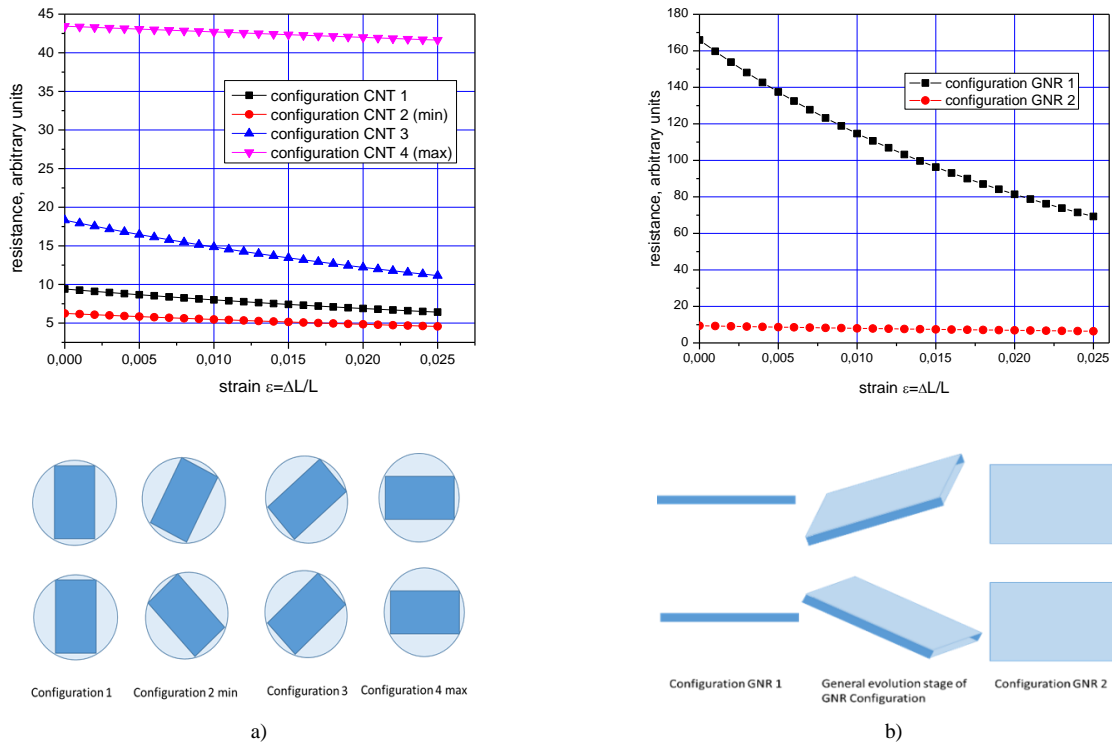
FIGURE 7 Simulation of nanocarbon composites resistances via strain: a) CNTs configurations, b) GNRs configurations

From the technological point of view, it is not so simple to provide such ideal orientations for host polymer materials similar to epoxy resins. The first problem of the nanocomposite morphology is the selection of CNTs and GNRs with identical parameters. The second problem is the polymer-nanocarbon mixture creation when we evidently should expect a homogenous random distribution of nanocarbon orientations.

Figure 8 demonstrates the marginal rotational disordering of CNTs inclusions from 'ideal' longtitudinal orientation. Deviations of orientations give the characteristic inter-cluster distances of 3.82 and 7.02 nm taking into account basic 5 nm in the ideal case.
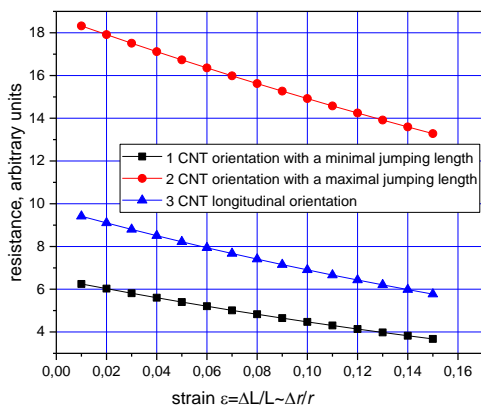
FIGURE 8 Simulation of nanocarbon composites resistances via strain for rotational deviations of CNTs inclusions

Figures 7 and 8 present the full-scale simulation of CNTs orientation deviations within a host material. The results show various sensitivity of the model nanocomposite as a potential pressure nanosensor in dependence of its morphology. Configurations of the 4th type (see Figure 6) are more sensitive and, evidently, more practically preferable.

The model uses morphologically compatible carbon nano-configurations with the same number of carbon atoms, the same surface area of model CNTs and GNRs, and the same chirality. In this way, the model CNTs and GNRs are interconnected by a simple topological transformation from a cylinder to a rectangular fragment.

3.2 COMPARISON OF MODELLING AND EXPERIMENTAL RESULTS SIMULATION OF STRESS-INDUCED RESISTANCE OF CARBON-BASED NANOCOMPOSITE SENSORS

In this section, we will discuss the correlation of simulation results for pressure and temperature nanosensors with the experimental data of the particular prototype of similar devices [25], where the developed technology of functionalised nanocomposite based on epoxy resin (ED-20, GOST 10587-84. Epoxy- Diane Resins Uncured, elasticity modulus E=3,05 GPa) with multi-wall CNTs inclusions was applied. The testing of the mentioned nanosensors with various CNTs morphologies and mass concentrations (1, 2, 3 %) was carried out for temperatures ranging from 27 till 90 °C and the pressure ranging from 1 till 30 Bars.

When testing the pressure sensor, the load ranged from 0 to 500 N, which corresponds to the change in pressure from 0 to 30 Bars. The typical dependence of the sensor resistance on the pressure changes, as compared with the

Shunin Yu, Fink D, Kiv A, Alfonta L, Mansharipova A,
Muhamediyev R, Zhukovskii Yu, Lobanova-Shunina T,
Burlutskaya N, Gopeyenko V, Bellucci S

simulation results, is shown in Figure 9a. Small deviations are connected with technological problems in the reproduction of perfect morphology, which reduces the percolation limit of the nanocomposite.

The typical dependence of the temperature sensor in the temperature range of 27 to 90 °C compared with the

simulation results is shown in Figure 9b. The discrepancy in behavior between the experimental and theoretical dependencies is associated with morphological imperfections of the real sensor induced the orientation dispersion of CNTs. This effect can diminish the hopping mechanism efficiency, especially, for the higher temperatures.

a)

b)
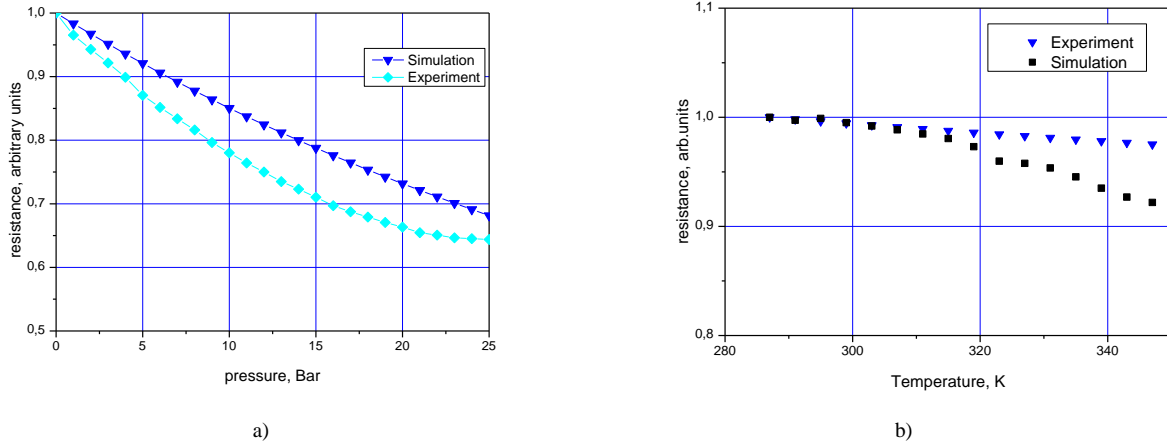
FIGURE 9 Comparison of real pressure and temperature nanosensor indications [25] with more adequate models morphologies simulation: a) pressure nanosensor ; b) temperature nanosensor

4 Polymer nanoporous structures based bionanosensors: biosensor model testing and experimental results

Since the sixties of the past century, it has been known that energetic (with tens of MeV or more) heavy (with atomic masses being usually larger than that of Ar) ion irradiation ("swift heavy ions", SHI) introduces very narrow (~ some nm) but long (typically 10-100 μm) parallel trails of damage

in irradiated polymer foils, the so-called latent ion tracks. The damage shows up primarily by the formation of radiochemical reaction products. Whereas the smaller ones readily escape from the irradiated zone, thus leaving behind themselves nanoscopic voids, the larger ones tend to aggregate towards carbonaceous clusters. Thus, emerging structural disorder along the tracks modifies their electronic behaviour (see Figure 10).
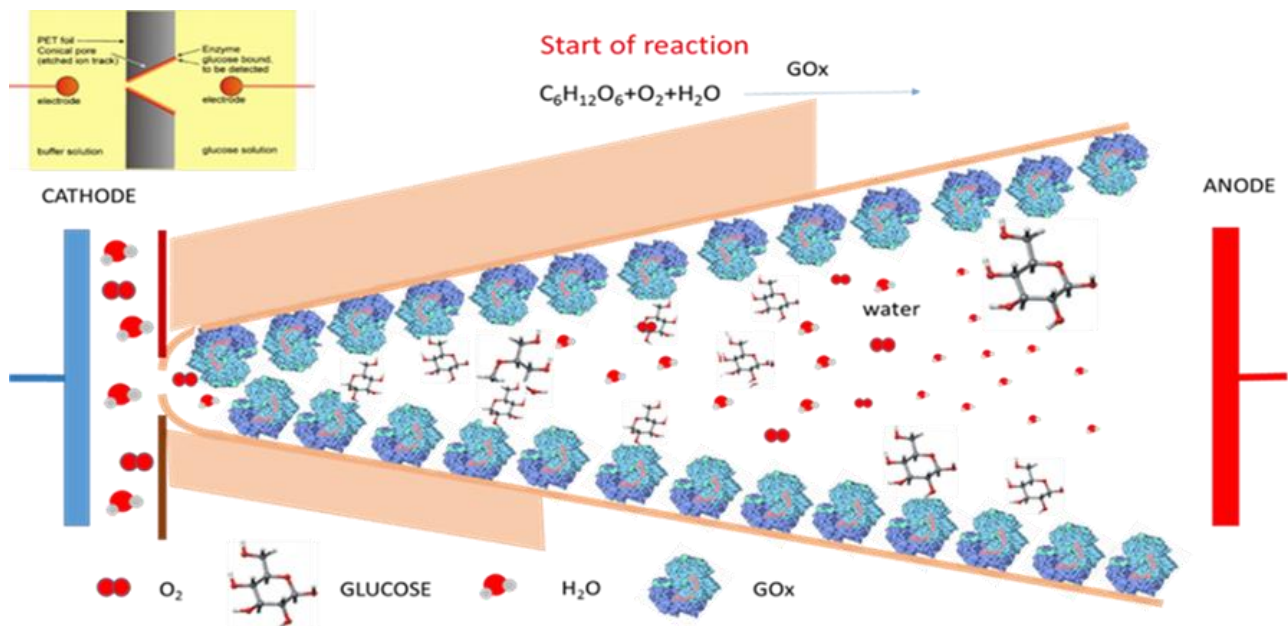
FIGURE 10 General scheme describing the detection scheme and modified polymer. Principle arrangement of experimental setup to study voltage-current dependences in ion track-containing foils embedded in electrolytes.

Shunin Yu, Fink D, Kiv A, Alfonta L, Mansharipova A,
Muhamediyev R, Zhukovskii Yu, Lobanova-Shunina T,
Burlutskaya N, Gopeyenko V, Bellucci S

Description of the sensing reaction of glucose with the enzyme GOx looks as follows:

a) the overall net reaction is: Glucose ($C_6H_{12}O_6$) + O_2 (due to enzyme-induced oxidation) $\rightarrow$ gluconic acid ($C_6H_{12}O_7$) + O;

b) This remaining O attaches to some H_2O to form peroxide H_2O_2 ;

c) the product: gluconic acid dissociates around pH=7: $C_6H_{12}O_7 \rightarrow C_6H_{12}O_7^- + H^+$; thus the conductivity of the liquid changes (essentially if the product is enriched in the track's confinement); this is what is measured by the sensor.

In particular, a complicated biochemical kinetics of basic reaction of glucose detection depends on track qualities (e.g., track creation mechanism, foil material properties), enzyme (GOx) distribution on the track surface, geometry of the etched track etc. All these factors are the subject for the nearest special research. Moreover, the detailed kinetics of reaction is the object of 3D-modelling to design the optimal geometry of nanosensor active space. This allows creating optimal nanosensors with the increased efficiency.

The newly created intrinsic free volume enables electrolytes to penetrate into the polymer, thus forming parallel liquid nanowires. In case of tracks penetration through all the foil, the conducting connections emerge between the front and back sides of the foil. The ion track technology is particularly intended to biosensing applications. In this case, the ion tracks are functionalized directly by attaching organic or bioactive compounds (such as enzymes) to their walls.

Using simulation of chemical kinetics glucose oxidation with glucose oxidase (see Figure 11), we have obtained theoretical calibration dependences, when the concentration of H^+ is proportional to the concentration of the detected glucose.

$$H_2O_2 \overset{catalaza}{\rightarrow} O_2 + 2H^+ + 2e^-,$$

$$w_1 = k_1[C_6H_{12}O_6][O_2][GOx], w_2 = k_2[H_2O_2] -$$
reaction rates.
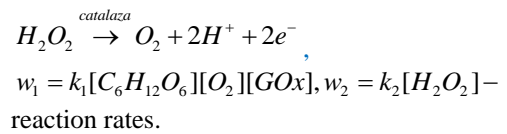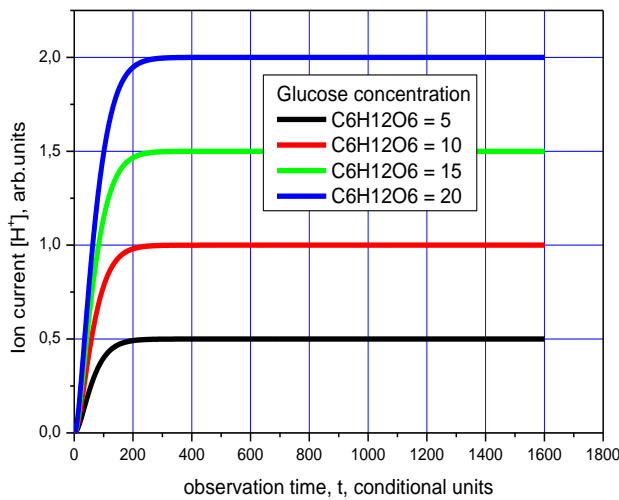
$$\begin{cases} \dfrac{d}{dt}[C_6H_{12}O_6] = -w_1 \\ \dfrac{d}{dt}[H_2O_2] = w_1 - w_2 \\ \dfrac{d}{dt}[C_6H_{12}O_6] = -w_1 + w_2 \\ \dfrac{d}{dt}[C_6H_{12}O_6] = 2w_1 \end{cases}$$

FIGURE 11 Simulation of H+ ion current via observation time in case of saturation and corresponding chemical kinetics equations

Experimental and theoretical calibration dependences demonstrate similar trends. The proposed device can serve to detect physiologically relevant glucose concentrations. The catalytic sensor can be made re-usable due to the formation of diffusible products from the oxidative biomolecular recognition event. Moreover, we can develop a multi-agent packet nanosensor, suitable for application as a human breathing analyser in relation to cancer detection, hepatitis, and so on.

The recent advancements in the field of nanosensor design allow monitoring and tracking biomolecules in such areas as the environment, food quality and healthcare. The presently developed ion track-based nanosensors provide high sensitivity, reliable calibration (see Figure 12), small power and low cost.

The creation of novel biosensors and their further improvement requires a careful study of the mechanisms of electrolytes passing through the tracks. Experimental and theoretical calibration dependences demonstrate similar trends. The proposed device can serve to detect physiologically relevant glucose concentrations. The catalytic sensor can be made re-usable due to the formation of diffusible products from the oxidative biomolecular recognition event. Moreover, we can develop a multi-agent packet nanosensor, which can be used as a human breathing analyzer in relation to cancer detection, hepatitis, and so on.

14

Shunin Yu, Fink D, Kiv A, Alfonta L, Mansharipova A,
Muhamediyev R, Zhukovskii Yu, Lobanova-Shunina T,
Burlutskaya N, Gopeyenko V, Bellucci S

a)

$$C_6H_{12}O_6 + O_2 \xrightarrow{GOx} C_6H_{12}O_7 + O$$
$$O + H_2O \rightarrow H_2O_2$$
$$H_2O_2 \xrightarrow{catalaza} \frac{1}{2}O_2 + H_2O$$
$$C_6H_{12}O_7 \rightarrow C_6H_{12}O_7^- + H^+$$
$$Anode:\ H_2O \rightarrow \frac{1}{2}O_2 + 2H^+ + 2e^-$$
$$Cathode:\ 2H^+ + 2e^- \rightarrow H_2$$
$$Ultimate\ \ reaction:$$
$$C_6H_{12}O_6 + H_2O \rightarrow C_6H_{12}O_7 + H_2$$
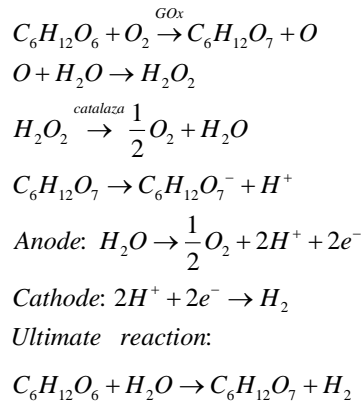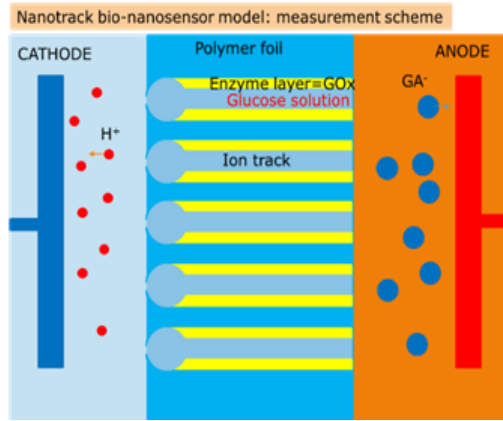
b)
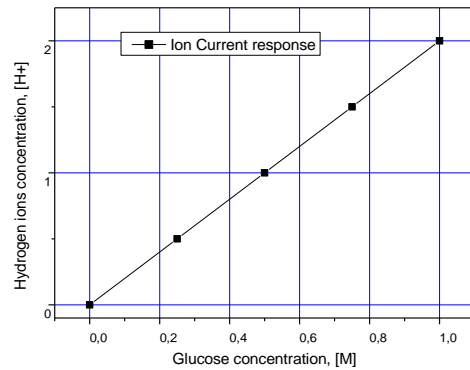
c)

FIGURE 12 a) General model of glucose detection process on the ion track-containing foils embedded in electrolyte and basic set of biochemical reaction; b) Experimental calibration dependenceerformance comparison of three identically produced track-based glucose detectors against a calibration curve I (+5 V) vs. glucose concentration; c) Theoretical model of typical calibration dependence based on chemical kinetics results: simulation of induced H$^+$ ion current via Glucose concentration.

5 Conclusions

A nanocomposite pressure and temperature nanosensor prototypes have been simulated. The hopping conductivity mechanism gives the adequate description of possible nanosensor qualities. An important problem of manufacturing sensors based on CNTs and GRNs is nanocarbon inclusions orientation, which determines the electrical properties of the future sensor.

Our work has demonstrated that ion track-based glucose sensors can be effectively created. Furthermore, they show good sensitivity, they cover a wide range of medical applica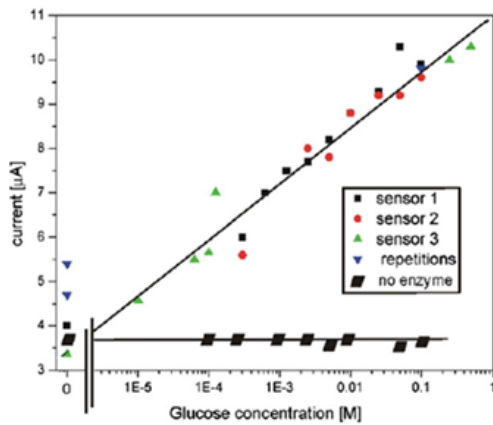tions, and they can be re-used at least 10 times. This study also proves that track-based biosensors with other enzymes can be similarly developed.

Both nanosensing schemes use simple electrical response outputs for device calibrations of parameters to be measured and can be considered as real-time tools.

References

[1] Shunin Yu N, Gopeyenko V I, Burlutskaya N, Lobanova-Shunina T, Bellucci S 2013 Electromagnetic properties of CNTs and GNRs based nanostructures for nanosensor systems *Proc. Internat. Conf. „Physics, Chemistry and Application of Nanostructures-Nanomeeting-2013, Minsk, Belarus* 250-3

[2] Shunin Yu N, Zhukovskii Yu F, Gopejenko V I, Burlutskaya N Yu, Bellucci S 2012 Properties of CNT- and GNR-Metal Interconnects for Development of New Nanosensor Systems *Nanodevices and Nanomaterials for Ecological Security Series: NATO Science for Peace Series B - Physics and Biophysics* 237-62

15

Shunin Yu, Fink D, Kiv A, Alfonta L, Mansharipova A, Muhamediyev R, Zhukovskii Yu, Lobanova-Shunina T, Burlutskaya N, Gopeyenko V, Bellucci S

[3] Fink D, Klinkovich I, Bukelman O, Marks R S, Kiv A, Fuks D, Fahrner W R, Alfonta L 2009 Glucose determination using a re-usable enzyme-modified ion track membrane sensor *Biosensors and Bioelectronics* **24** 2702–6

[4] Fink D., Gerardo Muñoz H, Alfonta L, Mandabi Y, Dias J F, de Souza C T, Bacakova L E, Vacı´k J, Hnatowicz V, Kiv A E, Fuks D and Papaleo R M 2012 Status and perspectives of ion track electronics for advanced biosensing *Nanodevices and Nanomaterials for Ecological Security Series: NATO Science for Peace Series B - Physics and Biophysics* 269-79

[5] Shunin Yu, Kiv A 2012 *Nanodevices and Nanomaterials for Ecological Security, Series: NATO Science for Peace Series B— Physics and Biophysics* 363

[6] Shunin Yu N, Schwartz K K 1997 Correlation between electronic structure and atomic configurations in disordered solids *Computer Modelling of Electronic and Atomic Processes in Solids* 241–57

[7] Shunin Yu N, Shvarts K K 1986 Calculation of the electronic structure in disordered semiconductors *Physica status solidi* (b) **135**(1) 15-36

[8] Shunin Yu. N, Zhukovskii Yu F, Gopeyenko V I, Burlutskaya N, Lobanova-Shunina T, Bellucci S 2012 Simulation of electromagnetic properties in carbon nanotubes and graphene-based nanostructures *Nanophotonics* **6**

[9] Shunin Yu N, Zhukovskii Yu F, Gopejenko V I, Burlutskaya N, Bellucci S 2011 Ab initio simulations on electric properties for junctions between carbon nanotubes and metal electrodes *Nanoscience and Nanotechnology letters* **3**(6) 816–25

[10] Shunin Yu N, Zhukovskii Yu F, Burlutskaya N, Bellucci S 2011 Resistance simulations for junctions of SW and MW carbon nanotubes with various metal substrates *Central European Journal of Physics.* **9**(2) 519–29

[11] Fink D, Kiv A, Shunin Y, Mykytenko N, Lobanova-Shunina T, Mansharipova A, Koycheva T, Muhamediyev R, Gopeyenko V, Burlutskaya N, Zhukovskii Y, Bellucci S 2015 The nature of oscillations of ion currents in the ion track electronics *Computer Modelling and New Technologies* **19**(6) 7-13

[12] Shunin Yu, Alfonta L, Fink D, Kiv A, Mansharipova A, Muhamediyev R, Zhukovskii Yu, Lobanova-Shunina T, Burlutskaya N, Gopeyenko V, Bellucci S 2016 Modelling and simulation of electric response of nanocarbon nanocomposites and nanoporous polymer based structures for nanosensor devices *Theses of the 14th International scientific conference INFORMATION TECHNOLOGIES AND MANAGEMENT 2016 April 14-15* 11-4

[13] Shunin Yu., Fink D, Kiv A, Alfonta L, Mansharipova A, Muhamediyev R, Zhukovskii Yu, Lobanova-Shunina T, Burlutskaya N, Gopeyenko V, Bellucci S 2016 Theory and modelling of physical and bio- nanosensor systems *Proc of the 5th Int Workshop Nanocarbon Photonics and Optoelectronics, 1-6 August 2016* 101

[14] Landau L D 1956-1957 The theory of a fermi liquid *Soviet Physics JETP* **3**(6) 920-5 E*xperimental and Theoretical Physics* **30** 1058-64

[15] Gurzhi R P, Shevchenko S I 1968 Hydrodynamic mechanism of electric conductivity of metals in a magnetic field *Soviet Physics JETP* **27**(6) 1019-22

[16] Mendoza M, Herrmann H J, Succi S 2013 Hydrodynamic model for conductivity in graphene *Scientific Reports* **3** 1052 1-6

[17] Drude P 1900 Zur Elektronentheorie der metalle *Annalen der Physik* **306**(3) 566

[18] Drude P 1900 Zur Elektronentheorie der Metalle II. Teil. Galvanomagnetische und thermomagnetische Effecte *Annalen der Physik* **308**(11) 369

[19] Landauer R 1957 Spatial Variation of Currents and Fields Due to Localized Scatterers in Metallic Conduction *IBM Journal of Research and Development* **1** 223–31

[20] Mott N F 1968 Metal-Insulator Transition *Reviews of Modern Physics* **40** 677-83

[21] Seager C H, Pike G E 1974 Percolation and conductivity: A computer study II *Physical Review B* **10** 1435-46

[22] Shunin Y, Bellucci S, Zhukovskii Y, Lobanova-Shunina T, Burlutskaya N, Gopeyenko V 2015 Modelling and simulation of CNTs- and GNRs-based nanocomposites for nanosensor devices *Computer Modelling & New Technologies* **19**(5) 14-20

[23] Shunin Yu N, Gopeyenko V I, Burlutskaya N Yu, Lobanova-Shunina T D, Bellucci S 2015 Electromechanical properties of carbon-based nanocomposites for pressure and temperature nanosensors", *EuroNanoForum 2015 1-12 June 2015*

[24] Shunin Yu, Bellucci S, Zhukovskii Yu, Gopeyenko V, Burlutskaya N, Lobanova-Shunina T 2015 Nanocarbon electromagnetics in CNT-, GNR- and aerogel-based nanodevices: models and simulations *Computer Modelling and New Technologies* **19**(1A) 35-42

[25] Abdrakhimov R R, Sapozhnikov S B, Sinitsin V V 2013 Pressure and temperature sensors basis of ordered structures of carbon nanotubes in an epoxy resin 2013 *Bulletin of the South Ural State University Series Computer Technologies Automatic Control Radio Electronics* **13**(4) 16-23

AUTHORS

Yuri N Shunin

Current position, grades: Professor and Vice-Rector on academic issues at Information Systems Management University and a leading researcher at the Institute of Solid State Physics, University of Latvia.
University studies: PhD (physics and maths, solid state physics, 1982) at the Physics Institute of Latvian Academy of Sciences and Dr. Sc. Habil. (physics and maths, solid state physics, 1992) at Saint-Petersburg Physical Technical Institute (Russia).
Scientific interests: His current research activities concern nanophysics, nanoelectronics, nanodevices, nanomaterials, nanotechnologies, nanorisks, nanoeducation, and nanothinking
Publications: over 470, 1 book with Springer
Experience: director of NATO ARW "Nanodevices and Nanomaterials for Ecological Security," Riga, Latvia, 2011, a visiting researcher at Gesellschaft für Schwerionenforschung mbH, Darmstadt, Germany (1995), INFN—Laboratori Nazionali di Frascati, Frascati-Roma, Italy (2010 to 2015), participation in EU FP7 Projects CATHERINE (2008 to 2011) and CACOMEL (2010 to 2014), education practitioner in Higher Education from 1975 till nowadays

Dietmar Fink

Current position, grades: Dr., at present he is a guest Professor of the University of Mexico. Earlier he was a Head of laboratory in Hahn-Meitner institute (Berlin), the Editor-in-Chief of International journal "Radiation effects and defects in solids".
Scientific interest: radiation effects in nanodevices
Experience: one of the founders of track electronics

Arnold Kiv

Current position, grades: Professor-researcher of Department of materials engineering, Ben-Gurion University of the Negev, Head of Department of physical and mathematical modelling, South-Ukrainian national pedagogical university after K. D. Ushinskij
Scientific interest: nanomaterials and nanoelectronics,
Experience: He is an expert in the theory of real structure of solids and physical processes in electronic devices. In last decade he obtained significant results in the field of nanomaterials, track nanostructures and track electronics.

Shunin Yu, Fink D, Kiv A, Alfonta L, Mansharipova A,
Muhamediyev R, Zhukovskii Yu, Lobanova-Shunina T,
Burlutskaya N, Gopeyenko V, Bellucci S

Lital Alfonta

Current position, grades: Professor of Department of Life Sciences, Ben-Gurion University of the Negev, Beer-Sheva
University studies: B.Sc. Hebrew University of Jerusalem, Jerusalem, Israel. Chemistry, M.Sc. Hebrew University of Jerusalem, Jerusalem, Israel. Biochemistry and Organic Chemistry
Scientific interest: Engineering of Electron Transfer Pathways, Genetic Code Expansion

Almagul Mansharipova

Current position, grades: Head of Department science KRMU, professor, member of Association aksam, Almaty, Kazakhstan
University studies: Kazakh Russian medical university
Scientific interest: Research in the field of medicine, cell biology, bioinformatics.
Publications: 150 papers, 3 patents.

Ravil Muhamedyev

Current position, grades: Head of Department CSSE&T, professor, International IT University, Almaty, Kazakhstan
University studies: International IT University, Almaty, Kazakhstan
Scientific interest: stochastic simulation, machine learning, simulation of anisochronous systems
Publications: 160 papers, 5 books

Yuri Zhukovskii

Current position, grades: Dr.Chem., Head of Laboratory of Computer Modeling of Electronic Structure of Solids, Institute of Solid State Physics (University of Latvia).
Publications: He is the author of over 120 regular and review papers in international scientific journals. His Hirsch index is 16.
Experience: From 1977 until 1995 a researcher at the Institute of Inorganic Chemistry, Latvian Academy of Sciences. Since 1995 a leading researcher at the Institute of Solid State Physics, University of Latvia. Within the last 20 years he has been granted several fellowships for collaboration, visiting activities and positions at seven universities and scientific centers of Canada, Finland, Germany, United Kingdom, and the United States. Actively engaged in developing active collaboration with some scientific groups in Belarus, Italy, Russia, and Sweden. Simultaneously, a contact person and participant in a number of collaboration projects under support of European Commission. His current research activities concern theoretical simulations on the atomic and electronic structure of crystalline solids (with 3D, 2D and 1D dimensionalities).

Tamara Lobanova-Shunina

Current position, grades: Associate Professor at Riga Technical University, Aeronautics Institute, PhD, Dr.edu
University studies: University of Latvia, She obtained her PhD (2009) on innovative education at South-Ukrainian National University
Scientific interests: current research activities concern nanotechnologies, nanomanagement, nanoeducation, nanorisks, and nanothinking in the EU FP7 Project CACOMEL (2010 to 2014), special interests are connected with the systemic approach to nanosystems applications.
Publications: 53 regular papers
Experience: a member of the NATO ARW Local Organizing Committee 'Nanodevices and Nanomaterials for Ecological Security', Riga, Latvia, 2011. A visiting researcher at INFN-Laboratori Nazionali di Frascati, Frascati-Roma, Italy (2010 to 2015). The Head of International Business Communications Department, Director of the study programme 'International Business Communications' at Information Systems Management University (till 2013). The Editorial Board member of the journal 'Innovative Information Technologies'.

Nataly Burlutskaya

Current position, grades: a researcher at the Information Systems Management University and the Institute of Solid State Physics, University of Latvia
University studies: Master degree in computer systems (2011) at Information Systems Management University, Riga, Latvia.
Scientific interests: current research activities concern theoretical simulations of the electronic and electrical properties of carbon nanotubes and graphene nanoribbons in the EU FP7 Project CACOMEL (2010 to 2014).
Publications: 30 regular papers
Experience: the secretary of organizing committee of NATO ARW "Nanodevices and Nanomaterials for Ecological Security," Riga, Latvia, 2011.

Victor Gopeyenko

Current position, grades: professor, Dr.Sc.Eng Vice-Rector on scientific issues at Information System Management University and the director of ISMU Computer Technologies Institute.
University studies: Riga Civil Aviation Engineering Institute (Latvia) obtained his doctor's degree (Dr. Sc. Eng., 1987) at Riga Civil Aviation Engineering Institute (Latvia).
Scientific interests: current research activities concern nanophysics, nanoelectronics, nanodevices, and nanotechnologies in the EU FP7 Project CACOMEL (2010 to 2014). His special interests concern carbon nanotubes and graphene systems applications and modeling.
Publications: 80 regular papers in international scientific journals
Experience: Was the member of local organizing committee of NATO ARW "Nanodevices and Nanomaterials for Ecological Security," Riga, Latvia, 2011, the editor-in-chief of the journal 'Information Technologies, Management and Society' and editorial board member of the journal 'Innovative Information Technologies'.

Stefano Bellucci

Current position, grades: PhD, Professor, currently coordinates all theoretical physics activities at INFN Laboratori Nazionali di Frascati (Italy).
Universisty studies: April 1982: Laurea in Physics (Magna cum Laude), University of Rome "La Sapienza" July 1984: Master in Physics of Elementary Particles, SISSA and University of Trieste, PhD in physics of elementary particles in 1986 at SISSA, Trieste, Italy.
Publications: over 400 papers in peer-reviewed journals (with h = 40), and more than 10 invited book chapters, the editor of ten books with Springer
Scientific interests: research interests include theoretical physics, condensed matter, nanoscience and nanotechnology, nanocarbon-based composites, and biomedical applications.
Experience: Worked as a visiting researcher at theBrandeis University, Waltham, MA, USA (1983 to 1985); at the M.I.T., Cambridge, MA, USA (1985 to 1986); the University of Maryland, USA (1986 to 1987); at the University of California at Davis, USA (1987 to 1988). Editorial board member of the Springer Lecture Notes in Nanoscale Science and Technology, as well as the editorial board member of the Global Journal of Physics Express and the Journal of Physics & Astronomy
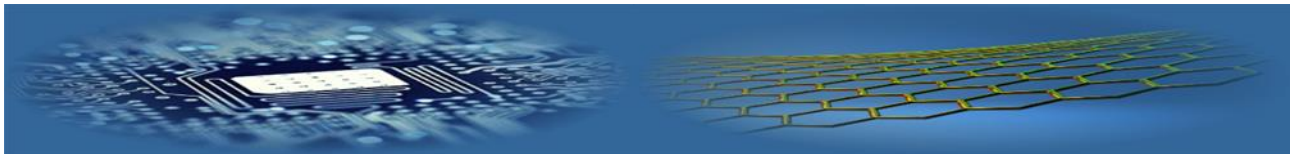
Development of the augmented reality applications based on ontologies

Yersain Chinibayev, Tolganay Temirbolatova*

International IT University, Manas Str. 34A/8A, 050040 Almaty, Kazakhstan

*Corresponding author: ttemirbolatova@gmail.com

Abstract

This article presents an analysis of the existing popular libraries for the development of augmented reality applications. Based on the analysis we propose a universal technology of construction of augmented reality applications using ontology. The technology is based on the geolocation using GPS and communicates with the resource through Linked Open Data.

1 Introduction

One of the applications of modern information systems and technologies – creation of qualitatively new features augmented reality with a view to their application in various branches of human activity [1, 2].

We know that in real life, a person receives 83% of information visually, 11% through the organs of hearing, and 6% through the channels of touch, smell and taste [3]. Modern development of hardware and software for Human Machine Interface (HMI) and computer graphics allow you to create a qualitatively new virtual worlds, enabling the use of all channels of perception of the information. Nowadays the main means displaying augmented reality (AR) are mobile devices, based AR solutions are used in all industries: tourism, medicine, etc. [4, 5].

Among the existing technologies in the construction of augmented reality applications (ARA) the most common solutions, demonstrating different approaches to the development of the ARA are: ARTAG [7], ARTOOLKIT [8], Layar [9], QUALCOMM AR PLATFORM [10], belonging to both the marker, so and markerless approaches [11]. Table 1 shows the description of the above systems.

The mentioned systems are used in the development of a specific task. However, existing solutions are only applicable in a certain area. The development of the ARA should take into account a several of specific issues of all AR systems. This problems are associated with the construction of virtual objects:

1. the organization of repository of the virtual objects and the means of access to it;
2. ensure the necessary degrees of realism of virtual objects;
3. matching of virtual objects with the scene.

TABLE 1 Description AR system

	Based on the markers	Advantages of the system	Disadvantages of the system
ARTAG	+	1. It supports multiple libraries to recognize the marker.	The following issues haven't been resolved: - general architecture,
ARTOOLKIT	+	2. Precisely defines the coordinates of the location of additional content.	- development of user interface, - the user's location in space
Layar	-	1. Determination of location using the GPS. 2. It contains detailed documentation and examples for creating layers. 3. Change shall be entered at the API level.	1. There is a difficulty in solving problems of the ARA with multiple user locations. 2. The complexity of application settings for a specific user. 3. The complexity of in calculating the specifics of a particular subject area.
Qualcomm AR	+	Recognize different types of objects in the video stream.	It doesn't recognize the user in the space

AR system can operate a whole set of virtual objects that are reproduced depending on the specific situation. Therefore it is necessary to organize the storage of objects in such a way that the system can get quick access to them.

Modern smart phones such as iPhone, HTC, Samsung have constant access to the Internet, and thus ensure the positioning of the user in the space. Defining user geolocation is done in two ways, the first category is an already stored specific location in the form of a cloud of linked data, in the second category user coordinates are being extracted in real-time and linked to user data. All the operated data is metadata, which can help you build an ontological model for future use.

2 Ontological modeling as an approach to overcome the limitations of existing solutions

The advantage of using ontology modeling in technology

development in the AR adapted applications is based on the change of an ontological module. It provides:

1. Software easy adaptation to changes in the subject area (SA - Many subject areas and problems solved).
2. Easy adaptation of the software to the needs of specific user / user group.
3. The ability to reuse ontological models and their fragments on different layers of a complex system.
4. The ability to make changes in the behavior of the system during operation, without the need to recompile the code.
5. Ontological model types can be reused at all stages of the software development of the ARA.
6. The user interface of the software has the ability to of intellectualization.

3 Technology of creation of the ARA, based on ontologies

The proposed constructing ARA technology uses multi-level ontology of Figure 1. The upper level ontology are:

- The real space - defined by the user geolocation.
- Stage space - set of objects of the scene formed (image).
- Replacement point - augmented object placement in real space.
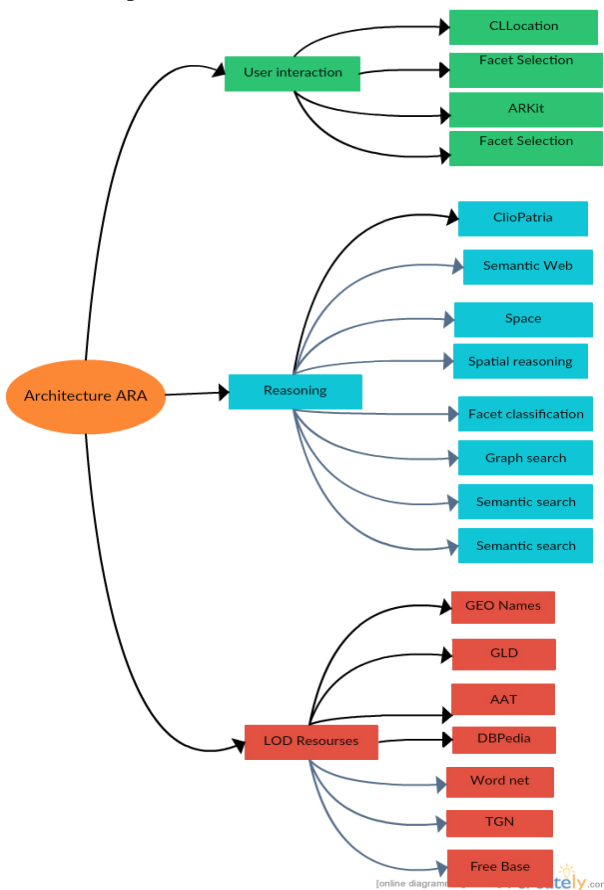
FIGURE 1 Architecture ARA

The scene in the applications of augmented reality is formed by combining a picture of the real world and objects augmented. Therefore, the real world - the space in which the user is moving, can be called complemented, and the set of all objects that are being augmented - space of addition. Space that is being augmented is discrete and divided into locations.

Functional description of the ARA presented in Figure 2. The proposed architecture creates applications where the user route depends on current preferences and interests, shows the user the information he needs, and helps to navigate in difficult situations. Thus, even the same path in real space, between the same objects, could be accompanied with different information, that allows the application to be configured as for the user and also for the current goals of content owners.
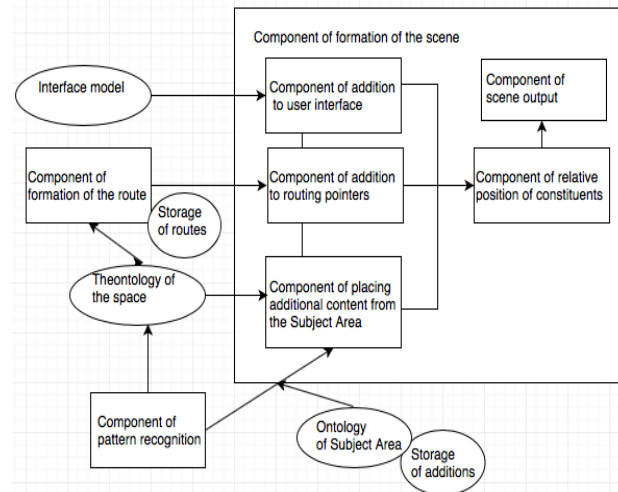
FIGURE 2 Architecture ARA based on ontologies (arrows denote the main directions of data streams)

The component that forms the scene is central in the application of augmented reality. It is responsible for the placement of the three types of add-ons:

1. The component of user interface additions forms user interface.
2. Component of addition for route pointers with the help of data provided by the components that form the route, allows you to display tips on the desired direction of movement and the distance between them.
3. Component of placement of the additional content from SA on the basis of data received from the pattern recognition component, determines where and how will the special content be reflected. This content is associated with a user's current position, as well as with specific objects of SA.

Formed additions should be located within the scene and displayed on the screen of the device, for which, the component of the mutual arrangement of additions and output component are responsible. The AR applications use extremely limited space on the screen to display the system functionality. However, it is possible to create interactive additions, the behavior of which will depend on explicit user action. This elements will be the user interface of AR applications. The declarative character of the interface model can significantly simplify the process of its development. This approach simplifies the division of responsibilities between the designers and programmers.

In order to highlight the place of ontological models in the ARA, main challenges are considered in Fig 3, resulting in the development of the ARA, and the possibility of using

semantically powerful tools to solve them. Identified the following tasks:
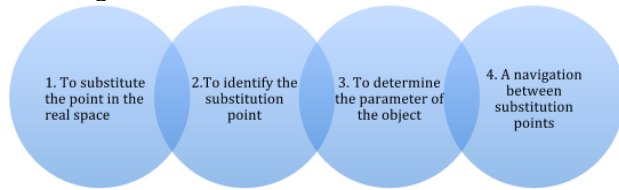
FIGURE 3 Defining the problem of constructing ARA

To solve the problem 1, it is required to construct an ontology domain concepts. Next, we need to build an applied ontology of real space using the concepts of the ontology.

For a more accurate indication of places of substitution points, it is prompted to enter the relative coordinates of the grid in separate locations. Built for solving the problem 1, the ontology can be used to simplify the solution of recognition problem of substitution points. To do this, use image recognition algorithms that can take into account not only the results of the analysis of the video stream, but the data about the place of location of the user in space.

Solution 3 requires use of the knowledge about supplement objects. This knowledge can be represented as a domain ontology. Subject ontology provided therein semantic existence metrics can be used to solve the problem of semantic navigation.

Based on the analysis of problems it is concluded about the need to describe the ontology model of SA and ontology of the space. Ontology SA (OSA) describes the basic concepts of SA and relations between them. As part of the OSA introduced semantic metric that allows to determine the proximity of concepts. Every concept is a set of possible additions. The ontology supports basic paradigmatic types of bonds (class-subclass instance of class, part-whole, necessary part- whole class attribute), connection type "contextually linked", as well as types of communication required for this domain.

4 The formal presentation of the solution of SA

Formal description of the visualization system is presented below. Multiple data in the system is displayed via the following formula:

$$\Sigma : \Xi \to \Xi , \tag{1}$$

$$O = \Sigma(I) , \tag{2}$$

where $I = (i_1, i_2, ..., i_n)$ – the set of input data, $n \in N$, $O = (o_1, o_2, ..., o_m)$ – the set of output data, m∈N.

Elements of I and O has a heterogeneous structure and are represented as a string. Ξ – a plurality of data, then $i_a \in \Xi$, $o_b \in \Xi$, $a = 1$, n , $b = 1$, m .

We introduce the variables:
- set of supported graphics visualization system objects in the scene, $U = (u_1, u_2, ..., u_k), k \in N$. Elements of U are the mathematical models of visual objects: three-dimensional bodies, raster images, diagrams, etc.

Specific scene is a subset U of U .
- set of supported imaging system of a Graphical

User Interface (GUI), $M = (m_1, m_2, ..., m_l), l \in N$, moreover $m = \sigma 1^d, \sigma 2^d, ..., \sigma l d^d$ – a set of states that can accept interface element m_d , $d \in 1$, l , $l_d \in N$ in response to user actions.

A specific set of interface elements that serve to control the visualization, is a subset of M the plurality of M , $M = \{mc1, mc2, ..., mct\}$, $mcg \in M$, $cg \in N$, $g = 1$, t , $t \in N$, $t \leq l$.
- $S = \{m_1 \times m_2 \times ... \times m_l\}$ – the set of conditions that can make all the interface elements in response to user actions.
- the set of all possible user actions, $E = \{e_1, e_2, ..., e_q\}$, $q \in N$, E . It is a subset of E .

The module Γ organizing interactive user interface with graphical visualization of the system can be represented as a mapping of the set of all possible actions the user E , and all supported elements M interface to the set of states S of these elements:

$$\Gamma : E \times M \to S . \tag{3}$$

Then the specific scene setting set in response to a user action at the time of its next reference to imaging system can be obtained using this mapping to the set M :

$$S ' = \Gamma(E, M) . \tag{4}$$

Multiple S' of all possible sets of scene settings in turn may be obtained kind of the union

$$S' = \bigcup E ' \subset E\Gamma(E', M) . \tag{5}$$

Visualizer Φ can be represented as a mapping of all supported visual objects Uand all possible setups scene S' on the P raster image, which is a matrix of dimensions $w \times h$, the elements of which are the color-coded using a color model (more often – RGB):

$$\Phi : U \times S' \to P , \tag{6}$$

$$P : W \times H \to C , \tag{7}$$

where $W = \{1, 2, ..., w\}$, $w \in N$, $H = \{1, 2, ..., h\}$, $h \in N$, C – a variety of colors used by the color model.

Getting the image P' with smooth boundaries of objects can be written as a superposition of the visualizer Φ and the smoothing operator Δ :

$$P \to P , \tag{8}$$

$$P' = \Delta(\Phi(U, S')) . \tag{9}$$

The module Ψ interaction the visualization system can be represented as a map of input and output data in the solver set of visual objects:

$$\Psi : \Xi \to U . \tag{10}$$

When the integration takes place only with the data set U of specific objects to be rendered can be written as follows:

$$U = \Psi(I \cup O) . \tag{11}$$

Each element of this set corresponds to an element of I input. Then feedback the visualization system can be written as follows: $U = \Psi(\Gamma(N) \cup \Sigma(\Gamma(N)))$.

Using the notations entered tuned to a specific imaging

system Y can be represented as follows:

$$Y = \langle \Phi, U, \Delta, \Gamma, M, E, \Psi, M, N \rangle . \qquad (12)$$

Components of the model Φ , Δ , Γ , M , E , M unified:

- Φ – imaging operator, displaying a plurality of graphical objects U .
- Δ – smoothing operator acting on the finished bitmap and generating a new image with smooth borders of objects.
- Γ – operator to organize a GUI that allows the user to set various settings using the graphical controls regardless of the logic of further use of the values of these settings.
- M – unified set of controls, such as buttons, text boxes, radio buttons, and so on. etc.
- E – set of supported user interaction with a plurality of elements M .
- M – once a certain set of controls needed to navigate through the displayed scenes. model components U , Ψ , N generally depend on the system:
- U – a set of objects that are visible the data system.
- Ψ – the operator carrying out the conversion of input and output data of the system into objects suitable for visualization module Φ .
- N –set of controls that provide feedback to the system.

The investigation of the applicability of the ontological engineering methods to the problem of describing the visual objects. Elements of U are connected to each other in relation to the parent-child relationship (inheritance of properties), the part-whole class- and instance. In this connection, the conclusion on the adequacy of applied ontology without axiomatic to address the objectives of the study. Therefore, $U = \langle T_U, R_U \rangle$, when T_U – thesaurus visual objects, R_U – a finite set of connections between visual objects. The set N can be obtained by comparing the types of elements of the sets I and M with the help of the operator Π select items from the set M , suitable for editing the corresponding data:

$$\Pi : \Xi \times M \to M , \qquad (13)$$

$$N = \Pi(I , M) . \qquad (14)$$

The practical implementation of such an operator in a software module is trivial comparison. Showing Ψ can be obtained by the operator kind of Ω .

$$\Omega : \Xi \times U \to \Psi \qquad , \qquad (15)$$

where Ψ – converting the set of operators.

In this case:

$$\Psi = \Omega(I \cup O , U) . \qquad (16)$$

The software implementation of the visualization system mapping Ψ can be generated semi-automatically, after the user has specified the relevant elements of the sets I and O object properties of a variety of U .

To unify the software implementation of the operator Θ can also be used an approach, based on ontological engineering. The operator will be modified as follows:

$$\Theta : K_\Sigma \times L \to \Xi , \qquad (17)$$

where L – ontology, describing syntax input-output programming language operators.

Θ denotes a unified parser, which is controlled by the ontology L .

The investigation of the applicability of the ontological engineering practices to the task of parsing the source code in a given language in order to extract input and output variables. To automatically generate a parser must submit Backus-Naur Form (BNF), the language of ontology. To represent the BNF, as well as for the presentation of visual objects of applied ontology enough without axiomatic. Therefore, $L= \langle T_L, R_L \rangle$, when T_L – thesaurus construction, and R_L - a finite set of relations between them. Total formal model of the system is represented as follows:

$$Y^* = \langle \Phi, U, \Delta, \Gamma, M, E, \Theta, L, \Omega, \Pi, M \rangle . \qquad (22)$$

5 Conclusions

This article presents the application development technology of augmented reality, based on ontologies. The results of the analysis of existing approaches to the development of augmented reality applications, demonstrated the need for a high-technology systems for building augmented reality. The article proposes the technology of constructing the application based on the ontological analysis to solve problems arising in the development of augmented reality applications.

References

[1] Craig A B 2013 Understanding Augmented Reality Concepts and Applications *Newnes*
[2] Huang Z, Hui P, Peylo C, Chatzopoulos D 2013 Mobile Augmented Reality Survey A Bottom-up Approach *arXiv preprint*
[3] http://zillion.net/ru/blog/236/dopolniennaia-rièalnost-prostranstvo-miezhdu-rièal-nostiu-i-virtualnostiu
[4] Yovcheva Z, Buhalis D, Gatzidis C 2012 Overview of Smartphone Augmented Reality Applications for Tourism *E-review of Tourism Research* 10
[5] Morris D, Sewell C, Barbagli F 2006 Visuohaptic Simulation of Bone Surgery for Training and Evaluation *IEEE Computer Graphics and Applications* **26**(6) 48–57
[6] Jurkov C 2012 Razrabotka prilozhenii dopolnennoi realnosti,

osnovannykh na ontologyi *Information Theories and Applications* **19**(4)
[7] Fiala M 2005 Artag, a fiducial marker system using digital techniques *IEEE Conference on computer vision and pattern recognition* 590-6
[8] Kato I P H, Billinghurst M 2000 ARToolkit User Manual *Human Interface Technology Lab*
[9] Layar. http://www.layar.com/, April 2012.
[10] Augmented Reality (Vuforia), https://developer.qualcomm.com/develop/mobile-technologies/augmented-reality, April 2012.
[Ferrari, 2001]Ferrari V, Tuytelaars T, Van Gool L 2001 Markerless augmented real time affine region tracker *Proceedings of the IEEE and ACM International Symposium on Augmented Reality* 87 – 96

Information and Computer Technologies

AUTHORS

Yersain Chinibayev, 1986, Kazakhstan

Current position, grades: PhD candidate
University studies: MSCS at KBTU
Scientific interest: Augumented Reality
Publications: 3
Experience: more than 7 years

Tolganay Temirbolatova, 1988, Kazakhstan

Current position, grades: PhD candidate
University studies: MSCS at NSU
Scientific interest: Big Data, Integration data, Ontologie, Mashine Learning
Publications: 10
Experience: more than 6 years
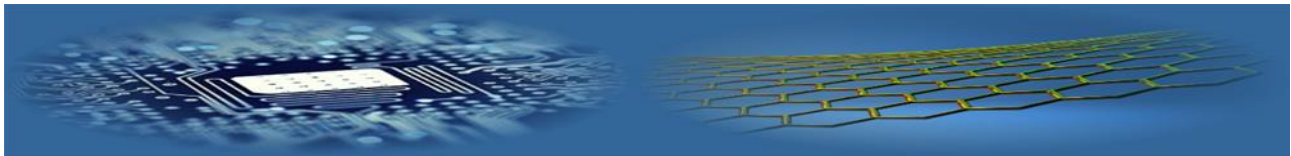
Comparison of Cuckoo Search, Tabu Search and TS-Simplex algorithms for unconstrained global optimization

Ghania Khensous[1, 2*], Belhadri Messabih[2], Abdellah Chouarfia[2], Bernard Maigret[3]

[1]Université des Sciences et de la Technologie d'Oran USTO-MB, Oran, Algérie
[2]Ecole Normale Supérieure d'Oran ENSO, Oran, Algérie
[3]CNRS, LORIA, Vandoeuvre-Les-Nancy, France

[*]Corresponding author: gh.khensous@yahoo.fr

Abstract

Metaheuristics Algorithms are widely recognized as one of the most practical approaches for Global Optimization Problems. This paper presents a comparison between two metaheuristics to optimize a set of eight standard benchmark functions. Among the most representative single solution metaheuristics, we selected Tabu Search Algorithm (TSA), to compare with a novel population-based metaheuristic: Cuckoo Search Algorithm (CSA). Empirical results reveal that the problem solving success of the TSA was better than the CSA. However, the run-time complexity for acquiring global minimizer by the Cuckoo Search was generally smaller than the Tabu Search. Besides, the hybrid TSA-Simplex Algorithm gave superior results in term of efficiency and run-time complexity compared to CSA or TSA tested alone.

1 Introduction

Global Optimization has been an active area of research for several decades since optimization problems are inherent in nearly every research area, ranging from engineering to the natural sciences such as Biology or Chemistry. It is also an active research topic in many other areas such as Mathematics, Business, and the Social Sciences [1]. As many real-world optimization problems become more complex, better optimization algorithms were needed.

In all optimization problems, the goal is to find the minimum or the maximum of the objective function. Therefore, the aim of optimization is to obtain the relevant parameter values allowing an objective function the generation of the minimum or maximum value. Thus, unconstrained optimization problems can be formulated as the minimization or the maximization of D-dimensional function [2]:

$$Min \ (or \ Max) \ f(x), \ x = (x_1, x_2, x_3, \ldots x_D) \quad (1)$$

The challenge of developing new methods, baptized Metaheuristics, which are better able to solve difficult problems, still attracts the interests of current researchers. Metaheuristic optimization is therefore a field of growing interest since a single metaheuristic optimization algorithm, which can solve all optimization problems of different types and structures, does not exist.

The metaheuristic optimization algorithms use two basic strategies while searching for the global optimum: exploration and exploitation [3]. The exploration process succeeds in enabling the algorithm to achieve the best local solutions within the search space, whereas the exploitation process expresses the ability to reach the global optimum solution around the obtained local solutions.

A metaheuristic algorithm must have some characteristics such as [4]: it must be able to reach rapidly the global optimum solution; the total calculation amount and the run-time required to reach the optimum must be acceptable for practical applications. The algorithmic structure of a metaheuristic has also to be simple enough to allow its easy adaptation to different problems. Besides, it is desired that the metaheuristics have very few algorithmic control parameters excluding the general ones like total Number of iterations or the size of the population (for the population based optimization algorithms).

There are a wide variety of metaheuristics and a number of properties allowing their classification. One classification dimension is single solution vs. population-based [5]: Single solution approaches focus on modifying and improving a single candidate solution such as Simulated Annealing (SA) and Tabu Search Algorithm (TSA). Whereas population-based approaches maintain and improve multiple candidate solutions such as Genetic Algorithms (GA) and Cuckoo Search Algorithm (CSA).

Several comparisons of the efficiency of metaheuristic algorithms have been published [6-11]: It has been shown that TSA represents one of the most efficient heuristic techniques to find good quality solutions in a short running time compared to population-based algorithms such as GA or Ant Colony Optimization (ACO) [12, 13]. It has been shown also that CSA gave superior results compared to GA, Particle Swarm Optimization (PSO) and Artificial Bee Colony (ABC) [4, 14-15].

In this paper, we applied therefore CSA and TSA for optimizing eight standard test functions with diverse

properties: modality, separability, and valley landscape to analyze their effectiveness in terms of solution quality and runtime. We then compared the both metaheuristics to the novel algorithm combining TSA and Nelder-Mead Simplex minimizer.

This paper is organized as follows: Section 2 describes the principles of the applied algorithms: CSA, TSA and Simplex algorithm as well as the test functions. In Section 3, we analyze and compare the results obtained in terms of run-time and solution quality. Section 4 concludes this paper.

2 Material and Method

2.1 CUCKOO SEARCH ALGORITHM

CSA is a novel population based stochastic search metaheuristic proposed by Yang and Deb in 2009 [16-18]. It is inspired by a natural mechanism; the parasitic breeding behavior of some cuckoo species that lay their eggs in the nests of host birds. Therefore, a pattern corresponds to a nest and similarly each individual attribute of the pattern corresponds to a cuckoo egg and the latter represents a new solution. In each computation steps, the new and potentially improved solutions replace the worse solutions (eggs in the nests).

CSA can be briefly described using the following three rules [17-19]:

1. Each cuckoo lays one egg at a time and dumps it in a randomly chosen nest.
2. Best nests with high quality of eggs will be passed to the next generations.
3. The number of available host nests is fixed, and a host bird can discover a foreign egg with a probability pa. In this case, the host bird can throw the egg away or abandon the nest and build a new one in a new location.

We have chosen this population based stochastic global search metaheuristic algorithm because it has been shown that CSA is superior with respect to GA, PSO and ABC [12-14]. Besides, several studies indicate that Cuckoo Search is a powerful algorithm and successful results have been achieved in various applications such as manufacturing optimization [20], physically - based runoff - erosion model [21] Query Optimization [22], Training Artificial Neural Networks [23] and PCB (Printed Circuit Boards) Drill Path Optimization [19] as well as Performing Phase Equilibrium Thermodynamic Calculations [15].

Although this metaheuristics is novel, many improvements are proposed in the literature such as ICS (acronyms of Improved Cuckoo Search) which is proposed to enhance the accuracy and the convergence rate of this algorithm [24]. In this version, a proper strategy for tuning the cuckoo search parameters is used instead of keeping these parameters constant.

Another modified cuckoo search algorithm is also presented in [25]: the authors implemented a CSA version where the step size is determined from the sorted, rather than only permuted fitness matrix.

In exploring the search space, Yang and Deb discovered that the performance of the CSA could be significantly improved by using Lévy Flights instead of simple random walk [18] since Lévy Flight can maximize the efficiency of

resource searches in uncertain environments. For this reason, we have selected this version of the CSA algorithm. In the other hand, this CSA version has outperformed both GA and PSO for all the test functions used in [16-17].

The different steps of the CSA implemented in our work (the minimization of test functions) can be summarized in the following flow chart [16-19].

In its original version, CSA is proposed for continuous problems; however, it can be extended for combinatorial discrete optimization problems [19, 26]. It can also be combined with others metaheuristics such as TSA [22], Scatter Search [23] and Greedy Randomized Adaptive Search Procedure (GRASP) [27].
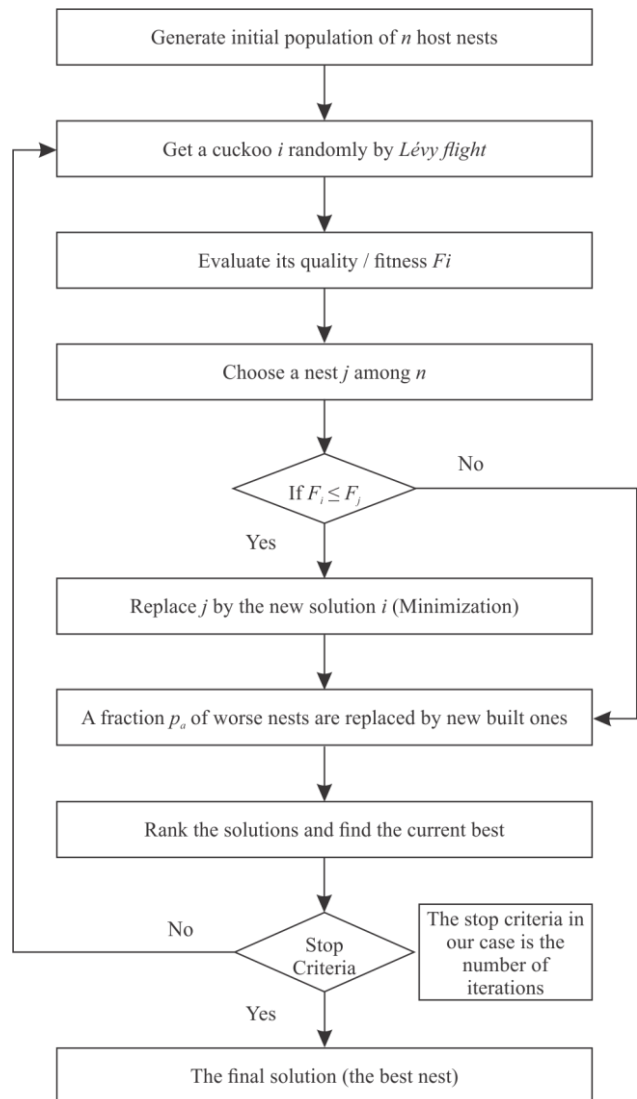
FIGURE 1 Flow Chart of CSA

2.2 TABU SEARCH ALGORITHM

TSA was first proposed by Fred Glover in 1986 [28]. It is inspired by human memory. It is so called because it avoids returning to recently visited solutions. At each iteration, the best neighbor is selected as a current solution. To avoid cycles, i.e.; the infinite repetition of a sequence of movements, the L latest movements are forbidden (L is the length of the tabu list, which is a short-term memory. It contains the best

conformations already visited). Then, the selected movements must be the best ones and not in the tabu list.

Although it might seem simple to reject a solution to a discrete combinatorial problem if it appears in the tabu list, this is not the case for continuous problems.

As for other metaheuristics, a random candidate solution within a neighborhood can be defined. If this solution has an objective value higher than the current solution (minimization), the decision whether to accept it or not is based on the content of the tabu list. However, rather than checking if the solution is already tabu it should be checked if the solution is within a certain distance of a solution in the tabu list [29]. A TSA with this property is called Enhanced Continuous Tabu Search (ECTS) [30].

ECTS is proposed for the global optimization of multi-minima functions, it results from an adaptation of combinatorial TSA that aims to follow Glover's basic approach as closely as possible. In order to cover a wide domain of possible solutions, this algorithm first performs the diversification: it locates the most promising areas, by fitting the size of the neighborhood structure to the objective function and its definition domain. For each located promising area, the algorithm continues the search by intensification within one promising area of the solution space.

The flow chart presented on Figure 2 outlines the different steps of the ECTS used in our work.

We have chosen this variant for its advantages [30]: first, its principle is rather basic, directly inspired from combinatorial Tabu Search. Secondly, the authors tested and compared the efficiency of ECTS to other published versions of Continuous Tabu Search and to some alternative algorithms like Simulated Annealing. The results revealed that ECTS showed a good performance for functions having a large number of variables.
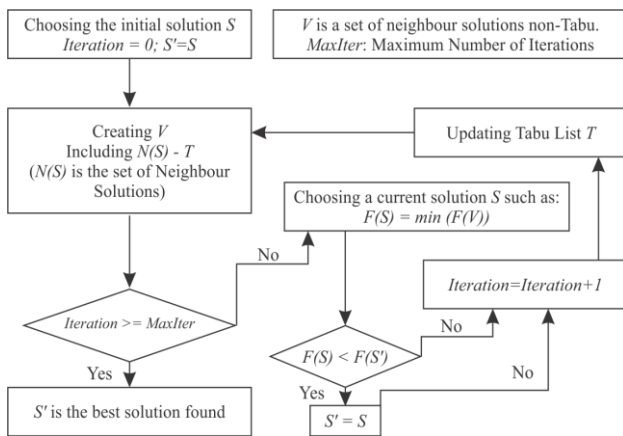
FIGURE 2 Flow Chart of TSA

Among the neighbourhood search methods, TSA is considered as one of the most prominent, being widely used and providing a powerful approach for solving a large range of optimization problems [31]. TSA, which also has the advantage that only function values are used, (differentiability and continuity being not required), is characterized by the use of "memories" during the search [32]. Additionally, TSA needs fewer parameters to be adjusted than the SA algorithm. Unlike other metaheuristics, TSA is not trapped in local minimum [29].

TSA is subject to several developments such as: Directed Tabu Search (DTS), which is a continuous TSA [33]. The

Memory Models are also introduced in order to improve Tabu Search with real continuous variables [34].

2.3 SIMPLEX ALGORITHM

The Nelder-Mead minimization method [35] is based on the comparison of function values at $n+1$ vertices of a general simplex. The simplex adapts itself via Reflection, Expansion as well as Contraction operations by replacing the vertex with the highest value by another point with lower value.

Figure 3 illustrates the principle of the Nelder–Mead Simplex algorithm.

(a) Reflect Transformation   (b) Expand Transformation

(c) Contract Outside Transformation   (d) Contract Inside Transformation

(e) Shrink

FIGURE 3 Nelder–Mead Simplex Algorithm's Principle

We have opted for the Nelder–Mead Simplex algorithm because it is a classical very powerful local descent algorithm, making no use of the objective function derivatives [36].

An overview of the algorithm is outlined in Figure 4 [37-38]:
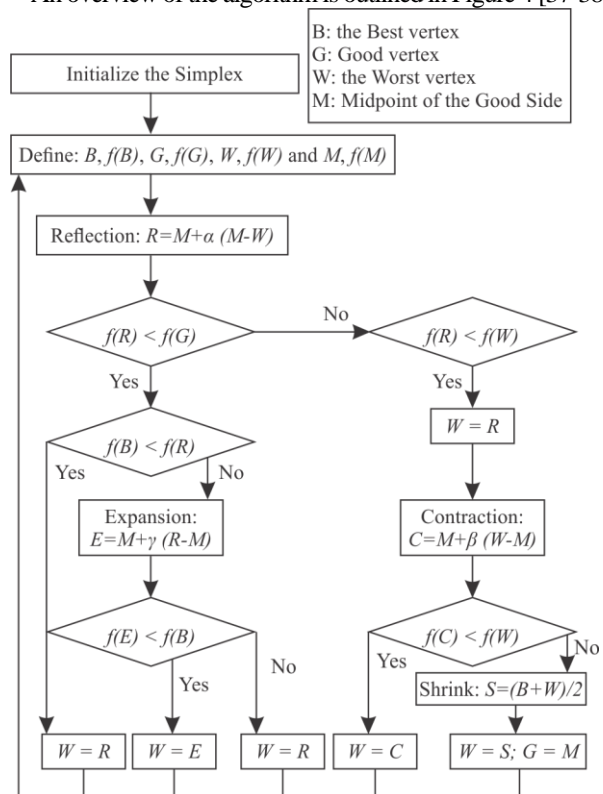
FIGURE 4 Flow Chart of Nelder-Mead Simplex Algorithm

25

2.4 HYBRID TSA-SIMPLEX ALGORITHM

In spite of the numerous advantages of the Tabu Search, it might not find a near-optimal solution for some problems, especially continuous ones [29], but it can find several good starting points for local search. For this reason, and in order to improve TSA effectiveness, we have applied the Nelder-Mead minimization to the TSA solutions. Therefore, the initial simplex is composed of the TSA solutions.

We have opted for the combination of these algorithms because many comparisons are made in this way. These comparisons concluded that hybrid search algorithms gave superior results compared with any of the algorithms tested individually [39-41].
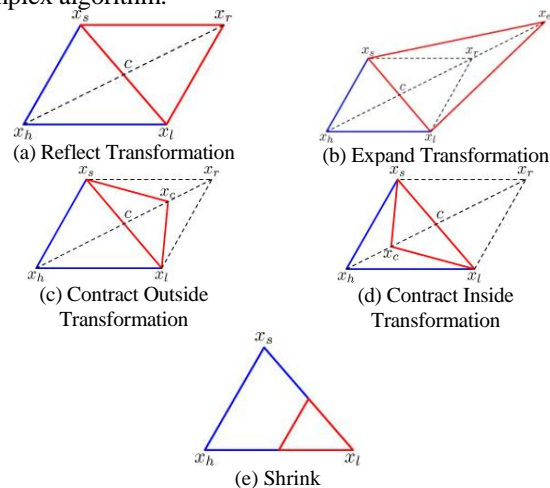
2.5 TEST FUNCTIONS

Test functions are important to validate new optimization algorithms and to compare the performance of various algorithms. There are many test functions in the literature [42-45], but there is no standard list or set of benchmark functions to be followed.

In order to make sure whether the tested algorithms can solve certain types of optimization efficiently, test functions should have diverse properties. So, we select a list of eight test problems usually used for checking the properties of the optimizers.

The details of the continuous test functions used in our work are summarized in the following table 1.

TABLE 1 Test Functions

Beale Function (Non-Separable, Non-Scalable and Unimodal)	
	Search Space: [-4.5;4.5]
$f_1(x,y) =(1.5-x+xy)^2 +(2.25-x+xy^2)^2+ (2.625-x+xy3)^2$	
	Global Minimum: $f_1(3 ;0.5)=0$
De Joung (or DJ) Function (Separable, Scalable, Unimodal)	
	Search Space: [-5.12;5.12]
$f_2(x,y) = x^2+y^2$	
	Global Minimum: $f_2(0 ;0)=0$
Goldstein and Price (or GP) Function (Non-Separable, Non-Scalable and Multimodal)	
$f_3(x,y)=[1+(x+y+1)^2 \times (19-14x+3x^2-14y+6xy+3y^2)] \times$	Search Space: [-2;2]
$[30+(2x-3y)^2 \times (18-32x+12x^2+48y-36xy+27y^2)]$	
	Global Minimum: $f_3(0 ;-1)=3$
Himmelblau Function (Non-Separable, Non-Scalable, and Multimodal)	
	Search Space: [-6;6]
$f_4(x,y) = (x^2+y-11)^2 + (x+y^2- 7)^2$	
	Global Minimum: $f_4(3 ;2)=0$
Matyas Function (Non-Separable, Non-Scalable and Unimodal)	
	Search Space: [-10;10]
$f_5(x,y) =0.26(x^2+y^2) - 0.48xy$	
	Global Minimum: $f_5(0 ;0)=0$
Rastrigin Function (Separable, Scalable and Multimodal)	
	Search Space: [-5.12;5.12]
$f_6(x,y) = 20 + (x^2-10 \cos(2\pi x)) + (y^2-10*\cos(2\pi y))$	
	Global Minimum: $f_6(0 ;0)=0$
Rosenbrock Function (Non-Separable, Scalable and Unimodal)	
	Search Space: [-10;10]
$f_7(x,y) =100(x^2-y)^2 + (x-1)^2$	
	Global Minimum: $f_7(1 ;1)=0$
Step Function (Separable, Scalable and Unimodal)	
	Search Space: [-100;100]
$f_8(x,y) = (x+0.5)^2 + (y+0.5)^2$	
	Global Minimum: $f_8(0.5;0.5)=0$

These functions have diverse properties in terms of modality, separability and valley landscape: According to [46], the modality of a function corresponds to the number of ambiguous peaks in the function landscape. If these peaks are encountered during an exploration process, there is a tendency that the algorithm may be trapped in one of such peaks. This will have a negative impact on the search process, since it can direct the search away from the true optimal solutions. So, a function with more than one local optimum is called multimodal. These functions are used to test the ability of an algorithm to escape from any local minimum.

Another test problem is formulated by separable and non-separable functions [46]. The dimensionality of the search space is an important issue with the problem. In general, separable functions are relatively easy to optimize, when compared with their inseparable counterpart, because each parameter of a function is independent of the other parameters. If all the variables are independent, then we can perform a sequence of n (n being the number of independent variables) independent optimization processes.

Finally, a valley occurs when a narrow region of little change is surrounded by areas of steep descent [46] (this region attracts the minimizers). The progress of a search process of an algorithm may be slowed down significantly on the floor of the valley. Functions with flat surfaces pose a difficulty for the algorithms, as the flatness of the function does not give the algorithm any information to direct the search process towards the minima.

3 Experiment

To verify the reliability of the CSA, TSA and Nelder-Mead Simplex algorithms, several well-known test functions as shown in table 1 are considered.

The parameters of the CSA, TSA and Simplex algorithms used in our experiments are given in the table 2 below.

TABLE 2 The parameters of the CSA, TSA and Simplex Algorithms

Algorithm	Parameters	
CSA	Number of Nests	= 25
	Discovery Rate	= 0.25
TSA	Tabu List Length	= 10
	Neighborhood Size	= 10
Simplex	Alpha	= 1.0
	Beta	= 0.5
	Gamma	= 2.0

We have executed each algorithm for 1000, 10000 and 100000 iterations. The table 3 shows the run times of the algorithms CSA, Simplex and TSA for 1000 iterations.

TABLE 3 The Run-time of CSA, TSA and Simplex Algorithms

Function	Algorithm	Run-time (seconds) for 1000 Iterations
f_1	CSA	0.181127
	TSA	999.355000
		0.004000
f_2	CSA	0.174693
	TSA	999.476000
	Simplex	0.002000
f_3	CSA	0.153440
	TSA	999.185000
	Simplex	0.0000000
f_4	CSA	0.384832

	TSA	999.486000
	Simplex	0.002000
f_5	CSA	0.137662
	TSA	999.496000
	Simplex	0.001000
f_6	CSA	0.258002
	TSA	999.363000
	Simplex	0.003000
f_7	CSA	0.422266
	TSA	1001.631000
	Simplex	0.003000
f_8	CSA	0.203946
	TSA	999.305000
	Simplex	0.001000

From this table, we can note that the simplex algorithm is the best in terms of running time and the TSA is the slowest algorithm. These findings remain true even for 10000 and 100000 iterations.

We have then executed each algorithm ten times for each benchmark function. The following table 4 shows the experimental results of the comparative performances in terms of best, worst and average solutions between the Cuckoo Search and Tabu Search Algorithms.

TABLE 4 Best, Worst and Average Solutions of CSA and TSA

Test function	CSA			TSA		
	Best	Worst	Average	Best	Worst	Average
f_1	0.00099507	0.1729	0,0420371609	0.003130	9.819423	1,3011135
f_2	0,0003587200	0,0032968000	0,0012535720	0,0000010000	0,0001410000	0,0000360909
f_3	3,0121	4,9408	3,93157	3,000088	97,698648	38,0309893
f_4	0,007139	0,10514	0,0340206	0,000055	0,021961	0,0043994
f_5	0,0000652940	0,0066796000	0,0024487004	0,0003460000	0,0355960000	0,0172967000
f_6	0,0966590000	1,9902000000	0,9387889000	0,0001740000	0,0189600000	0,0041338000
f_7	0,0332870000	1,4028000000	0,5478952000	0,0124640000	3,8449870000	1,0535761000
f_8	0,12119	2,5204	0,87182667	0,0019300000	0,0195940000	0,0111310909

From the table 4 above, we can note that TSA is more efficient since TSA solutions are better than the CSA ones for six functions. However, TSA is slower than CSA.

Besides, we can note that CSA is better for Non-Separable, Non-Scalable and Unimodal functions (Beale and Matyas functions).

In order to improve the TSA run-time, we have executed

the hybrid algorithm TSA-Simplex: we first execute the TSA for only 10 iterations. We have then applied the Nelder-Mead minimization (1000 iterations) to the TSA solutions. Therefore, the initial simplex is composed of the TSA solutions.

The following table 5 shows the results of this combination.

TABLE 5 TSA-Simplex Results

Test function	Best	Worst	average	Runtime average
f_1	0,0000000000	0,1651646790	0,0337103523	9,90962
f_2	0,0000000000	0,00077629	0,000077629	9,90236
f_3	3,0000000000	30,1994131088	14,2549998587	9,9053
f_4	0,0000000000	0,0062818	0,00155021	9,90369
f_5	0,0000000000	0,01367587	0,00136759	9,90418
f_6	0,0000000000	0,00019708	0,000022294	9,90489
f_7	0,0000000000	3,13065288	0,77918326	9,90416
f_8	0,0000000000	0,00650235	0,00103485	9,90568

The table 5 above shows obviously that the hybrid algorithm finds the exact solution to all the benchmark functions even in acceptable run-time. These findings remain true even when minimizing functions with 3, 4 and 5 dimensions (3, 4 and 5 variables instead of 2) for all benchmarks used in our work.

4 Conclusion

In this study, we have selected three metaheuristic

algorithms: CSA, TSA and Simplex method for the test of eight difficult optimization functions with diverse properties: modality, separability, and valley landscape to analyze their effectiveness in terms of solution quality and runtime. The functions were systematically optimized by the different metaheuristics and the results were tracked and compared.

The results show clearly that TSA is more reliable than CSA since the best TSA solutions are better than the CSA ones in 6 functions (f_2, f_3, f_4, f_6, f_7 and f_8) among 8 (see table 4), whereas CSA is faster than TSA (see table 3). Note also

that CSA gives good results for Non-Separable, Non-Scalable and Unimodal functions (f_1, f_5).

To improve the runtime of the TSA, we have combined it with simplex algorithm (as it has the best run-time). The hybrid algorithm is the more reliable as it successfully optimized all functions and found the global minima for each one within reasonable run-time.

With regard to the future, we believe that the application of these metaheuristics to solve real-world problems such as molecular docking is promoting [47-51]. On the other hand, the CPU time could be drastically reduced by using a parallel version of these metaheuristics [52-54] that could be easily implemented on GPUs (Graphical Processing Units).

References

[1] Grebner C 2012 New Tabu Search Algorithms for the Exploration of Energy Landscapes of Molecular Systems *WÜRZBURG*

[2] Tuba M, Subotic M, Stanarevic N 2011 Modified cuckoo search algorithm for unconstrained optimization problems *Proceedings of the European Computing Conference, Paris*

[3] Rashedi E, Nezamabadi-pour H, Saryazdi S 2009 GSA: A Gravitational Search Algorithm *Information Sciences* **179** 2232–48

[4] Civicioglu P, Besdok E 2011 A conceptual comparison of the Cuckoo-search, particle swarm optimization, differential evolution and artificial bee colony algorithms *Artif Intell Rev* DOI 10.1007/s10462-011-9276-0

[5] Layeb A 2009 *Introduction aux métaheuristiques* Université Mentouri de Constantine

[6] Bajeh A O, Abolarinwa K O 2011 Optimization: A Comparative Study of Genetic and Tabu Search Algorithms *International Journal of Computer Applications* (0975-8887) **31**(5)

[7] Kannan S, Slochanal S M R, Padhy N P 2005 Application and Comparison of Metaheuristic Techniques to Generation Expansion Planning Problem *IEEE Transactions on Power Systems* 20(1)

[8] Madić M, Marković D, Radovanović M 2013 Comparison of MetaHeuristic Algorithms for Solving Machining Optimization Problems *Facta Universitatis Series: Mechanical Engineering* **11**(1) 29-44

[9] Silberholz J, Golden B 2010 *Comparison of Metaheuristics* University of Maryland

[10] Azimi Z N 2004 Comparison of Metaheuristic Algorithms for Examination Timetabling Problem *J. Appl. Math. & Computing* **16**(1-2) 337-54

[11] Arora T, Gigras Y 2013 A Survey of Comparison between Various Metaheuristic Techniques for Path Planning Problem *International Journal of Computer Engineering & Science*

[12] Pirim H, Bayraktarn E, Eksioglu B 2008 Tabu Search: A Comparative Study *Wassim Jaziri* ISBN 978-3-902613-34-9, 278 I-Tech, Vienna, Austria

[13] Pappas C, Srinivasan R K, Barnes J W, Sarkar S 2004 *A Comparison of Heuristic, Meta-Heuristic and Optimal Approaches to the Selection of Conservation Area Networks* University of Texas at Austin

[14] Sangita Roy, Sheli Sinha Chaudhuri 2013 Cuckoo Search Algorithm using Lèvy Flight: A Review *I.J. Modern Education and Computer Science* **12** 10-5

[15] Seif-Eddeen K Fateen, Bonilla-Petriciolet A 2014 On the Effectiveness of Nature-Inspired Metaheuristic Algorithms for Performing Phase Equilibrium Thermodynamic Calculations *The Scientific World Journal*

[16] Yang X-S, Deb S 2010 Engineering Optimisation by Cuckoo Search *Int. J. Mathematical Modelling and Numerical Optimisation* **1**(4) 330–43

[17] Yang X-S, Deb S 2009 Cuckoo search via Lévy flights *Proc. of World Congress on Nature & Biologically Inspired Computing (NaBIC 2009), December 2009, India. IEEE Publications, USA* 210-4

[18] Yang X-S 2010 *Nature-Inspired Metaheuristic Algorithms Second Edition* Luniver Press

[19] Wei Chen Esmonde Lim, Kanagaraj G, Ponnambalam S G 2014 PCB Drill Path Optimization by Combinatorial Cuckoo Search Algorithm *Scientific World Journal* Article ID 264518 http://dx.doi.org/10.1155/2014/264518

[20] Syberfeldt A, Lidberg S 2012 Real-World Simulation-Based Manufacturing Optimization using Cuckoo Search *WSC Simulation Conference*

[21] Santos C A G, Freire P K M M, Mishra S K 2012 Cuckoo Search via Lévy Flights for Optimization of a Physically - Based Runoff - Erosion Model *Journal of Urban and Environmental Engineering (JUEE)* **6**(2) 123-31

[22] Mukul Joshi, Praveen Ranjan Srivastava 2013 Query Optimization: An Intelligent Hybrid Approach using Cuckoo and Tabu Search *International Journal of Intelligent Information Technologies* **9**(1) 40-55

[23] Al-Obaidi A T S 2013 Improved Scatter Search Using Cuckoo Search *IJARAI - International Journal of Advanced Research in Artificial Intelligence* **2**(2)

[24] Ehsan Valian, Shahram Mohanna, Saeed Tavakoli 2011 Improved Cuckoo Search Algorithm for Global Optimization *International Journal of Communications and Information Technology, IJCIT*

[25] Tuba M, Subotic M, Stanarevic N 2012 Performance of a Modified Cuckoo Search Algorithm for Unconstrained Optimization Problems *WSEAS Transactions on Systems* E-ISSN: 2224-2678 **11**(2)

[26] Gherboudj A 2013 *Méthodes de résolution de problèmes difficiles académiques* Université de Constantine **2**

[27] Hongqiang Zheng, Yongquan Zhou, Qifang Luo: 2013 A hybrid Cuckoo Search Algorithm-GRASP for Vehicle Routing Problem *Journal of Convergence Information Technology (JCIT)* **8**(3)

[28] Glover F 1990 *Tabu Search: A Tutorial* University of Colorado

[29] Schulz P G 2006 *Creative Design in Optimization Metaheuristics Applied to Multi-modal Continuous Functions* Kongens Lyngby

[30] Chelouah R, Siarry P 2000 Tabu Search applied to global optimization *European Journal of Operational Research* **123** 256-70

[31] Py Y 2008 Local Search Techniques: Focus on Tabu Search *Wassim Jaziri Ed.* ISBN 978-3-902613-34-9 278

[32] Morales L B, Garduño–Juárez R, Aguilar–Alvarado J M, Riveros-Castro F J 2000 A Parallel Tabu Search for Conformational Energy Optimization of Oligopeptides *J Comput Chem* **21** 147–56

[33] Hedar A, Fukushima M 2006 Continuous Optimization: Tabu Search directed by direct search methods for nonlinear global optimization *European Journal of Operational Research* **170** 329–49

[34] Connor D A M 2006 Memory Models for Improving Tabu Search with Real Continuous Variables *Proceedings of the Sixth International Conference on Hybrid Intelligent Systems*

[35] Nelder J A, Mead R 1965 A Simplex method for function minimization *The Computer Journal*

[36] Chelouah R, Siarry P 2005 A hybrid method combining continuous tabu search and Nelder–Mead simplex algorithms for the global optimization of multiminima functions *European Journal of Operational Research* **161** 636-54

[37] Mathews J H, Fink K K 2004 *Numerical Methods Using Matlab* Prentice-Hall Inc. Upper Saddle River, New Jersey USA, ISBN: 0-13-065248-2

[38] Tomick J J 1995 *On convergence of the Nelder-Mead Simplex algorithm for unconstrained stochastic optimization* The Pennsylvania State University

[39] Hou T J, Wang J M, Xu X J 1999 A Comparison of Three Heuristic Algorithms for Molecular Docking *Chinese Chemical Letters* **10**(7) 615–8

[40] Koduru P, Das S, Welsh S M 2006 A Particle Swarm Optimization-Nelder Mead Hybrid Algorithm for Balanced Exploration and Exploitation in Multidimensional Search Space *Proceedings of the ICAI - International Conference on Artificial Intelligence, Las Vegas, Nevada, USA*

[41] Mashinchi M H, Orgun M A, Pedrycz W 2011 Hybrid optimization with improved tabu search *Applied Soft Computing* 1993-2006

[42] Molga M, Smutnicki C 2005 Test functions for optimization needs

[43] Andrei N 2008 An Unconstrained Optimization Test Functions Collection *Advanced Modeling and Optimization* **10**(1)

[44] Yang X S 2010 *Test Problems in Optimization* Department of Engineering, University of Cambridge, UK

[45] Adorio E P 2005 *MVF - Multivariate Test Functions Library in C for Unconstrained Global Optimization* Department of Mathematics U.P. Diliman

[46] Jamil M, Yang X S 2013 A Literature Survey of Benchmark Functions For Global Optimization Problems *Int. Journal of Mathematical Modelling and Numerical Optimization* **4**(2), 150–94

[47] Huang S Y, Zou X 2010 Review Advances and Challenges in Protein Ligand Docking *International Journal of Molecular Sciences*

[48] Kitchen D B, Decornez H, Furr J R, Bajorath J 2004 Docking and Scoring in Virtual Screening for Drug Discovery: Methods and Applications *Nature Reviews*

[49] Sousa S F, Fernandes P A, Ramos M J 2006 *Protein–Ligand Docking: Current Status and Future Challenges* Université de Porto-Portugal

[50] Huang S Y, Grinter S Z, Zou X 2010 Scoring functions and their evaluation methods for protein–ligand docking: recent advances and future directions *Phys. Chem. Chem. Phys.* **12** 12899–908

[51] Wardono B, Fathi Y 2004 A tabu search algorithm for the multi-stage parallel machine problem with limited buffer capacities *European Journal of Operational Research*

[52] Fiechter C N 1994 A parallel tabu search algorithm for large traveling salesman problems *Discrete Applied Mathematics*

[53] Matsumura T, Nakamura M, Tamaki S 2000 *A Parallel Tabu Search and Its Hybridization with Genetic Algorithms* University of the Ryukyus, Japan

AUTHORS

Khensous Ghania, **17.01.1981, Oran - Algeria**

Current position, grades: Ph.D. Computer Sciences student at the USTO-MB University (Université des Sciences et de la Technologie d'Oran- Mohamed BOUDIAF); Assistant Lecturer at Ecole Normale Supérieure d'Oran (ENSO), Algeria.
Scientific interest: Optimization, Bioinformatics, Artificial Intelligence.

Messabih Belhadri, 1958, Oran - Algeria

Current position, grades: Senior Lecturer at the USTO-MB University, Oran- Algeria.
Ph.D. degree in Computer Sciences from the University of Paris 7, France, in 1997.

Chouarfia Abdellah, 1955, Mostaganem - Algeria

Current position, grades: Professor at the USTO-MB University, Oran- Algeria.
Ph.D. degree in software engineering from the University Paul Sabatier of Toulouse France in 1983.

Maigret Bernard, 1944, Nancy - France

Current position, grades: Emeritus Research Director at CNRS - France.
Ph.D. degree in theoretical physique from the University of Paris, France in 1976.
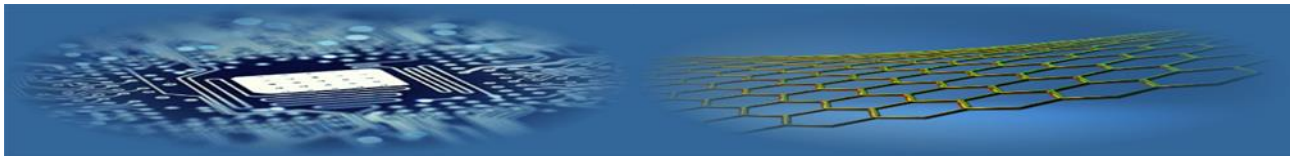
Handwritten offline Hindi character recognition using advanced feature extraction techniques

Dayashankar Singh[1*], J P Saini[2], D S Chauhan[3]

[1]*Assistant Professor, Deptt. of CSE MMMUT, Gorakhpur (UP), India*
[2]*Professor, Deptt of ECE BIET, Jhansi, India*
[3]*Vice-Chancellor GLA University Mathura (UP), India*

Corresponding author: dss_mec@yahoo.co.in

Abstract

Feature extraction technique plays an important role in character recognition since last so many years. In this paper, two advanced feature extraction techniques namely 16-Directional Gradient Feature Extraction Technique (16-DGFET) and 24-Directional Gradient Feature Extraction Technique (24- DGFET) have been proposed and implemented. This paper demonstrates the concept of Handwritten Hindi Character Recognition (HCR), feature extraction mechanisms adopted for character recognition starting from Conventional Feature Extraction Technique (CFET), Gradient Feature Extraction Technique (GFET), and Directional Gradient Feature Extraction Technique (DGFET). In DGFET, few techniques have been initiated which involve dividing the gradient values to 8/16 directional values, these techniques attained recognition accuracy of around 94%. We have aimed at further splitting of the gradient values in 24 parts in order to find if it achieves the objective of increasing the performance of character recognition with more accurate analysis and acceptable training time. An experimental evaluation and comparative analysis have been made at the end of the paper to prove the result whether further splitting is providing a better result in comparison to 8 or 16 parts division taking in account the training time, the accuracy of recognition and performance appraisal. The network used here is Multilayer Perceptron (MLP) with Error Back Propagation (EBP) algorithm to train the network.

A sample of count 1000 has been taken for experimentation including the personnel of different age groups involving both male and female handwriting. A comparative synthesis is made for 8/16-Directional and 24-Directional input values comparing the recognition performance and training time.

1 Introduction

Artificial Neural Network has its effective implementation in certain areas due to its application potentials; Character Recognition is one among them, character recognition being an area of pattern recognition aims at feature extraction to identify the character samples.

Many efforts have been applied in scientific scenario for the development of an effective recognition system which could effectively identify and analyse the entity, object or characters. Identifying a typed/printed character is easy while handwritten character recognition raises a difficulty because every individual has its own style of writing including its size, style and orientation angle. A number of works have been reported for character recognition of languages such as English, Chinese, Japanese, Arabic, etc. but only a few attempts have been made for resolution of Hindi Character aiming at Handwritten Hindi Character Recognition. In this paper, a MLP network has been used featured with Advanced Feature Extraction, with neurons trained with EBP algorithm to obtain offline recognition of handwritten Hindi Characters. Feature Extraction Mechanisms which have been implemented in this paper are Directional Values Gradient Feature Extraction with splitting of gradient values into 16 and 24 parts/directions

respectively. [13 - 15]

While application of 8-DGFET, the performance obtained is 95% and when applied with 16-DGFET the accuracy performance raised to 96% with a little rise in training time. The work aims at further dividing it in 24 parts and then analysing the network performance in recognizing the character. On further division in 24 sectors, the result found that there was a slight enhancement in performance accuracy i.e. 97% with a great rise in training time of neurons which could be considered ineffective. As while developing a character recognition system both performance accuracy and little training time serve as essential parameters. The network architecture that considers the input layer and the number of hidden and output layer and training algorithm is also considered while deriving the conclusion.

The organization of paper is as follows- Section II provides a background study of neural network, the language selected, the training methods, the training algorithm used with specifying the reason of its adoption. Section III discusses the pre-requisites to perform the recognition, operation to be performed before application to the neural network for training. Section IV highlights several mechanisms discussed so for character recognition.

Section V provides comparison of 8 Directional, 16-

Directional and 24- Directional Gradient Feature Extraction mechanism defining which scheme proves to be effective in achieving the Character Recognition objectives with consideration of training time of neuron.

2 Research background

2.1 HINDI LANGUAGE

Hindi, the national language of India is the second most widely spoken language of India. It is being used as an official language in various Government offices and sectors which include banks, sales tax offices, Railway, Passport office, Embassy, etc. Around 40 million people speaks Hindi language all over India, especially by the north Indians. The characters involve 13 vowels and 36 consonants directing from left to right. [1]
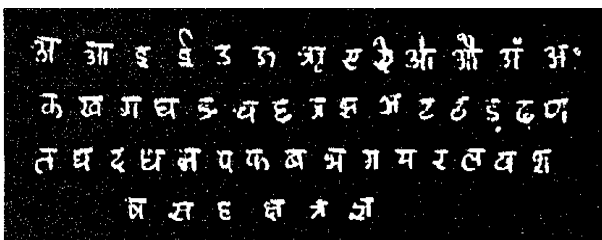

FIGURE 1 Hindi Characters of alphabet [1]

2.2 NEURAL NETWORK

A Neural Network can be defined as a highly-interconnected network with a number of processing elements termed as neurons, having the ability to gain knowledge which could be used for further future applications. The inspiration on these parallel processing elements is attained from the biological neurons.

2.3 FEATURE EXTRACTION

Feature Extraction is an essential component in Pattern/ Character Recognition. It aims at finding an appropriate mapping for the characters reducing the dimension of the pattern. The neural network here is incorporated with advanced mechanism for feature Extraction with several methods for it. Edge detection, Boundary detection, etc. are also some methods for Character Recognition.

The Hindi Character recognition follows the following steps:
- Sample acquisition
- Pre-processing operations including image thinning, compression, Skeletonization and normalization
- Directional Gradient Feature Extraction
- Classification and Recognition

2.4 TRAINING MECHANISM

A neural network is trained to perform certain applications. The network training involves feeding the input vectors into the system and performing weight adjustments to obtain the desired output/target vector.

The learning or training mechanism includes- Supervised Training, Unsupervised Training, and Reinforcement training.

Supervised Training: Supervised training involves an assumption of teacher during training aiming to minimize the error between the desired output and attained output. The input vector and the target vector are together termed as training pair. Generally, a network requires several such training pairs. Every time a result is obtained on application of input vector is matched with the desired output. If it not, the weight is manipulated and again fed to the network tending to minimize the error. This continues until a result is obtained with error potentially low [7, 8].
- Unsupervised Learning: Involves no pre-feeding of output vector. The only provided value is the input vector thus no comparison could be made to determine the correctness of the result obtained. The training is performed to the time the system is found to obtain a consistent result. The network here tries to learn on its own. [7, 8]
- Reinforcement Learning: The learning performed based on rewards or criticism is Reinforcement learning. If positive or reward defines a good training and in case of criticism is regarded as error or inappropriate output. [7, 8]

2.5 PERCEPTRON

The architecture of neural network consists of several neurons to which input are provided such that each input "x_i" is multiplies to its respective weight "w_i". The result is summed up using Σ unit. The output is then compared with the predefined threshold value and if is found greater is set to 1 otherwise the value is taken 0. The perceptron learning is categorized under supervised learning. It can be a single layer model or multi-layer model comprising of several hidden layers. In the present word, we have taken 2 hidden layers. The number of neurons at the output layer is the number of characters to be recognized.

2.6 PERCEPTRON TRAINING ALGORITHM

This training algorithm is used to train the perceptron which involves presentation of the input pattern one at a time and adjusting the weights to minimize the error raising the accuracy. "Delta Rule" is a generalized perceptron training algorithm to train the neurons. Δ provides the difference between target output "T" and the obtained output "A" i.e. $\Delta = T-A$.

In case $\delta=0$, means no training us required and the attained output is the desired output. In other cases, training is required. Each input is multiplied with its respective weights and a learning coefficient η is multiplied to the product to control the average weight change. Accordingly, the weight is adjusted by applying the formula: $W_{i+1}= W_i + \Delta$.

2.7 ERROR BACK PROPAGATION ALGORITHM

The recognition performance of the network depends on the training algorithm and structure of the network. Here, in this paper have adopted Error back propagation algorithm as it provides a better training/learning rate. This network does not have any feedback connection but only requires back propagation of errors during training. The errors obtained at the output layer are the result of hidden layer errors. These

errors serve as a basis of adjustment of connecting weights interleaved between the hidden layer and the input layer. The adjustment of weight continues to the time the error is found to be below the tolerance level.

The implementation of error back propagation algorithm includes the weight updating and is biased in the direction where the performance function falls rapidly- the negative part of the gradient. The iteration is represented as $W_{n+1} = W_n - \alpha_n g_n$.

Here W_n represents the weight, α is the learning rate and g_n is the gradient value. The gradient value is calculated for each pixel and after each iteration and is compared with the threshold value. If is smaller is passed else sent for next iteration. The implementation of gradient descent algorithm takes place in two modes – Incremental mode and Batch mode. In this paper, Batch Gradient Descent (traingd) is adopted for training the network. The parameters adopted for traingd are- epoch (defining the number of iterations), show, goal, min, lr (learning rate). The lr should be neither too high nor too low. The smaller the lr the learning time will be raised and if is too high could make the algorithm unstable.

2.8 OBJECTIVE OF THE WORK

The basic objective of the paper includes:
- Directional Gradient Feature Extraction using back propagation feed forward network.
- Analysing the performance if the directional gradient feature extraction measure is further split to 24 parts ie. What will be the performance of Character Recognition if we propose 24-Directional Gradient Feature Extraction in comparison to 16-Directional Gradient Feature Extraction?
- Comparison parameters covers - Recognition performance accuracy, network training time and classification time.

3 Pre-requites of feature extraction

3.1 PRE-PROCESSING

The handwritten samples of Hindi characters are collected from several personnel including male and female of different age groups. The samples are then scanned by scanner and image is converted into binary form.

3.2 IMAGE SMOOTHENING

Smoothening of the images by removing unnecessary variations from the image is called image smoothing. These variations are the noise. Gaussian filter approach is adopted for it.

3.3 IMAGE THINNING

It is also referred as skeletonization which is applied to binary pixel image aims at removal of extra pixel that are not part of backbone of a character. This image thinning results in transformation of broad strokes of image to thin lines. [4, 6]

3.4 NORMALIZATION AND IMAGE COMPRESSION

After skeletionization of the image, normalization is done by placing the character to the top left corner of the computer screen in 30*30-pixel window. [1, 3, 6]

4 Feature Extraction Methods

4.1 CONVENTIONAL FEATURE EXTRACTION TECHNIQUE (CFET)

It involves the selection of region holding the character. The screen is taken to be of 30*30 pixels. If a line is passing through a pixel; the pixel value is taken to be 1 whereas the left pixels are assigned the value 0. This combination of pixel value is stored in the character database for every Hindi character meant for recognition purpose. In Hindi, every character holds a different font size varying person to person; hence there is a possibility that the character taken from individual for recognition has a different line. Hence this generalized method of character recognition cannot be specialized. It also requires a large storage space to hold the pixel value combination for every character. This technique requires more training time and yields less recognition accuracy. [1, 2, 12]

4.2 GRADIENT FEATURE EXTRACTION TECHNIQUE (GFET)

This method incorporates the use of **"Sobel Operator"** to obtain the gradient values for each pixel. This sobel operator is used in gradient values calculation. E.g. if the screen has resolution of 30*30, gradient value is calculated for each pixel. The sobel operator uses a horizontal or vertical template for gradient component extraction [5, 13 - 15].

Vertical Template   Horizontal Template

FIGURE 2 Sobel operator template [13 - 15]

The gradient component is evaluated using the following expression:

Horizontal Component is represented by

$$Gx = grad_v(i,j) = g(i-1,j+1) + 2g(i,j+1) +$$
$$g(i+1,j+1) - f(i-1,j-1) - \qquad , \quad (1)$$
$$2g(i,j-1) - g(i+1,j-1)$$

$$Gy = grad_h(i,j) = g(i-1,j-1) + 2g(i-1,j) +$$
$$g(i-1,j+1) - g(i+1,j-1) - \qquad . \quad (2)$$
$$2g(i+1,j) - g(i+1,j+1)$$

After obtaining the values the gradient strength and its direction can be evaluated using the formula:

$$G(i,j) = \left(grad_v^2(i,j) + grad_h^2(i,j) \right)\hat{\ } \, 0.5,$$

$$\theta = arctan\left(G_y / G_x \right)$$

4.3 DIRECTIONAL GRADIENT FEATURE EXTRACTION (8-DGFE)

Further enhancement was made in the field of feature extraction by dividing the gradient values into 8 equal parts to obtain directional value ranging from 1 to 8. For gradient value -1, the directional value was taken to be 0. The directional gradient value was calculated according to the gradient angle range.

Before calculation a padding operation was performed to transform the 30*30-pixel image to 32*32 matrixes. This padding involved the addition of 0 across the boundary of image. The pixel surrounded by 8 black pixels was assigned the gradient value -1. Next the 32*32 matrix was converted to 1024*1 matrixes and fed to feed forward neural network for character recognition.

The division was such that if angle ranged between 0-45 degrees was taken the value 1, for angle between 46-90 degree was assigned the value 2 and so on. This division can be represented as follow in the figure 3. [13, 14, 15]. The directional values can be calculated as per following table given below as table 1.

TABLE 1 Direction equivalent of gradient values

Calculated Gradient values	Equivalent Directional values
grad = -1	0
0 < = grad < 0.786	1
0.786 < = grad < 1.58	2
1.58 < = grad < 2.37	3
2.37 < = grad < 3.14	4
3.14 < = grad < 3.94	5
3.94 < = grad < 4.72	6
4.72 < = grad < 5.46	7
5.46 < = grad < 6.28	8

The division of gradient values into 8 equal parts can also be represented as follows in figure 3.
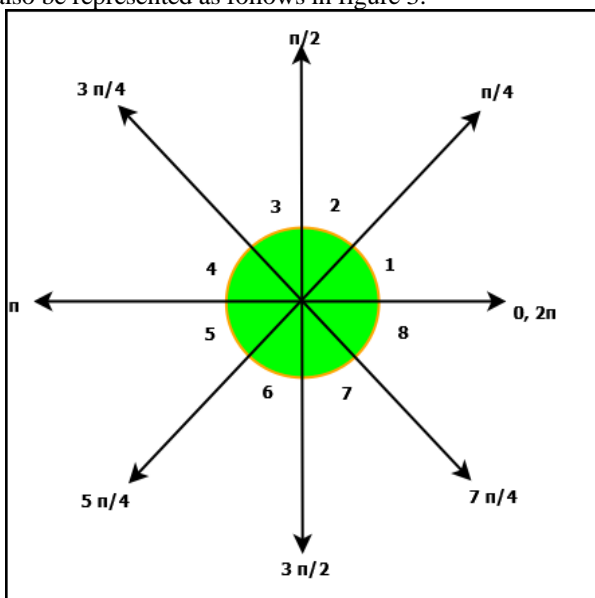

FIGURE 3 8 Directional Values equivalent to gradients

4.4 16- DIRECTIONAL GRADIENT FEATURE EXTRACTION (16-DGFE)

The image is normalized into 30 * 30 matrixes and then transformed to 32*32 matrixes by adding zeros across the boundaries. Gradient value is calculated for each pixel using the sobel operator. The same mechanism as for 8-DGFET is adopted with a difference that the gradient was partitioned to 16 equal parts. The division can be represented as in table 2 and figure 4.

The division of gradient values into 16 equal parts can also be represented as follows: For this feature extraction technique, the same parameter of training, classify have been taken as we have taken for 8-DGFET.

TABLE 2 8 directional values equivalent to gradients

Calculated Gradient values	Equivalent Directional values
grad = -1	0
0<= grad <0.395	1
0.395<= grad <0.795	2
0.795<=grad<1.19	3
1.19<=grad<1.57	4
1.57<=grad<1.97	5
1.97<=grad<2.37	6
2.37<=grad<2.76	7
2.76<=grad<3.14	8
3.14<=grad<3.55	9
3.55<=grad<3.94	10
3.94<=grad<4.33	11
4.33<=grad<4.72	12
4.72<=grad<5.12	13
5.12<=grad<5.50	14
5.50<=grad<5.89	15
5.89<=grad<6.28	16

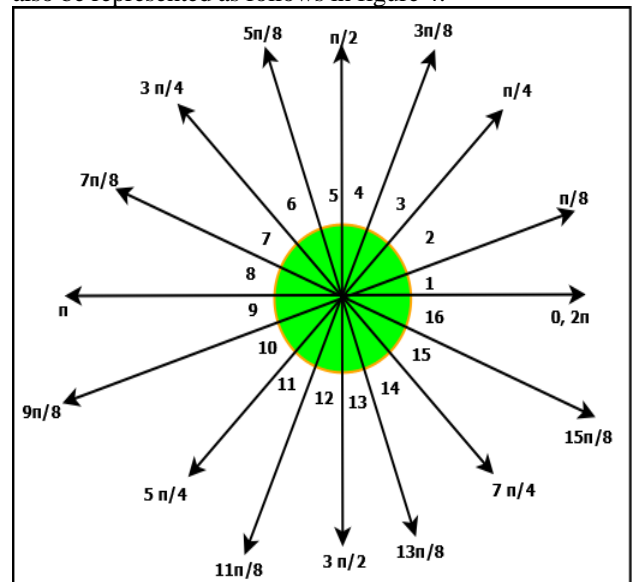The division of gradient values into 16 equal parts can also be represented as follows in figure 4.

FIGURE 4 16 Directional Values equivalent to gradients

4.5 24-DIRECTIONAL GRADIENT FEATURE EXTRACTION (24-DGFE)

The paper aims at further splitting the gradient value into 24 equal parts i.e. to the angle of 15 degree variations.

The work aims at finding that if further splitting could successfully improve the performance and accuracy of

33

character recognition with consideration to neuron training time or could result in no better or effective result. An effective approach does not compromise with the neuron training time i.e. if further splitting of gradient values is found to bring no potential difference compared to that found in 16-DGE and it consumes much training time, and then the approach cannot be considered efficient.

The mechanism remains the same with the only difference in the number of sectors partitioned. The directional value is calculated as per following table 3.

TABLE 3 24 directional values equivalent to gradients

Calculated Gradient values	Equivalent Directional values
grad=-1	0
0<=grad<0.26	1
0.26<=grad<0.52	2
0.52<=grad<0.79	3
0.79<=grad<1.05	4
1.05<=grad<1.31	5
1.31<=grad<1.57	6
1.57<=grad<1.83	7
1.84<=grad<2.10	8
2.10<=grad<2.36	9
2.36<=grad<2.62	10
2.62<=grad<2.88	11
2.88<=grad<3.14	12
3.14<=grad<3.41	13
3.41<=grad<3.67	14
3.67<=grad<3.93	15
3.93<=grad<4.19	16
4.19<=grad<4.45	17
4.45<=grad<4.71	18
4.71<=grad<4.98	19
4.98<=grad<5.23	20
5.23<=grad<5.50	21
5.50<=grad<5.76	22
5.76<=grad<6.02	23
6.02<=grad<6.28	24

The division of gradient values into 24 equal parts can also be represented as follows in figure 5.
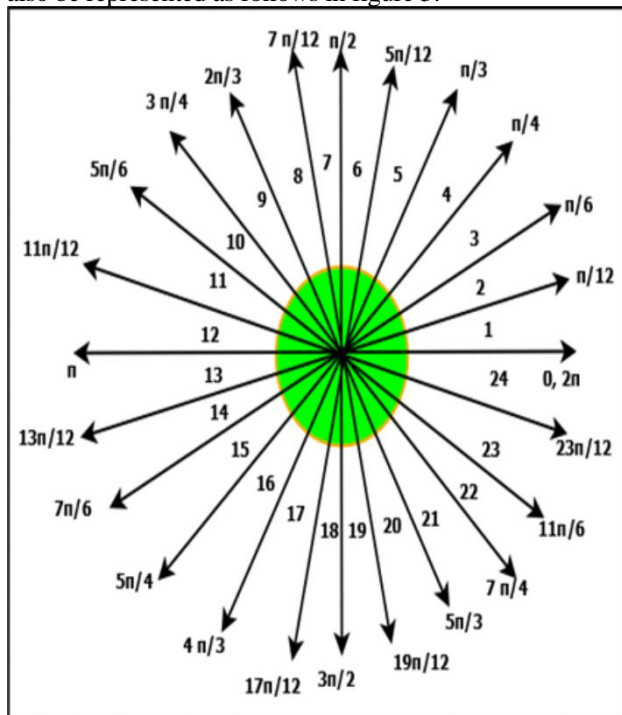

FIGURE 5 24 Directional Values equivalent to gradients

5 Experimental Result and Comparative analysis

In this paper, Back propagation neural network with 12 number of hidden units has been used for training the network.The gradient descent training method has been implemented for training the back propagation neural network. This training method calculates the gradients and compare it with threshold value 10^{-10}.Whenever gradient exceeds the threshold valus,network performs next iteration. The batch steepest descent training function is traingd.

For performing the experiment in Matlab, 1000 number samples of Hindi characters have been collected from different person of different department of different age groups. Out of 1000 samples, 500 samples were used for training purpose and remaining 500 samples were used for testing purpose. Flowchart for performing the experiment.
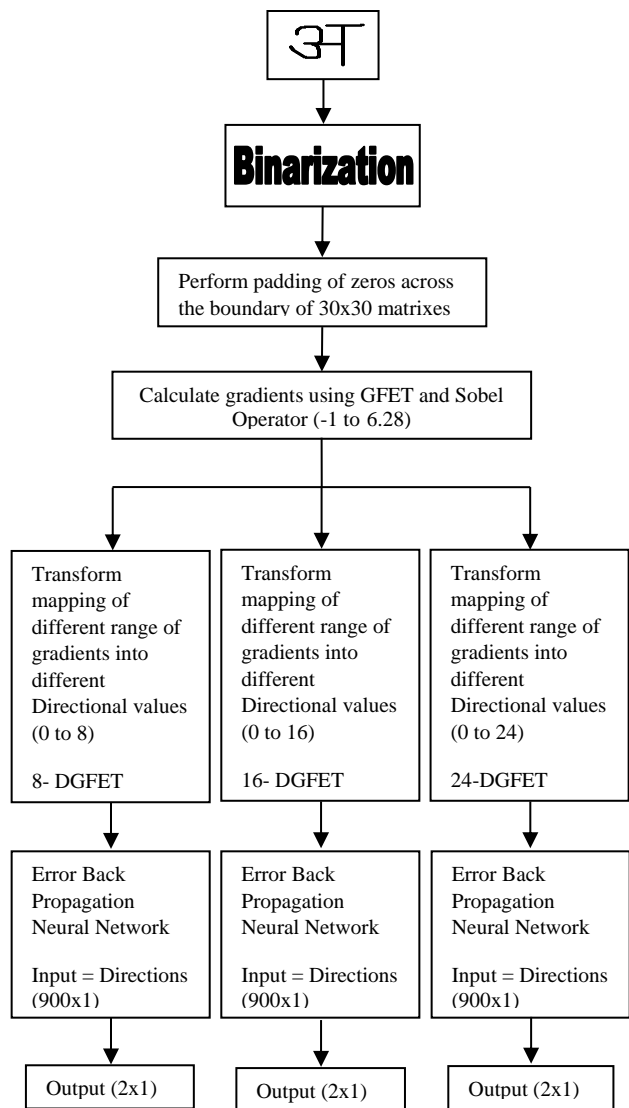

FIGURE 6 Flowchart

5.1 PROCEDURE

The various steps of implementing all the feature extraction techniques are given in procedure
- Normalize handwritten Hindi character in 30x30 pixels

- Convert 30x30 pixel images into binary i.e. perform binarization.
- Convert above 30*30 binary values into 32x32 matrixes by padding with zeros across the boundary.
- Apply Sobel operator on above 32x32 matrixes for calculating the gradient values.
- Calculated gradient values will be in a 30x30 matrix (Gradient values will be between 0 to 2π). If pixel is surrounded with all zeros, set the gradient value -1.
- Set the gradient values into 8/16/24 directions as per tables given above.
- All three methods of feature extraction will supply 30x30 matrix directional values in 900x1 column matrix to the feed forward neural network independently as an input.
- The above values can be used for training and simulation both
- Set goal as a 2x1 matrix (e.g. for first vowel of Hindi character, goal = [1 0] ´ and for first consonant of Hindi character, goal = [0 1] ´.

Results of experiment have been given in following table 4.

TABLE 4 Results of experiment

Advanced Feature Extraction Techniques	Input to Neural Network	Number of Hidden Units	No of Iterations	Training Time (sec)	Classification Time (ms)	Performance on Training set (%)	Performance on Test Set (%)
8-DGFE	30x30 inputs	12	50	416.53	65.62	100	95
16-FGFE	30x30 inputs	12	50	665.37	62.52	100	96
24-DGFE	30x30 inputs	12	50	884.85	60.38	100	97

From above table, it has been analyzed that recognition accuracy is increasing at the cost of training time as we move from 8-DGEF to 24-DGEF. 24 Directional gradient feature extraction technique is giving high accuracy up to 97% and requires less classification time, this feature extraction technique requires some more training time. But, once system is fully trained then training time does not matter more, only recognition accuracy matters more. In this way, 24- DGFE technique is developed and implemented for handwritten Hindi character recognition.

6 Conclusion and Future Scope

In this paper, three feature extraction techniques have been implemented for handwritten Hindi character recognition. The 24-DGFE technique is yielding recognition accuracy little bit more but it requires more training time as compared to other methods. This concludes that as we keep on splitting the gradient values in increasing number of directional values, the recognition accuracy is little bit increasing but training time is increasing more. If we focus on recognition accuracy, then the 24-DGEF technique is better. This accuracy can be further increased by implementing some innovative feature extraction technique. In this paper, since, scanned samples have been taken therefore this automatic character recognition system can be used for any other character of any other language by giving it proper training.

Acknowledgments

References

[1] Verma B K 1995 Handwritten Hindi Character Recognition Using Multilayer Perceptron and Radial Basis Function Neural Network *IEEE International Conference on Neural Network* **4** 2111-5

[2] Sutha J, Ramraj N 2007 Neural Network Based Offline Tamil Handwritten Character Recognition System *IEEE International Conference on Computational Intelligence and Multimedia Application* **2**(13-15) 446-50

[3] Hailong Liu, Xiaoqing Ding 2005 Handwritten Character Recognition using gradient feature and quadratic classifier with multiple discrimination schemes *Eighth IEEE International Conference on Document Analysis and Recognition* August 29-1 Sept. 2005 **1** 19-23

[4] Weipeng Zhang, Yuan Yan Tang, Yun Xue 2006 Handwritten Character Recognition Using Combined Gradient and Wavelet Feature *IEEE International Conference on Computational Intelligence and Security* **1** 662-7

[5] Cheng-Lin Liu 2007 Normalization-Cooperated Gradient Feature Extraction for Handwritten Character Recognition *IEEE Transactions on Pattern Analysis and Machine Intelligence* **29**(8) 1465-9

[6] Hertz J, Krogh A, Palmer R 1991 *Introduction to the theory of neural computation* Addison-Wesley Publishing Company, USA

[7] Wasserman P D *Neural Computing Theory and Practices*

[8] Rajasekaran S, Vijaylakshmi Pai G A *Neural Networks, Fuzzy Logic, and Genetic Algorithms*

[9] Yeung D S 1994 A neural network recognition system for handwritten Chinese character using structure approach *Proceeding of the World Congress on Computational Intelligence* **7** 4353-8

[10] Almualim H, Yamaguchi S 1987 A method for recognition of Arabic cursive handwriting *IEEE Trans. on Pattern and Machine Intelligence* **PAMI-9**(5) 715-22

[11] Sutha J, Ramraj N 2007 Neural Network Based Offline Tamil Handwritten Character Recognition System *IEEE International Conference on Computational Intelligence and Multimedia Application* **2**(13-15) 446-50

[12] Verma W K 1995 *New training methods for multilayer perceptrons* Ph.D Dissertation, Warsaw Univ. of Technology, Warsaw

[13] Dayashankar Singh, Maitreyee Dutta, Sarvpal H Singh 2009 Comparative Analysis of Handwritten Hindi Character Recognition Technique *Proceeding of IEEE International Advanced Computing Conference, ISBN: 978-981-08-2465-5, Thaper University, Patiala, India, March 6-7*

[14] Dayashankar Singh, Maitreyee Dutta, Sarvpal H Singh 2009 Neural Network Based Handwritten Hindi Character Recognition *Proceeding of International Conference of ACM (Compute 09), ISBN: 978-1-60558-476-8, Bangalore, India, Jan. 9-10*

[15] Dayashankar Singh, Sanjay Kr. Singh, Maitreyee Dutta 2010 Handwritten Character Recognition Using Twelve Directional Feature input and Neural Network *International Journal of Computer Application (IJCA) (ISBN: 0975-8887)* **1**(3) 94-8 New York, USA

[16] Smith S J, Baurgoin M O 1994 Handwritten character classification using nearest neighbor in large database *IEEE Trans. on Pattern and Machine Intelligence* **16** 915-9

AUTHORS	

Dayashankar Singh, 10th June, 1969

Current Position: Assistant Professor, CSED, M M M University of Technology, Gorakhpur.
University Studies: Panjab University, Chandigarh, India
Scientific Interests: Neural Network, Artificial Intelligence, Image Processing, Database, Network Security
Publication: More than 35 research papers have been published in various International Journals/Conferences
Experience: More than 14 years of teaching and research experience

Prof. J.P. Saini, 26th June, 1966

Current Position: Professor, ECED, BIET, Jhansi and Director, AITH, Kanpur, India
University Studies: Indian Institute of Technology, Kanpur, India
Scientific Interests: Artificial Neural Network (ANN), Reliability Engineering and Analog Electronics
Publication: More than 100 research papers have been published in various International Journals/Conferences
Experience: More than 25 years of teaching and research experience

Prof. D S Chauhan, 18th September, 1949

Current Position: Vice Chancellor, GLA University Mathura
University Studies: Indian Institute of Technology, New Delhi, India
Scientific Interests: Power System & Control System.
Publication: More than 200 research papers have been published in various International Journals/Conferences
Experience: More than 35 years of teaching and research experience
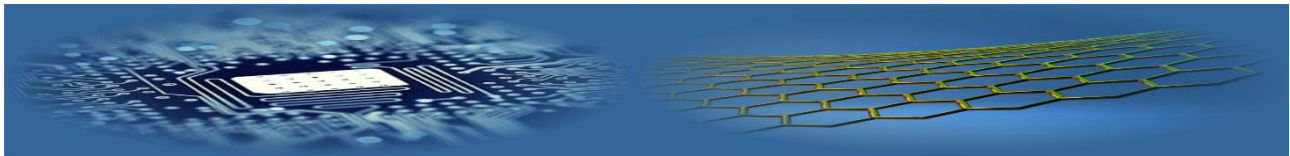
Modelling of non-point source pollution transport for the Charyn River Basin

Jalal K Jamalov*, Daniyar B Nurseitov, Kairat A Bostanbekov

National Open Research Laboratory of Information and Space Technologies, Kazakh National Research Technical University named after K.I. Satpayev., Satpayev Str. 22a, Almaty, Kazakhstan

Corresponding author: gg.mazei@gmail.com

Abstract

The results of pollution transport simulation for the Charyn river (the Republic of Kazakhstan, Central Asia) obtained using software package BASINS 4.1 are shown in this article [1]. Modules created in the process of the study as well as the method of adaptation of the model of pollution transport are described. The calculations include the modeling of the hydrology of the river basin and the calculation of the concentration of non-point sources of pollution. The comparison with the data of natural hydrological observation post.

1 Introduction

The Charyn is the river in Almaty region of the Republic Kazakhstan. It is located in the Charyn gorge where the Charyn canyon belongs. It is the largest left-bank tributary of the Ili river. Its headwaters are located above the climatic snowline, on the southern slope of the Ketmen range. The river length is equal to 428 km, catchment area - 9.0 thousand square kilometres. The main tributaries are Karkara (the right one) and Temirlik (left). Currently, monitoring of water flow is being carried out by the only remaining station of RSE "Kazhydromet" on the Charyn river located in Sarytogay tract. According to the data of this station the average annual water discharge makes up 37.7 m³/s.

2 Theory and calculations

The region under study is the basin of the Charyn river shown in Figure 1. To implement calculations multifunctional system of environmental analysis BASINS 4.1 was used. This system was developed by the Environment Protection Agency for the purposes of setting standards of the maximum total daily load (TMDLs) for waterbodies with impaired water quality and to allow local and state agencies to conduct analysis of watersheds. To simulate the transfer of pollution the main input data were determined, and the algorithm for calculations was developed. In Figure 2 a graphical model describing the developed algorithm is given.

Input parameters for BASINS 4.1 software are the following ones:
1) Digital Elevation Model (DEM);
2) River Net;
3) Land Use data;
4) State Soil data;
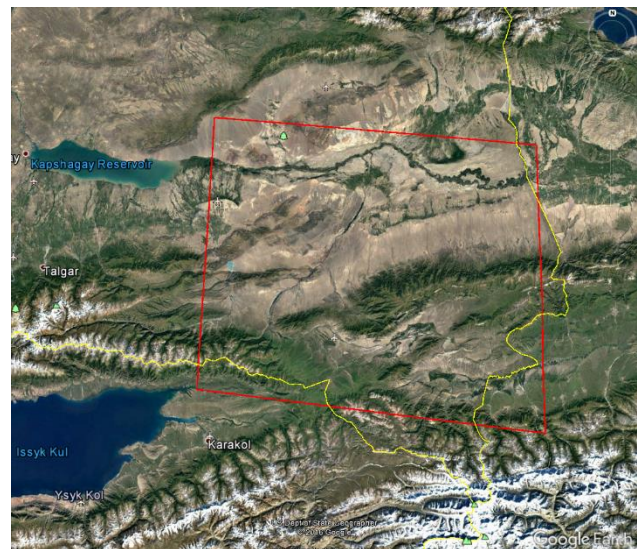5) Meteorological data.

FIGURE 1 The region under study

The digital elevation model (DEM) is the information on terrain elevations in the area under study presented in GeoTIFF format. This format is an input one to be us³ed in the Watershed Delineation tool (WDT) [2] intended for determination of the boundaries of the basin and the construction of watershed lines. The major part of DEMs is generated by the processes involving land remote sensing technology, the search and analysis of online resources that may provide this information were conducted. As a result, the DEM of the Global Explorer Data portal was used [3]. To construct the lines of watersheds and to determine the basin boundaries in addition to elevation data (DEM) the data of river flows location (River Net) were used. The USGS HydroSHEDS has developed files of streams and river networks based on digital elevation models obtained by NASA [4] (in the course of SRTM).

The data are given in vector format and contain the information on the location of river flows of the entire
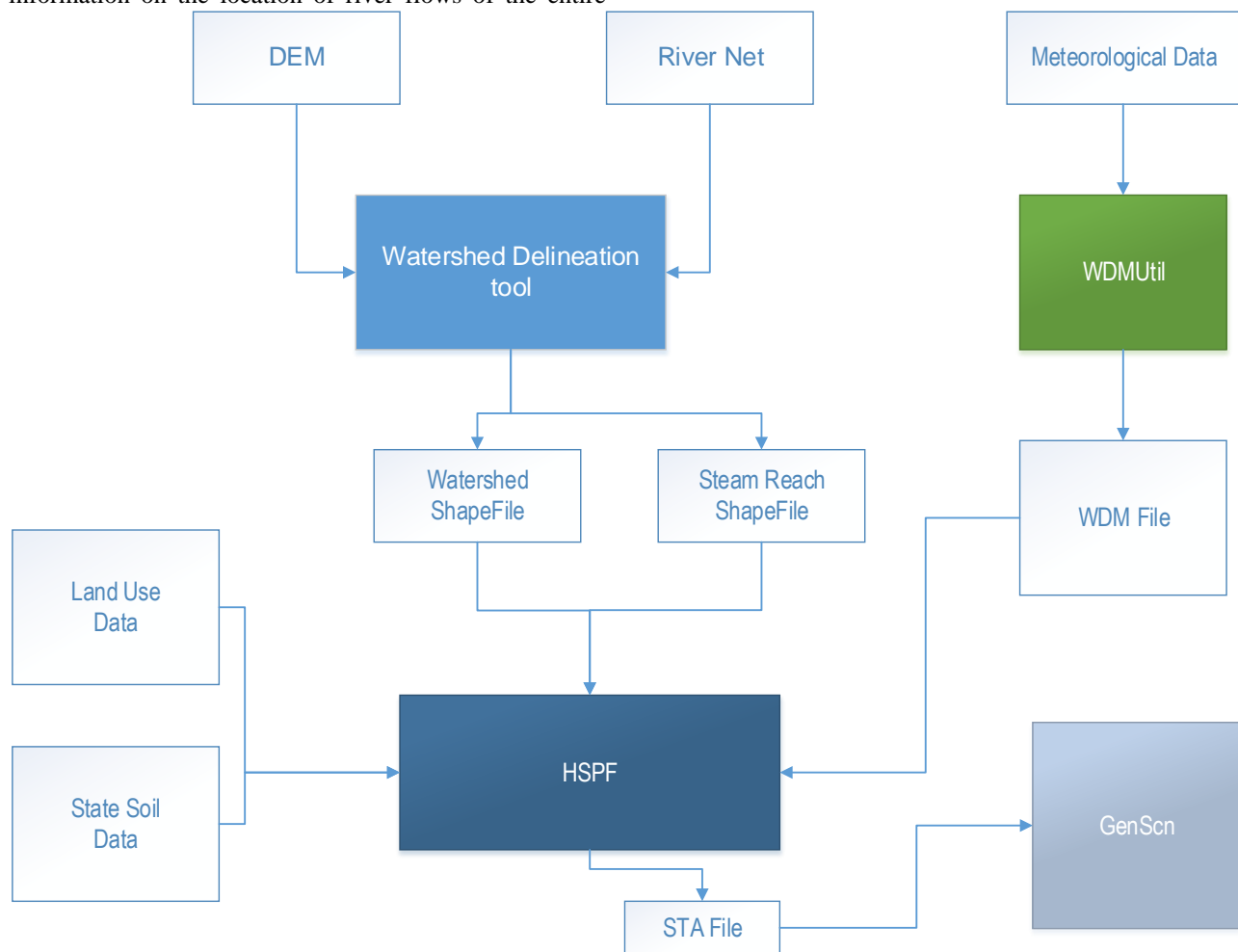
Asian region.

FIGURE 2 Flow chart of calculations

The results of the WDT usage are:
1) basin boundary lines;
2) sub-basin lines;
3) river network line file.

The files were visualized using Google Earth, where: 1) the boundary of the river Charyn basin (translucent blue color); 2) river Charyn (blue marker); 3) sub-basins of the river Charyn (red marker), see Figure 3.

For the purposes of hydrological processes simulation HSPF model was used. This model requires the following input data:
1) sub-basin lines;
2) the river network lines;
3) land-use maps;
4) soil maps;
5) meteorological data.

The application of the data of land cover in BASINS allows evaluating the categories of land use in the watershed. To minimize the errors of the HSPF model results land cover data resolution should be as high as possible, especially for small catchment basins. Land use maps Global Land Cover 2000 were downloaded in TIFF format from the website of the Joint Research Centre of the European Commission (Joint Research Centre) [5]. Soil data were obtained from the FAO GeoNetwork website [6].
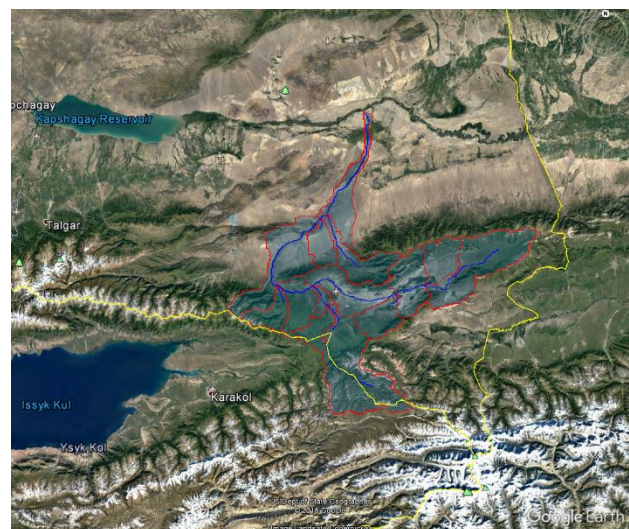

FIGURE 3 Image by Google Earth with superimposed data of calculations

In HSPF model land use and soil maps are used for determining the area and hydrological parameters of each category of soil and land resources. Application of the tool Spatial Analyst allows calculating cross areas between tabular data of land cover and sets of soil cover by the method of superimposition.

38

3 Meteorological data processing

As for hydrological processes, these vary over time and depend on the changes in the state of environment, while for evaluation of pollution of scattered sources the succession of hourly precipitation, evaporation, temperature and other meteorological data are required.

Initially, meteorological data were downloaded from the website of the National Climatic Data Center (NOAA's National Climate Data Center) [7]. Then, meteorological data of ALMATY station were used (marked with a yellow square), Figure 4.
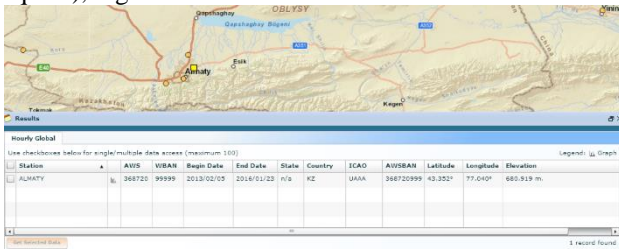

FIGURE 4 Meteorological station ALMATY

The obtained data are stored in a text file (txt), Figure 5.

FIGURE 5 Meteorological data of the NOAA's National Climate Data Center

As it is seen in figure 5, the value of PRECIP = 999.9, that implies the lack of the data on precipitation, as well as on evaporation. However, these two parameters are very essential ones for calculations of water discharge and simulation of hydrological processes. Therefore, meteorological data to be used in the BASINS system were downloaded from the database of reanalysis ERA Interim, created by the European Centre for Medium-Range Weather Forecasts (ECMWF). The data are presented in GRIB format for the period from 1 January 1980 to 1 August 2016. The IDV (Interactive Data Visualization) software allowed exporting meteorological parameters concerning the point of 43.2 latitude and 79.0 longitude into CSV text format intended for presenting tabular data. The tabular data are stored in the form of time series, where the first column is the date and time, and each subsequent column is the value of the corresponding meteorological parameter. Since the model requires hourly time series, while the downloaded data were presented with a 6-hour interval, the values were interpolated. For this purpose, a script in Python for reading the data from the CSV file and conducting linear interpolation was written. Then the obtained values with hourly intervals and time shifting for +6 hours, as the initial data correspond to UTM, were stored in a new CSV. The python code listing is shown below.

```python
import os
import sys
import math
import numpy as np
from scipy.interpolate import interp1d
import matplotlib.pyplot as plt
from matplotlib.colors import LogNorm, ListedColormap,
BoundaryNorm
import datetime


try:
    infile = sys.argv[1]; outfile = sys.argv[2];
except:
    print "Usage:",sys.argv[0], "infile outfile"; sys.exit(1)

# read infile
fin = open(infile,'r')
header = fin.readline()
lines = fin.read().split('\r\n')
values = []
for line in lines:
    values.append(line.split(';')[1])


y = values
x = np.linspace(0,len(y)*6-6,len(y))

f = interp1d(x,y)
#f2 = interp1d(x,y,kind='cubic')

xnew = np.linspace(0,len(y)*6-6,len(y)*6-5)
ynew = f(xnew)
#ynew2 = f2(xnew)

#plt.plot(x, y, 'o', xnew, ynew, '--', xnew, ynew2, '-')
#plt.show()

fout = open(outfile,'w')
fout.writelines(header)

Time = datetime.datetime(1979,1,1,9,0,0)
for line in ynew:

fout.writelines(Time.strftime('%Y-%m-%d %H:%M:%S')+';'+'{0:.10f}'
.format(line)+'\n')
    Time += datetime.timedelta(hours=1)


fin.close()
fout.close()
```

For structuring time series of meteorological data WDM format was used [reference]. The characteristic features of

WDM files are the following ones:
1) these files are supported in HSPF model;
2) allow storing a large number of time series;
3) ensure reading, movement of the data stored in the file. To import the data from test files into WDM format a script for utilities WDMUtil was written.

```
(ATCScript "WDMUtil Export Format - Hourly Values"
        (LineEnd LF)
        (NextLine)
        (ColumnFormat Fixed
                        1-4:Year
                        6-7:Month
                        9-10:Day
                        12-13:Hour
                        15-16:Minute
                        21-36:Value
        )
        (Attribute Scenario "OBSERVED")
        (Attribute Location "Charyn")
        (Attribute Constituent "ATEM")
        (Attribute Description "Temperature")
        (Attribute LATDEG "43.2")
        (Attribute LNGDEG "79")
        (Test (And (IsNumeric Value)
                        (IsNumeric Year)
                        (IsNumeric Month)
                (IsNumeric Day)
                        (IsNumeric Hour)
                        (IsNumeric Minute)
                        (> Year 1700)
                        (< Month 13)
                        (> Day "0")
                        (< Day 32)
                        (< Hour 26)))
        (While (Not EOF)
                                (Date Year
                                Month
                                Day
                                Hour
                                Minute)
                        (Value Value)
                        (NextLine)
        )
        (Fill H 1 -999 -999 -999)
)
```

As a result, a WDM-format file with the required meteorological parameters, in the required units with hourly intervals was obtained, see Figure 6.
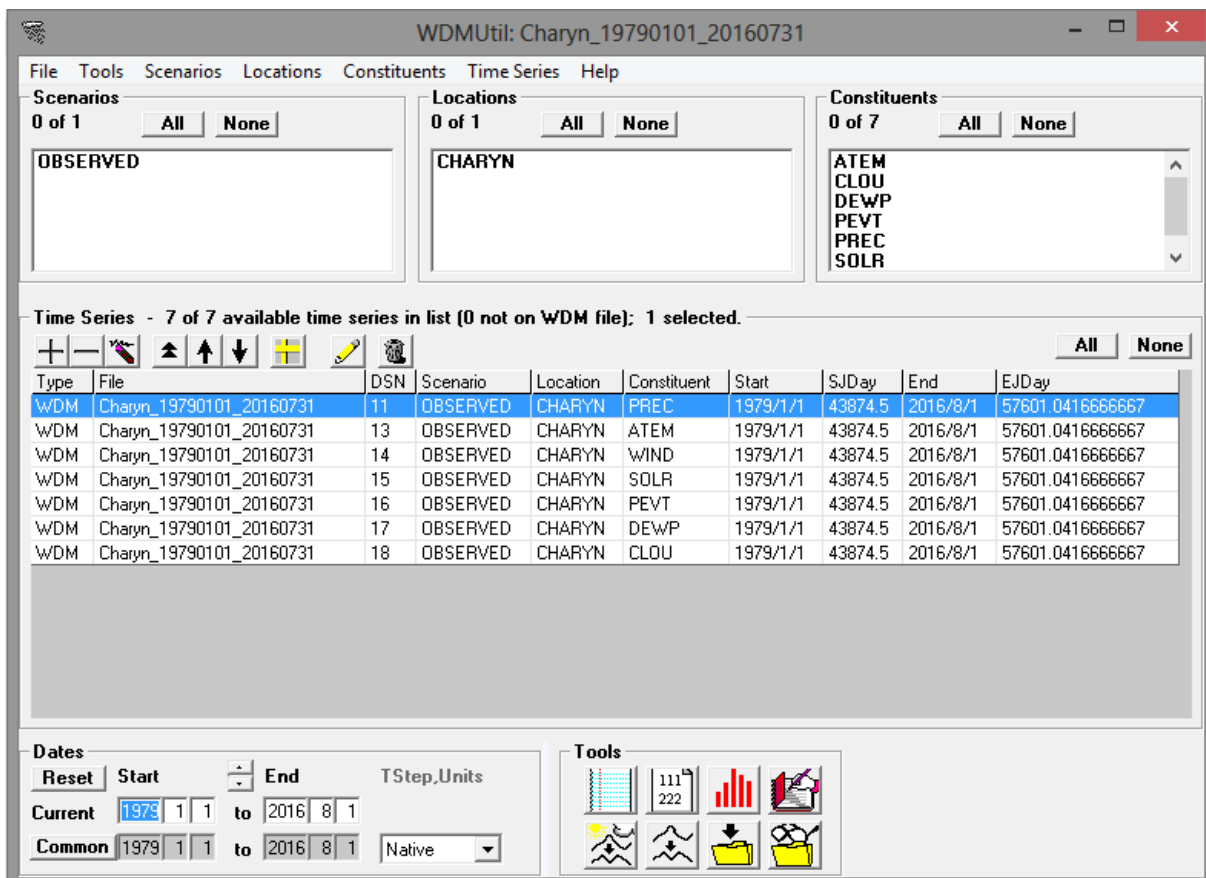

FIGURE 6 Meteorological parameters in WDM format opened by means of WDMUtil

As shown in Figure 6 in the "Constituent" column indicated all meteorological parameters used to calculate:

TABLE 1 Description of meteorological parameters

Data set	Description Parameter
PREC	hourly precipitation
CLOU	hourly cloud cover
ATEM	hourly temperature
WIND	hourly windspeed
SOLR	hourly solar radiation
PEVT	hourly potential evapotranspiration
DEWP	hourly dewpoint temperature

As a result of calculations in HSPF model for the River Charyn were obtained 15 river reaches of each of these specific parameters, see Figure 7.
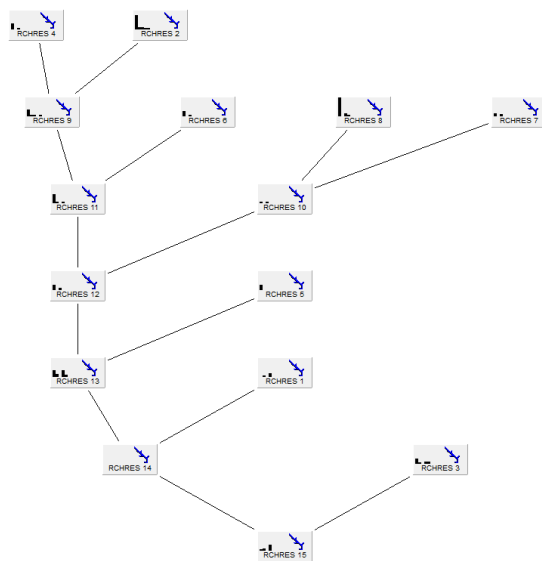

FIGURE 7 The Charyn river reaches in HSPF model

Reaches correspond to the main flow of the river and its lateral tributaries, as shown in Figure 8.
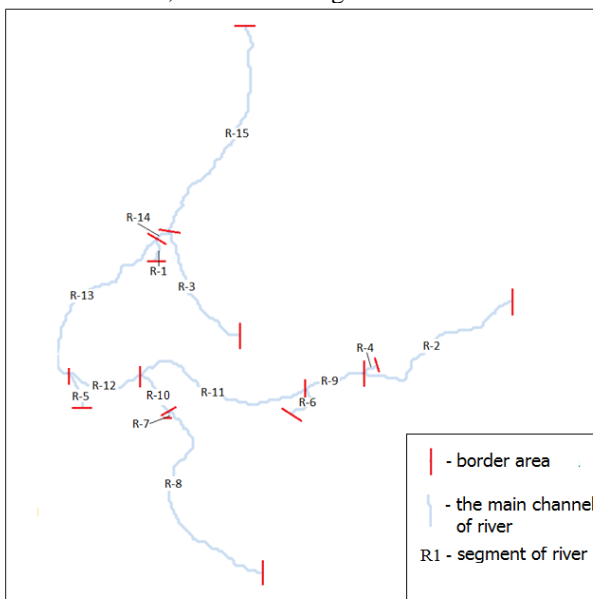
FIGURE 8 Schematic representation of the results of HSPF model

As seen in Figure 8, river reach R-15 is the final one. It is the area where the hydrological post - Sarytogay tract - monitoring the river water flow is situated. This fact allowed comparing the simulation results with the data of field observations.

4 Results

The following indicators were found for the following non-point sources of pollution:
1) BOD (Biochemical oxygen demand);
2) Dissolved oxygen (Dissolved oxygen);
3) Nitrate nitrogen (NO3);
4) Ammonium Nitrogen (Total Ammonia) (TAM).

4.1 BIOCHEMICAL OXYGEN DEMAND

Biochemical oxygen demand is the amount of oxygen consumed for aerobic biochemical oxidation by the action of microorganisms and decomposition of unstable organic compounds contained in the tested water. According to the observation data for the year 2006 obtained at the station located in Sarytogay tract, monthly average BOD concentration makes up 0.81 mg/L.

FIGURE 9 Changes in the concentrations of BOD

Average annual BOD concentration at reach R-15 obtained as a result of calculations equaled to ¬ 0.72 mg/L.

FIGURE 10 Changes in the computed concentrations of BOD

4.2 DISSOLVED OXYGEN

According to the observation data for the year 2006 obtained at the station located in Sarytogay tract, average monthly

dissolved oxygen concentration equals to 9.94 mg / L.
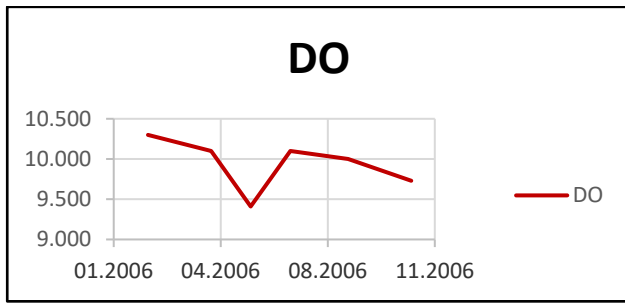
FIGURE 11 Changes in the concentrations of dissolved oxygen

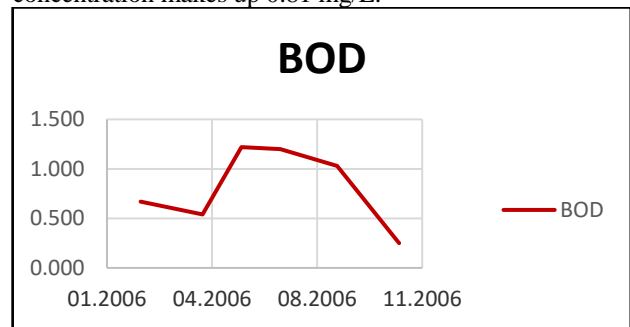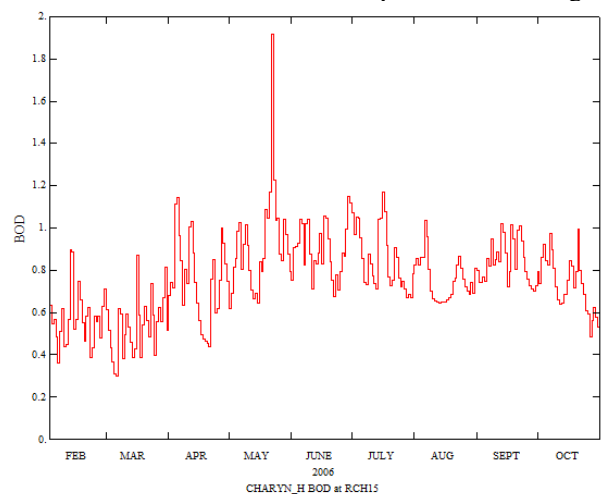Average annual concentration of dissolved oxygen at river reach R-15 obtained as a result of calculations made up 11.6 mg/L.
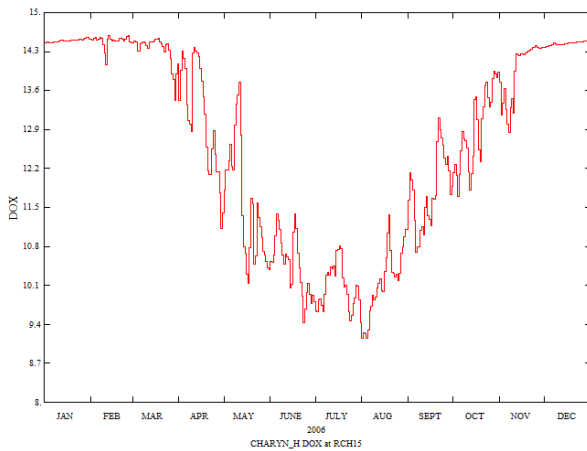
FIGURE 12 Changes in the computed concentrations of dissolved oxygen

4.3 NITRATE NITROGEN (NO3)

According to the observation data for the year 2006 obtained at the station located in Sarytogay tract, average monthly value of NO3 concentration = 0.58 mg/L.
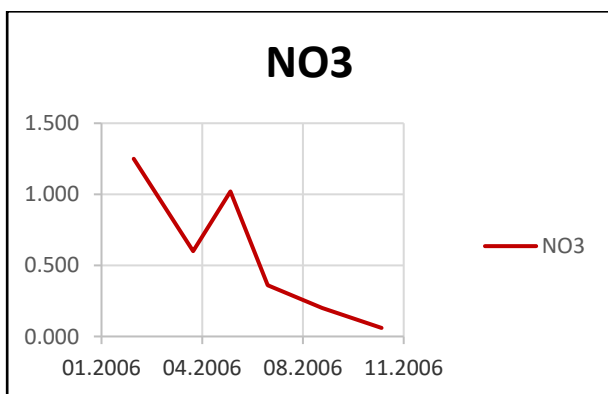
FIGURE 13 Changes in the concentrations of NO3

Average annual concentration of NO3 at river reach R-15 obtained as a result of calculations made up 0.51 mg/L.
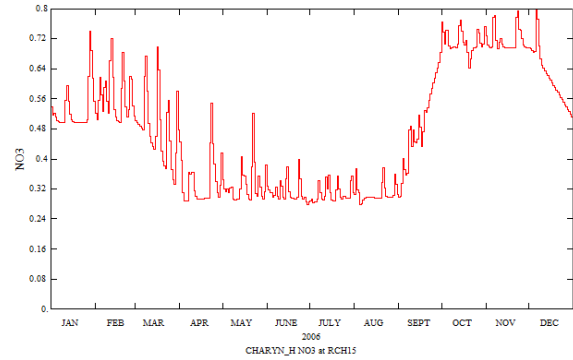
FIGURE 14 Changes in the computed concentrations of NO3

4.4 AMMONIUM NITROGEN (TAM)

According to the observation data for the year 2006 obtained at the station located in Sarytogay tract, average monthly concentration of TAM = 0.012 mg/L.
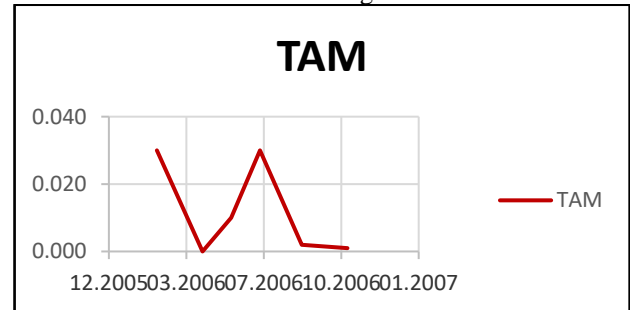
FIGURE 15 Changes in the concentrations of TAM

Average annual concentration of NO3 at river reach R-15 obtained as a result of calculations made up¬ 0.01 mg/L.
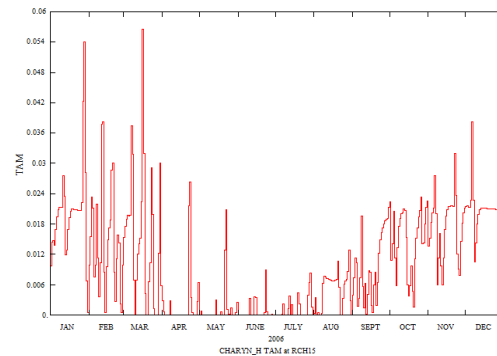
FIGURE 16 Changes in the computed concentrations of TAM

5 Conclusion

The main result of this work is approbation of BASINS software by the example of the modeling of transport pollution in small River Charyn in the south-eastern part of the Republic of Kazakhstan (Central Asia). The practice has shown that a simple installation of the product is not enough for the calculations. It was necessary to adapt the model to local conditions. However, some input parameters of the model had to assembled from a variety of sources, transform and adjust.

Also, to verify the adequacy of the model was produced searching existing data and lead an expedition with data

collection by field studies were carried out.

Comparisons on the following parameters:
1) Deviation of BOD value - 0.09 mg/L, error - 11%
2) Deviation of DO value – 1.66 mg/L, error - 16%
3) Deviation of NO3 value - 0.07 mg/L, error - 12%
4) Deviation of TAM value - 0.002 mg/L, error - 16%

It can be noted that the model adequately reflects the situation on the transport of pollutants. Accuracy is the permissible value for the assessment of the environmental situation in the region.

In future will be planned to expand the usage of this model for large river basins, to consider the possibility of calculation of point sources taking into account the daily load. After multiple calculations are also planning to create an automated system using distributed computing, similar to the [7].

Acknowledgements

References

[1] «EPA's Better Assessment Science Integrating Point and Nonpoint Sources (BASINS)» *Exposure Assessment Models* https://www.epa.gov/exposure-assessment-models/basins

[2] Andrew Battin, Russel Kinerson, Ph.D., Mohammed Lahlou, Ph.D. EPA's Better Assessment Science Integrating Point and Nonpoint Sources (BASINS) *A Powerful Tool for Managing Watersheds 2014*

[3] *Global Data Explorer* http://gdex.cr.usgs.gov/gdex/

[4] *U.S. Releases Enhanced Shuttle Land Elevation Data* http://www2.jpl.nasa.gov/srtm/

[5] «The European Commission's science and knowledge service» *Joint Research Centre* http://forobs.jrc.ec.europa.eu/products /glc2000/glc2000.php

[6] *FAO GeoNetwork* http://www.fao.org/geonetwork/srv/en/main .home

[7] Zaurbekov D L, Bostanbekov K A, Jamalov J K, Kim D K, Nurseitov D B, Tursunov I E, Zakarin E A 2013 Service-Oriented GIS System for Risk Mapping of Oil Spills Integrated with High Performance Cluster *The Second International Conference on Informatics Engineering & Information Science (ICIEIS2013) 343-354*

AUTHORS

Jalal Jamalov, 02.03.1991, Kazakhstan

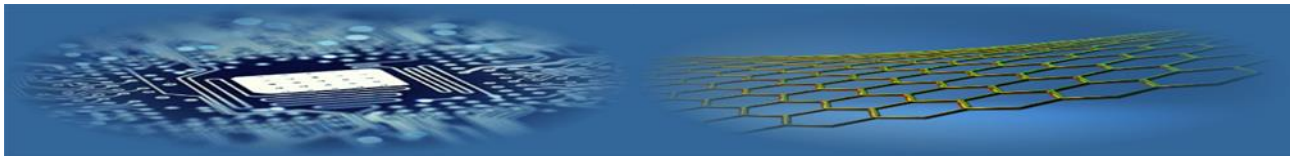**Current position, grades:** PhD student of Kazakh National Technical University.
University studies: Master degree in computer engineering and software from International University of Information Technologies.
Scientific interest: Computer modeling and ecological problems.
Publications: 1. Water resources of Central Asia and their use.Materials International Scientific-Practical Conference devoted to the summing-up of the "Water for Life" decade declared by the United Nations. Volume 1. Almaty, Kazakhtan, September 22–24, 2016.
2. Numerical solution of the inverse problem Streeter-Phelps closed system for two incubation periods// Water resources of Central Asia and their use. International scientific-practical conference dedicated to summing up the results of the UN Declaration of the Decade "Water for Life". Book 1. Almaty, Kazakhstan, 22-24 September 2016 p. 56-63.
3. Example simulation of water protection measures in the Kazakh part of the basin. Or (scenario calculation) // Russian Foundation for Basic Research, Institute of Arid Zones, Southern Scientific Centre of the Russian Academy of Sciences, Southern Federal University. Collection of articles "Ecology, Economics, Computer Science. System analysis and modeling of economic and ecological systems. Mathematical methods and models in environmental studies." Volume 1. Rostov-on-Don, 2016. p. 33-43.
Experience: Experience in software development, web applications and GIS technologies.

Daniyar Nurseitov, 22.03.1980, Kazakhstan

Current position, grades: Head of National Open Research Laboratory Information and Space Technologies at Kazakh National Research Technical University.
University studies: Candidate of physical and mathematical sciences from Novosibirsk State University.
Scientific interest: Inverse problems, computer modeling and ecological problems.
Publications: 1. Analysis of ill-posedness and numerical methods of solving a nonlinear inverse problem in pharmacokinetics for the two-compartmental model with extravascular drug administration // Journal of Inverse and Ill-Posed Problems. Volume 20, Issue 1, P. 39–64, March 2012.
2. An optimization method in the Dirichlet problem for the wave equation // Journal of inverse and ill-posed problems. Volume 20, Issue 1, Number 2, P. 193–211.
3. Inverse problems for the ground penetrating radar // Journal of Inverse and Ill-Posed Problems. Volume 21 Number 6, P. 885–892, 2013
Experience: Leadership experience five successful scientific projects.

Kairat Bostanbekov, 05.07.1988, Kazakhstan

Current position, grades: PhD student of International University of Information Technologies.
University studies: Master degree in computer engineering and software from Kazakh National Technical University.
Scientific interest: Computer modeling and ecological problems.
Publications: 1. Integrated workflow-based system for risk mapping of oil spills with using high performance cluster // International Journal of New Computer Architectures and their Applications (IJNCAA): Vol. 3, Issue 4. P.115–131, 2013.
2. Service-Oriented GIS System for Risk Mapping of Oil Spills Integrated with High Performance Cluster // The Second International Conference on Informatics Engineering & Information Science (ICIEIS2013):Kuala Lumpur, Malaysia, Nov. 12-14, P.343-354, 2013.
3. Geoinformacionnaia model bioraznobrazia i uyazvimosti bioty Severnogo Kaspia [Geoinformation models biodiversity and vulnerability of biota of the Northern Caspian] // Geoinformatika P.55-63, 2016.
Experience: Experience in software development, web applications and GIS technologies.

Performance evaluation of computer-aided knit design using software package based on ontological knowledge model

O Kochetkova[1*], A Kaznacheeva[2], A Kochetkov

[1]Volgograd State Agricultural University, 26 Universitetskiy prospekt, 400002, Volgograd, Russia
[2]National Institute of Financial Markets and Management, 14 Bolshaya gruzinskaya Str, 123242, Moscow, Russia

[*]Corresponding author: editor9@academicpapers.org

Abstract

The article represents the original approach to computer-aided warp knit fabrics on the base of universal algorithms and modern methodology which allows to apply the methods of projecting with the given technologies. The ontological approach is represented for development and improvement of knowledge model which provides the description of object domain of computer-aided warp knit fabrics and its formalized presentation. The elaborated software allows to perform fully the proceedings of art and technological and parametric projecting of warp knit fabrics. The performance evaluation of computer-aided warp knit fabrics on the basis of algorithmical and ontological approach is elaborated. To solve this problem we used the method of hierarchy analysis of Thomas Saati. The results of the evaluation represent that software grounded on ontological approach in totality of functional means is more effective than CAD on the base of algorithmical approach.

1 Introduction

Computer-aided warp knit fabrics (WKF) design, as less studied and the most complicated knitted technology object in terms of its structure, is a complicated multiple-task problem, which solution is obstructed by the fact that the knowledge of this object domain is not enough structured and formalized.

Therefore, the task of intellectualization of computer-aided warp knit fabrics on the basis of universal algorithms and modern methodology of projecting to increase the effectiveness of technological preparation is actual nowadays.

2 Materials and methods

In our study, we have proposed an ontological approach to development and improvement of a knowledge model that describes the object domain of computer-aided design of warp-knitted fabrics and its formalized representation (Kochetkova 2012a). A system conceptual model of WKF, as the object of functional, design, and process engineering, has been developed to organize structured information that allows the expert support subsystem of computer-aided design to generate and manipulate knowledge in the object domain effectively.

3 Results and discussion

Conducted theoretical studies allowed us to develop program-methodical package of WKF which structure and composition (Figure 1) reflect the generalized algorithm for solving the knit design problem on the basis of ontological model of knowledge (Kochetkova 2012b).

Within the framework of the "PMA-WKF"

(poly(methacrylic) acid - warp knit fabrics), subsystems for art-technological and structural-parametric knit design were developed through forming a pattern matrix, reproducing knitwear pattern, selecting materials, establishing structure and parameters of the WKF and selecting knitting machines.

As is obvious from Figure 1, "PMA-WKF" consists of four functional blocks: 1) database; 2) knowledge base; 3) simulation and design system; 4) ontological descriptions output block.

Raw materials and types of WKF interweaving. It also includes graphical objects libraries, intended to produce different patterning effects to move from the pattern matrix to the WKF structure matrix as well as to ensure the coupling of the art-technological and structural-parametric subsystems of the computer-aided design.

The knowledge base is intended for storing of ontological representations of the knowledge model components (task, solution method, and object domain), as well as procedural component of the problem solving process, i.e., the standard techniques of methods strategies implementation presented in the subsystem "Methods". Special attention in this functional block should be paid to the internal organization of solution methods subsystem. It consists of components that contain the ontological representations for solving different classes of problems, and is used for storing this knowledge in a form that is handy for their search and further application (Kochetkova 2012a).

The modeling and design system is used for visual modeling of the problem solution and further use of the resulting ontological models by design solutions formation procedures. Multi-window interface subsystem represents on-line data input interface. Output of the results is carried out upon receipt of all required ontological descriptions of knowledge model components and implementation of

project procedures in subsystems of art-technological and structural-parametric design of the WKF.

The ontologies obtained by means of this system are displayed in the ontological descriptions output block that

allows control of the design process at all stages of its implementation. Consider the operation stages of the user working with "PMA-WKF" program-methodical package (Figure1).
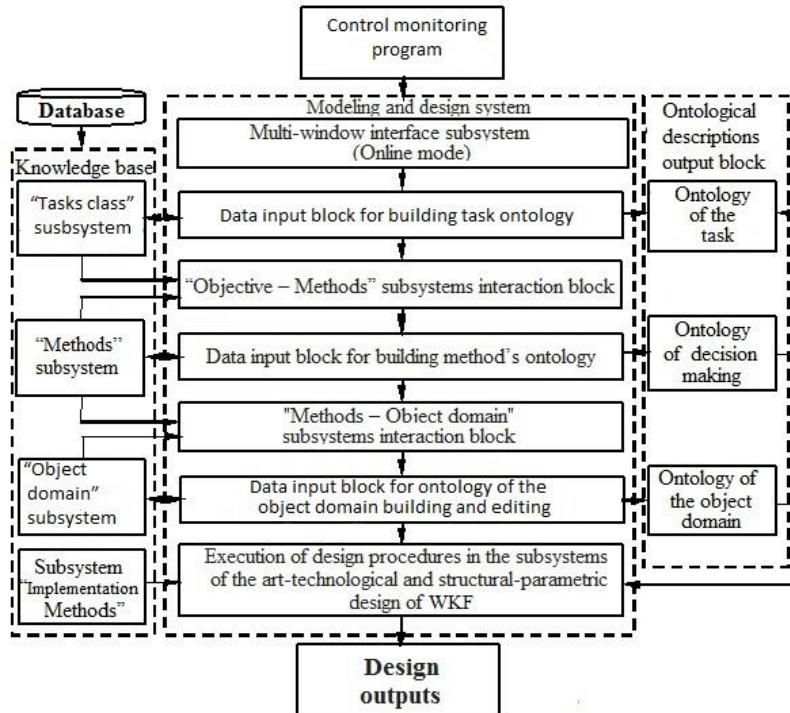

FIGURE 1 The structure and composition of the "PMA-WKF" package

Stage I. The description of a certain problem situation is put into the program. In the course of dialogue with the designer, informal and abstract description of a problem situation is transformed into the description of the specified task.

Stage II. On the basis of the received specification, the formulated task is attributed to one of the design objectives (either art-technological or structural-parametric), and the selection of appropriate ontological description components is conducted out of "Tasks class" subsystem. Then, using the data input block, the software package constructs the ontology of task by filling it with a specific content.

Stage III. Using the "Methods" subsystem, the software package selects the problem solving method. This subsystem contains various decision making methods in the context of their specific application to a particular class of design tasks. All knowledge that affect the choice of method is transmitted into the "Task – Methods" subsystems interaction block, where they are interpreted in terms of selected method to identify the indication axioms. Ontology of subsystems interaction is dynamically changed in each specific case; therefore, it is assumed setting in the subsystems interaction block the base ontology template of a given type with the most common concepts and relations that are applicable to any interaction.

Stage IV. To fill the method with data of object domain, the interaction ontology of the "Methods - Object domain" subsystem is developed, which interprets the method in terms of the object domain. Data needed by method to find project solution of the task in the object domain, is selected from the "Object domain" subsystem. At the object level, software package data input block is used to build the final version of ontology for adjustments of existing components

of the object domain ontology descriptions. The designer has the opportunity to update the ontology with new concepts and relationships, as well as to change its structure.

Stage V. The desired design solution is formed on the basis of obtained ontological knowledge model, the data from object domain and executed implementation procedure, defined by the selected ontology method.

One of the most important "PMA-WKF" blocks is a knowledge modeling system carried out by the user, and subsequent design process. It was implemented as a set of data input blocks for reflection of existing ontological descriptions of knowledge model components and design outputs. The object-oriented programming language C# (C Sharp), combining object-oriented and context-oriented concepts, was selected as the implementation medium.

Testing of the "PMA-WKF" program-methodical package in terms of solving the problem of computer-aided art-technological and structural-parametric design of wefting warp-knitted fabrics has shown its correctness and suitability for solving the problems concerned the engineering preparation of sewing production.

The major task of computer-aided design development, improvement and introduction into manufacturing is the evaluation of their performance efficiency, i.e. the optimal use of the available analyzable resources system to achieve the ultimate results. In this regard, the application of efficiency assessment methods, conduction of comparative analysis, comparison of the investigated objects, as well as identification and selection of priorities is quite relevant. To solve this task, we used the hierarchy analysis technique developed by **T Saati** (Saati 1993). The method is based on the decomposition of complex problem, i.e. its presentation

in the form of a structured set of components or criteria, whose interrelationships are formed in a hierarchical version of the presentation. The top of the hierarchy is the common goal, i.e. the desired state of the system. The next level is detailing of total goal in terms of selecting criteria, components or forces that influence the achievement of the indicated result. The lower level of the hierarchy contains possible alternatives, whose priority needs to be evaluated.

The hierarchy analysis technique involves the operation of pairwise comparison of individual hierarchy components (Diligensky, 2004). The results of the evaluation are presented in the form of a set of pairwise comparisons matrices:

$$B = \begin{bmatrix} b_{11} & b_{12} & ... & b_{1n} \\ b_{21} & b_{22} & ... & b_{2n} \\ ... & ... & ... & ... \\ b_{n1} & b_{n2} & ... & b_{nn} \end{bmatrix}. \qquad [1]$$

In the matrix B, each element b_{ij} determines the expert's subjective opinion regarding the significance of the estimated i-th component of the hierarchy with respect to j-th component. Such matrices are compiled for comparison of the importance of each lower level elements relative to higher level. The assessment of the hierarchy elements is carried out in accordance with a nine-point scale of relative importance. On the basis of expert judgment matrices, the local priorities are calculated for each specific matrix, as well as the quality criteria of expert evaluations. Local priorities are formalized in the form of the main eigenvector of matrix V. Common way of finding eigenvectors is an approach based on finding the geometric mean. In accordance with this technique, the eigenvector component of i-th row is given by formula: $v_i = \sqrt[n]{b_{i1} \times b_{i2} \times ... \times b_{in}}$.

Then all the components v_n of the eigenvector are normalized per unit through dividing by the sum, and these values define the local importance of relatively assessed elements. Experts' evaluation quality criteria are found on the basis of the calculation of judgments consistency indicators for each matrix of pairwise comparisons with regard to the maximum eigenvalue of the matrix.

The final stage of the method is finding of the integral generalized ratings of alternatives importance. The local priorities contraction procedure consists in determination of the weighted sums for all the elements of the same level that take into account the weighting factors (priority vectors) of higher level in the hierarchy. After determining the values of global priorities, a definitive conclusion is made about the relative importance of the evaluated alternatives.

Let conduct performance evaluation of the warp-knitted fabrics design using "PMA-WKF" by a set of the following indicators: generality, structuredness and formalization level of object domain knowledge, as well as the quality of the designed technological process. To identify, compare and prioritize we confront the investigated object with software products, based on algorithmic approach.

The elements of the considered software products include: 1) the art-technological design subsystem; 2) the structural-parametric design subsystem; and 3) servicing subsystems. The efficiency is determined by several factors: functionality, time resources, used resources, and the calculation accuracy. Figure 2 shows the hierarchy of the

system for evaluation of effectiveness factors. The lower level forms the system describing variables x = (xi), i = 1, n. The resulting efficiency y is formed taking into account the weighting coefficients at the previous levels.
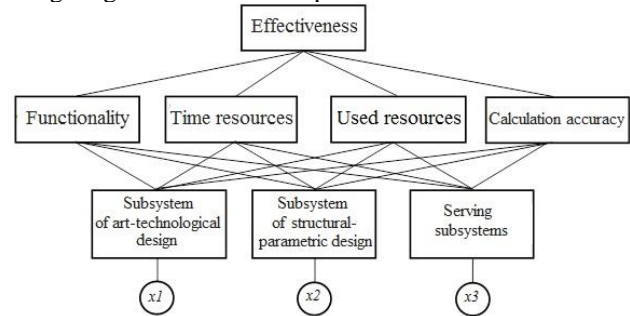
FIGURE 2 The hierarchy of the system for evaluation of effectiveness factors

In general form, the hierarchical synthesis operator can be written as follows (Diligensky 2004):

$$v_{ij(l+1)}^{l+1} = \sum_{j(l)=1}^{n(l)} v_{ij(l)}^{l} v_{ij(l+1)}^{l+1}, l = \overline{1, L,} \qquad [2]$$

where L – is the number of hierarchy levels; n(L) – is the number of elements at the levels [n(1)=n, n(L)=1].

Quantitative estimation of y(x) is determined by the formula:

$$y = \sum_{i=1}^{n} v_{i1}^{L} x_i, y \in [0, 1]. \qquad [3]$$

Three the pairwise comparisons matrices filled in by the experts are presented below.

Matrix V₁¹

1	3	0.5	0.4
0.33	1	0.25	0.67
2	4	1	0.29
2.5	1.5	3.5	1

Matrix V₁¹

1	3	0.5	0.4
0.33	1	0.25	0.67
2	4	1	0.29
2.5	1.5	3.5	1

Matrix V₂²

1	4	2
0.25	1	0.33
0.5	3	1

Matrix V₃²

1	0.5	1.5
2	1	1
0.67	0.33	1

The uniformity indicators of the experts' judgments for compiled matrices equal to following: G11 = 0.016; G12 = 0.048; G22 = 0.050; G32 = 0.035. All indicators are less than 0.1 that testifies the consistency of composed matrices of paired comparisons. The values of the priorities vectors, resulted from processing the expert matrices of pairwise comparisons in accordance with the hierarchy (see Fig.2), are given in Table 1.

TABLE 1 The values of the priorities vectors

j	1	2	3	4
v_j^1	0.19	0.11	0.27	0.43
v_{1j}^2	0.56	0.33	0.28	0.25
v_{2j}^2	0.12	0.45	0.17	0.37
v_{3j}^2	0.32	0.22	0.55	0.38

Experts' performance evaluations of three systems in a nine-point scale are presented in Table 2, where 1 – corresponds to software products, created on the basis of the algorithmic approach; 2 – is the "PMA-WKF" program-methodical package; 3 – is the hypothetical version, which includes the best elements of software products 1 and 2.

TABLE 2 Performance evaluation of software products and WKF design

Design Subsystems	Software products		
	1	*2*	*3*
x1	7	9	9
x2	8	7	8
x3	7	8	8

4 Conclusions

Calculations of the efficiency of the systems under consideration, carried out according to the formulas (3) and (4), gave the following values: system 1, $y = 0.68$; system 2, $y = 0.82$; system 3, $y = 0.87$. Following the results of the obtained estimates, we can conclude that due to a combination of functional properties, "PMA-WKF" package is more efficient than the computer-aided systems based on algorithmic sapproach, by 14%.

Therefore the development and improvement of CAD by development and introduction of programming and methodical complex, which center is the ontological model of knowledge, is a valuable for science and practice.
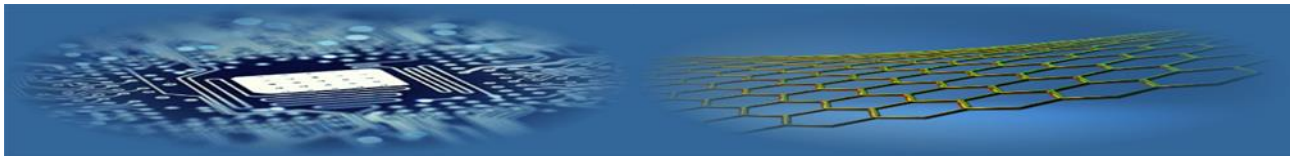
References

[1] Diligensky N V 2004 Matematicheskoe modelirovanie i oboschennoe otsenivanie proizvodstvenno-ekonomicheskih system [Mathematical Modeling and Generalized Estimation of Production Economic Systems Efficiency] *Proceedings of the 6th International Conference "Control and Modeling Problems in Package Systems."* 96-106 Samara

[2] Kochetkova O V, Kaznacheeva A A 2012 *Razrabotka metoda i sredstv predstavleniya modeli znaniy spetsialista v uchebno-issledovatel'skih SAPR [Development of a Method and Means of the Representation of the Specialist's Knowledge Model in Research and Training CAD]* Volgograd: Volgograd State Agricultural University

[3] Kochetkova O V 2012 Razrabotka modeli znaniy i eyo ontologicheskoy predstavlenie v algodritmah avtomatizirovannogo proektirovaniya osnovovyazannogo trikotazha [Development of Knowledge Model and its Ontological Representation in CAD Algorithms for warp-knitted Fabrics] *Contemporary Problems of Science and Education* **6** http://www.science-education.ru/106-7535

[4] Saati T 1993 *Decision-Making. Analytic Hierarchy Process* Moscow: Radio and Communication

AUTHORS

Olga Kochetkova, 29.06.1955, Volgograd, Russia

Current position grades: Vice-Rector for Informatization, Head of Department of Information Systems and Technologies, Volgograd State Agrarian University, doctor of technical sciences, professor
University studies: Volgograd State Technical University
Scientific interest: ontological engineering, conceptual design, computer-aided design
Publications: more than 250, six monographs
Experience: 25 years

Anastasia Kaznacheeva, 30.10.1973, Karaganda, Kazakhstan

Current position grades: Ph.D., associate professor, National Institute of Financial Markets and Management, Moscow
University studies: Karaganda State Technical University
Scientific interest: ontological engineering, conceptual design, computer-aided design
Publications: more than 35, two monographs
Experience: 16 years

Alexey Kochetkov, 29.09.1980, Volgograd, Russia

Current position grades: Ph.D., associate professor, Volgograd State Agrarian University
University studies: Volgograd State Pedagogical University, Volgograd State Agrarian University
Scientific interest: modeling, analysis and business process reengineering, information technology in education
Publications: 32, one monograph
Experience: 10 years

Effect of texture on mechanical and magnetic properties of steel from the petroleum distillation column

E Dragomeretskaya*

South Ukrainian National Pedagogical University named after K.D. Ushinsky, 26 Staroportofrankovskaya Street, Odessa 65020, Ukraine

*Corresponding author: drag_8181@mail.ru

Abstract

Texture, mechanical properties and coercive force of steel 09G2S from the column fragment of petroleum distillation after prolonged use studied. Anisotropy of mechanical properties and coercive force take place. Significant pair wise linear correlations and appropriate regression equations with coefficients reliability of approximation not less than 0.90 were found between magnitudes of the coercive force, tensile strength, yield strength, elongation and texture characteristics. Found correlations may be used for nondestructive mechanical properties control of investigated steel by means of monitoring of coercive force.

1 Introduction

Low alloy steels of type A515 and A516 are widely used in equipment of refinery complex, in particular for the production of distillation petroleum columns [1]. During the exploitation of the above equipment arise problems of mechanical properties of steel control, as well as the further safe operation estimation. Uniaxial tensile tests, fatigue, experiments on the long-term strength, etc. are carried out to study the mechanical properties [2, 3]. Cutting of samples from appropriate plots of material is necessary for such research. This requires stopping of the equipment operation. Therefore the development of non-destructive monitoring methods of the structural state and properties of the steel is important. The method of coercive force measuring is one of perspective non-destructive monitoring methods of structural condition of steels. Crystallographic texture as well as shape and size of grains, and elastic stresses have a main influence on the coercive force and her anisotropy [4]. Possibility of the structural state evaluation, of accumulated fatigue damage level, value of internal stress by measurement of coercive force was demonstrated in number of studies (e.g., [5-8]). In [6] was found a linear correlation of coercive force with the pole density on inverse pole figures (IPF) as well as with broadening of appropriate X-ray diffraction lines with increasing of the hydraulic pressure in the steel pipeline at testing. However relationship of coercive force (H_c) anisotropy with mechanical and structural characteristics of ferromagnetic construction steels is studied deficiently.

This work aimed to ascertainment of reasons anisotropy coercive force measured by non-destructive method, as well as relationship of coercive force with texture and mechanical characteristics of low-alloy steel of petroleum distillation column after long-term use.

2 Experimental material and methods

Low alloy steel of type 09G2S thickness of 20 mm from the column fragment of petroleum distillation after long-term use was by material for the study. The studied steel has the following chemical composition: 0.11 wt% C; 1.47 Mn; 0.70 Si; 0.13 Cr; 0.05 Ni; 0.06 V; 0.02 A1; 0.02 P; 0.009 S; 0.05 Cu; 0.04 Nb; 0.03 wt% Mo; Fe balance.

The coercive force H_c was measured non-destructively using a magnetic analyzer (coercimeter) KRM-Ts-MA by overlay of pole tips of the portable measuring device on surface of the test product. The area of the test products between the pole tips of the magnetic converter is periodically magnetized to saturation by current pulses with amplitude of at least 2 A. Automatic compensation of residual magnetization field is then carried out. Value of coercive force is automatically calculated by the current magnitude of magnetic field compensation. Readings of device are dependent only from the metal properties but independent of confounding factors such as the protective coating (paint, film, etc.) to 6 mm on controlled metal or equivalent to this gap the corrosion metal, roughness, curvature etc. The maximum error does not exceed 2%. [13]. Coercive force was measured through every 15° from longitudinal direction (LD) up to the transverse direction (TD) orienting the measuring probe without damaging the product.

Samples for mechanical testing by uniaxial tension (Figure 1) with the diameter of working part of 3 mm were cut from the column fragment through every 15° from longitudinal direction (LD) up to the transverse direction (TD).

FIGURE 1 Sample after the test

The arithmetic average of test results of at least three specimens in every of above directions has been taken as the

value of the corresponding mechanical characteristics. Mechanical testing was performed on a setup 1246-R. Velocity of the active grip was 2 mm / min. Mechanical properties were determined according to standard procedures [10].

The X-ray method was used for the study of texture [11]. Scanning θ-2θ of the sample without texture (which was manufactured from sawdust of investigated steel after recrystallization), as well as of specimens cut out in the ND, DD, and in TD was performed by means X-ray diffractometer DRON-3M by Bragg-Brentano geometry in the radiation of Kα - Mo. Texture was investigated in the ND near the outer convex surface of the column, in the middle of fragment thickness, and near of her inner concave surface. Appropriate surfaces were chemically polished up

to 0.1 mm before recording for removing of layer distorted by machining. On obtained data were constructed IPF for respective directions described above. The three-dimensional distribution function of the crystals orientation in space of ideal orientations were calculated by us from the IPF LD and the IPF TD according to the method described in earlier our work [12].

Metallographic structure of end surfaces of samples orthogonal to the RD and TD was examined by the microscope Axioplan 2 of firm KARL ZEISS.

3 Results and Discussions

Results of mechanical tests and measurement of the coercive force H_c are shown in Table 1.

TABLE 1 Mechanical properties and coercive force of steel samples, cut out in different directions from the fragment of distillation petroleum column

Angle with the LD, º	Tensile strength σ_m, MPa	Conditional yield strength $\sigma_{0.2}$, MPa	Relative elongation, $\varepsilon = \Delta l\,/\,l$, %	Coercive force, H_c , A/cm
0	400±2.0	255±1.4	31.0±0.4	5.9±0.12
15	405±2.2	258±1.8	30.2±0.4	6.1±0.12
30	416±2.3	265±2.1	28.8±0.4	6.3±0.12
45	425±2.2	272±2.3	28.0±0.4	6.5±0.12
60	421±2.0	268±2.0	28.4±0.4	6.5±0.12
75	417±2.0	266±1.5	29.4±0.4	6.4±0.12
90	415±1.8	260±2.5	30.0±0.4	6.2±0.12

Anisotropy of mechanical characteristics and coercive force take place. The minimal values of the strength properties of σ_m, $\sigma_{0.2}$, and the coercive force H_c are observed in the LD. Their maximal values occur in the LD+45°, and in the TD they take an intermediate value. Elongation ε shows the opposite behavior.

Anisotropy coefficient η was calculated by the formula

$$\eta = \left(F_{max} - F_{min}\,/\,F_{min} \right) \cdot 100\% \,,\qquad (1)$$

here F_{max} and F_{min} are maximal and minimal values of the corresponding property.

Anisotropy coefficients of σ_m, $\sigma_{0.2}$, H_C and ε amounted respectively 6.25%, 6.27%, 10.71% and 10.17%.

Strong linear correlations of the H_c value with values of mechanical characteristics σ_m, $\sigma_{0.2}$ and ε take place. Corresponding regression equations with high reliability approximation coefficients R^2 have the form

$$\sigma_m = 38.2H_c + 174.8\,;\ R^2 = 0.92,\qquad (2)$$

$$\sigma_{0.2} = 26.1H_c + 99.6\,;\ R^2 = 0.93,\qquad (3)$$

$$\varepsilon = -4.6H_c + 58.0\,;\ R^2 = 0.89.\qquad (4)$$

Experimental inverse pole figures obtained by us are presented in Figure 2.
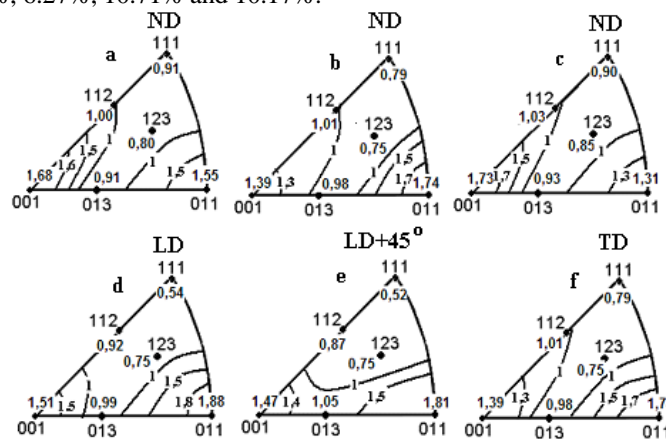
FIGURE 2 IPF's of steel column: a, c correspond to the convex and concave surface of the column respectively; b corresponds to the middle of the thickness of the metal; d-f correspond to the LD, LD+45º and TD

Texture of polycrystalline bodies presents a continuous distribution of crystals by orientations. At the same time there are certain preferable orientations of crystals, which are for clarity usually described using ideal orientations. Important components of the low carbon steel rolling

texture are arranged along three fibres orientations [11]:
1. α-fiber with the fiber axis <110> parallel to the rolling direction including the main components of {001} <110>, {112} <110> and {111} <110>.
2. γ-fiber with the fiber axis <111> parallel to the

COMPUTER MODELLING & NEW TECHNOLOGIES 2016 **20**(4) 48-51 **Dragomeretskaya E**

normal direction including the main components of {111} <110> and {111} <112>.

3. ε-fiber with the fiber axis <110> parallel to the transverse direction including the main components of {001} <110>, {111} <112>, {554} <225> and {011} <100>.

When referring to ideal orientations {hkl} <uvw> in the cylindrical sample we mean that planes of family {hkl} are located in a plane tangent to the cylindrical surface, and a set of crystallographic directions <uvw>, owned by {hkl}, are parallel to cylinder axis.

From Figure 2 it can be concluded that parallel to the side surface of the column metal are arranged families of crystallographic planes {001} and {110} since their pole density is greater than 1 that corresponds to the state without

texture. Crystallographic directions <110> and <100> of families mainly coincide with the LD, TD and LD + 45°. A three-dimensional ODF was calculated by us in the space of ideal orientations on the base of IPF LD (Figure 2(b)) and IPF RD (Figure 2(d)). Texture can be described as a combination of ideal orientations with the volume content, which are presented in the Table 2 as it was determined by the analysis of the ODF.

Effect of crystals orientation on the coercive force electrical steel previously is investigated in several studies [e.g. 14, 15]. Summarizing, can be concluded that the anisotropy of coercive force in the steel dependent not only from crystal orientation (i.e. from texture) but and from features of the magnetic domains formation.

TABLE 2 The composition and volume content of ideal orientations in the texture of steel of distillation oil column

Ideal orientation	{100} <010>	{100} <011>	{100} <013>	{110} <110>	{110} <111>	{110} <001>
Volume content	0.20	0.12	0.11	0.18	0.14	0.25

Crystallographic texture, shape and size of the grains, and the elastic stresses have a mainly influence on the coercive force and its anisotropy [4] as mentioned above. Metallographic analysis showed that the investigated steel has a typical ferrite – pearlite microstructure with average grain size of 22 μm (Figure 3). This microstructure can hardly be the main cause of the anisotropy of the coercive force.
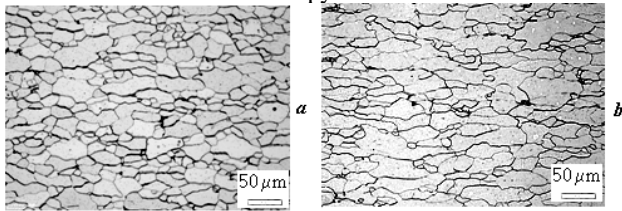

FIGURE 2 Ferrite – pearlite structure of the investigated steel: *a*, *b* have been photographed from the LD and TD direction

These features are caused by the magnitude of the external magnetizing field, if the steel does not magnetized to saturation. But when the coercive force is measured using the coercimeter, steel is magnetized to saturation, since the magnetizing field is sufficiently large (B = 1.5 T) [13]. Therefore, we can assume that the behaviors of domains in the magnetization and demagnetization play a secondary role in formation of the coercive force anisotropy, but the main role belongs to the energy of the magnetic crystallographic anisotropy in the investigated steel.

Let's estimate the energy of the magnetic crystallographic anisotropy in the investigated material. Suppose that the coercive force is associated only with the energy of the magnetic crystallographic anisotropy (external applied mechanical stresses are absent, structure of the investigated steel is homogeneous). Energy of the magnetic crystallographic anisotropy as a first approximation is expressed by the following equation [4] for the material with cubic lattice.

$$W_k \approx K_1 \left(\alpha_1^2 \alpha_2^2 + \alpha_2^2 \alpha_3^2 + \alpha_1^2 \alpha_3^2 \right),$$ (5)

here α_1, α_2 and α_3 are direction cosines of the magnetization with respect to the cube axes; K_1 is anisotropy constant.

Let's will call of function energy of magneto-crystalline anisotropy the expression

$$\psi = \left(\alpha_1^2 \alpha_2^2 + \alpha_2^2 \alpha_3^2 + \alpha_1^2 \alpha_3^2 \right).$$ (6)

The direction cosines of orientations indicated in Table 2 are presented in Table 3. Numerical values of the function Ψ of magnetic crystallographic anisotropy energy calculated from (3) for combinations of ideal orientations as well as corresponding volume content (Table 2) and considering direction cosines (Table 3) are shown in Table 4.

TABLE 3 Ideal orientations and functions of the magnetic crystallographic anisotropy energy

α_1	α_2	α_3
cosφ	sinφ·sin90º	sinφ·cos90°
cos(φ+45º)	sin(φ+45º)·sin 90°	sin(φ+45º)·cos90°
cos(φ+18.43º)	sin(φ+18.43º)·sin90º	sin(φ+18.43º)·cos90º
cos(φ+90º)	sin(φ+90º)·sin45º	sin(φ+90º)·cos45º
cos(φ+54.7º)	sin(φ+54.7º)·sin 45º	sin(φ+54.7º)·cos45º
cos φ	sinφ·sin 45º	sinφ·cos45º

TABLE 4 The calculated numerical values of function Ψ of the magnetic crystallographic anisotropy energy

Angle with LD,º	0	15	30	45	60	75	90
Ψ	0.09	0.16	0,21	0.24	0.23	0.19	0.15

Function Ψ takes the maximal value in the direction of LD + 45º. The minimal value of Ψ is observed in the LD. Function Ψ has an intermediate value in the TD. This is consistent with the character of coercive force anisotropy (Table 1). A strong linear correlation between the values of Ψ function and H takes place, as showed the correlative analysis conducted by us. The corresponding regression equation with a coefficient of reliability correlation $R^2 = 0.91$ has the form

$$\Psi = 0.23 H_c - 1.23 .$$ (6)

Thus, the character of the observable coercive force anisotropy in the studied steel of the oil distillation column can be explained, mainly by influence of the magnetic crystallographic anisotropy energy. Correlations (2) - (4) can be used to non destructive control the mechanical

Mathematical and Computer Modelling

characteristics of steel 09G2S by measure of the coercive force during operation of oil distillation column.

4 Conclusion

(1) Mechanical properties, the coercive force, and the texture in the fragment of steel petroleum distillation column after prolonged use studied.

(2) Anisotropy of mechanical properties and coercive force take place. Minimal values of strength properties σ_m and $\sigma_{0.2}$ coercive force H_c are observed in the longitudinal direction, their maximum values occur in a diagonal direction, and in the transverse direction

abovementioned properties takes the intermediate values. Elongation ε shows the opposite behavior.

(3) Strong linear correlations of the coercive force H_c with mechanical characteristics tensile strength σ_m, proof strength $\sigma_{0.2}$, and elongation ε are found. Reliability coefficients of linear approximations were no less than 0.89.

(4) Energy of the magnetic crystallographic anisotropy that is associated with orientation of crystals (i.e. with the texture), is main factor of coercive force anisotropy in the investigated steel. A strong linear correlation (with a correlation coefficient of at least 0.9) was found between calculated values function of magnetic crystallographic anisotropy energy and experimental values of coercive force.

References

[1] *Towers, Columns,* http://instruct.uwo.ca/engin-sc/cbe497/Doc/Icarus/ir08.pdf

[2] *Pressure Vessel Inspection Code: In-Service Inspection, Rating, Repair, and Alteration,* https://law.resource.org/pub/us/code/ibr/api.510.2006.pdf

[3] *Damage Mechanisms Affecting Fixed Equipment in the Refining Industry*, http://www.silcotek.com/hs-fs/hub/22765/file-815218612-pdf/docs/api_rp_571.pdf

[4] Terunobu Miyazaki, Hanmin Jin 2012 *The Physics of Ferromagnetism* Springer Berlin Heidelberg

[5] Zhang Yu, Wang Z, Wang Y, Zhang Z, Zhang Yi 2015 Astudy on the relationship between hardness and magnetic properties of ultra-high strength steel *Advanced Materials Research* **106** 78-81

[6] Solomakha R, Pittala R D, Bezlyudko G, Baskaran B V *Practical evaluation of fatigue and stress state, and residual life of metal by non-destructive method for measuring magnetic characteristic "The coercive force" – A case study"* http://www.ndt.net/article/apcndt2013/papers/243.pdf

[7] Altawalbeh N A M, Thuneibat S A Al, Olaimat M M 2012 ANew Electromagnetic Technique for Controlling Stress in Metals *Applied Physics Research* **4**(3) 48-52

[8] Gorkunov E S, Mitropolskaya S Yu, Zadvorkin S M, Shershneva L S, Vichuzhanin D I, Tuyeva, E A 2010 Relation of the magnetic properties of control-rolled pipe steel to its structural anisotropy, internal stresses and damage http://www.ndt.net/article/ecndt2010/reports/1_01_24.pdf

[9] Lobanov L M, Nehotyaschiy V A, Rabkina M D, Usov V V, Shkatulyak N M, Tkachuk E N 2010 Anisotropy of the coercive force and texture of deformed steel *Deformation and fracture of material* **10** 19–24 *(In Russian)*

[10] *Tensile Testing* 2004 Materials Park, Ohio

[11] Randle V, Engler O 2000 Introduction to Texture Analysis: Macrotexture, Microtexture and Orientation Mapping, CRC PRESS, Boca Raton, London, New York, Washington

[12] Usov V V, Tarlovsky V A 1991 The calculation method of the three-dimensional orientation distribution function and integral texture characteristics of cubic polycrystals from inverse pole figures *Zavodskaya Laboratoriya* **7** 25-8 *(In Russian)*

[13] *Nomenclature / Instruments and equipment for non-destructive testing / magnetic analyzer KRM-Ts-MA* http://promsouz.com/pribori14.html *(In Russian)*

[14] Campos M F, De Campos M A, Landgraf F J G, Padovese L R 2011 Anisotropy study of grain oriented steels with Magnetic Barkhausen Noise *Journal of Physics: Conference Series* **303** *012020*

[15] Paltanea V, Paltanea G, Gavrila H 2012 Magnetic Anisotropy in Silicon Iron Alloys *Electrical and Electronic Engineering* **2**(6) 383-8

AUTHORS

Elena Dragomeretskaya, 1981, Ukraine

Current position grades: finished graduate school, Leading specialist of postgraduate and doctoral studies
University studies: South Ukrainian National Pedagogical University named after K.D. Ushinsky
Scientific interest: Influence of crystallographic texture on the anisotropy of physical and mechanical properties
Publications: 14
Experience: more than 10 years

AUTHORS' INDEX

Alfonta L	7
Bellucci S	7
Bostanbekov K A	37
Burlutskaya N	7
Chauhan D S	30
Chinibayev Y	18
Chouarfia A	23
Dragomeretskaya E	48
Fink D	7
Gopeyenko V	7
Jamalov J K	37
Kaznacheeva A	44
Khensous G	23
Kiv A	7
Kochetkov A	44
Kochetkova O	44
Lobanova-Shunina T	7
Maigret B	23
Mansharipova A	7
Messabih B	23
Muhamediyev R	7
Nurseitov D B	37
Saini J P	30
Shunin Yu	7
Singh D	30
Temirbolatova T	18
Zhukovskii Yu	7

NANOSCIENCE AND NANOTECHNOLOGY

Theory and modelling of real-time physical and bio- nanosensor systems

Yu Shunin, D Fink, A Kiv, L Alfonta, A Mansharipova, R Muhamediyev, Yu Zhukovskii, T Lobanova-Shunina, N Burlutskaya, V Gopeyenko, S Bellucci

Our research pursues two important directions of real-time control nanosystems addressed to ecological monitoring and medical applications. We develop physical nanosensors (pressure and temperature) based on functionalized CNTs and GNRs nanostructures. The model of nanocomposite materials based on carbon nanocluster suspension in dielectric polymer environments (epoxy resins) is regarded as a disordered system of fragments of nanocarbon inclusions with different morphologies. Using the effective media cluster approach, disordered systems theory and conductivity mechanisms analysis we have formulated the approach of conductivity calculations for carbon-based polymer nanocomposites and obtained the calibration dependences. We also develop bio-nanosensors based on polymer nanotracks with various enzymes, which provide the corresponding biocatalytic reactions and give reliably controlled ion currents. Particularly, we describe a glucose biosensor based on the enzyme glucose oxidase (GOx) covalently linked to nanopores of etched nuclear track membranes. Using simulation of chemical kinetics glucose oxidation with GOx, we have obtained theoretical calibration dependences. Our objective is to demonstrate the implementation of advanced simulation models providing a proper description of electric responses in nanosensoring systems suitable for real time control nanosystems. Comparisons with experimental calibration dependences are discussed. Prospective ways of developing the proposed physical and bio- nanosensor models and prototypes are considered.

Keywords: real-time nanosensors, functionalized nanocomposites, physical nanosensors bionanosensors

INFORMATION AND COMPUTER TECHNOLOGIES

Development of the augmented reality applications based on ontologies

Yersain Chinibayev, Tolganay Temirbolatova

This article presents an analysis of the existing popular libraries for the development of augmented reality applications. Based on the analysis we propose a universal technology of construction of augmented reality applications using ontology. The technology is based on the geolocation using GPS and communicates with the resource through Linked Open Data.

Keywords: Augmented reality, ontological modelling, ontological engineering, Linked Open Data

Comparison of Cuckoo Search, Tabu Search and TS-Simplex algorithms for unconstrained global optimization

Ghania Khensous, Belhadri Messabih, Abdellah Chouarfia, Bernard Maigret

Metaheuristics Algorithms are widely recognized as one of the most practical approaches for Global Optimization Problems. This paper presents a comparison between two metaheuristics to optimize a set of eight standard benchmark functions. Among the most representative single solution metaheuristics, we selected Tabu Search Algorithm (TSA), to compare with a novel population-based metaheuristic: Cuckoo Search Algorithm (CSA). Empirical results reveal that the problem solving success of the TSA was better than the CSA. However, the run-time complexity for acquiring global minimizer by the Cuckoo Search was generally smaller than the Tabu Search. Besides, the hybrid TSA-Simplex Algorithm gave superior results in term of efficiency and run-time complexity compared to CSA or TSA tested alone.

Keywords: Metaheuristic Algorithms, CSA, TSA, Global Optimization, Nature Inspired Algorithms

Handwritten offline Hindi character recognition using advanced feature extraction techniques

Dayashankar Singh, J P Saini, D S Chauhan

Feature extraction technique plays an important role in character recognition since last so many years. In this paper, two advanced feature extraction techniques namely 16-Directional Gradient Feature Extraction Technique (16-DGFET) and 24-Directional Gradient Feature Extraction Technique (24- DGFET) have been proposed and implemented. This paper demonstrates the concept of Handwritten Hindi Character Recognition (HCR), feature extraction mechanisms adopted for character recognition starting from Conventional Feature Extraction Technique (CFET), Gradient Feature Extraction Technique (GFET), and Directional Gradient Feature Extraction Technique (DGFET). In DGFET, few techniques have been initiated which involve dividing the gradient values to 8/16 directional values, these techniques attained recognition accuracy of around 94%. We have aimed at further splitting of the gradient values in 24 parts in order to find if it achieves the objective of increasing the performance of character recognition with more accurate analysis and acceptable training time. An experimental evaluation and comparative analysis have been made at the end of the paper to prove the result whether further splitting is providing a better result in comparison to 8 or 16 parts division taking in account the training time, the accuracy of recognition and performance appraisal. The network used here is Multilayer Perceptron (MLP) with Error Back Propagation (EBP) algorithm to train the network.

A sample of count 1000 has been taken for experimentation including the personnel of different age groups involving both male and female handwriting. A comparative synthesis is made for 8/16-Directional and 24-Directional input values comparing the recognition

performance and training time.

Keywords: Pattern Recognition, Hindi Character Recognition, Gradient Feature Extraction Technique (GFET), Directional Gradient Feature Extraction (DGFET), Multilayer Perceptron (MLP), Error Back Propagation (EBP)

MATHEMATICAL AND COMPUTER MODELLING

Modelling of non-point source pollution transport for the Charyn River Basin

Jalal K Jamalov, Daniyar B Nurseitov, Kairat A Bostanbekov

The results of pollution transport simulation for the Charyn river (the Republic of Kazakhstan, Central Asia) obtained using software package BASINS 4.1 are shown in this article [1]. Modules created in the process of the study as well as the method of adaptation of the model of pollution transport are described. The calculations include the modeling of the hydrology of the river basin and the calculation of the concentration of non-point sources of pollution. The comparison with the data of natural hydrological observation post.

Keywords: Simulation, BASINS, Watershed Delineation, HSPF, pollution transport in water, BOD, nitrate, dissolved oxygen

Performance evaluation of computer-aided knit design using software package based on ontological knowledge model

O Kochetkova, A Kaznacheeva, A Kochetkov

The article represents the original approach to computer-aided warp knit fabrics on the base of universal algorithms and modern methodology which allows to apply the methods of projecting with the given technologies. The ontological approach is represented for development and improvement of knowledge model which provides the description of object domain of computer-aided warp knit fabrics and its formalized presentation. The elaborated software allows to perform fully the proceedings of art and technological and parametric projecting of warp knit fabrics. The performance evaluation of computer-aided warp knit fabrics on the basis of algorithmical and ontological approach is elaborated. To solve this problem we used the method of hierarchy analysis of Thomas Saati. The results of the evaluation represent that software grounded on ontological approach in totality of functional means is more effective than CAD on the base of algorithmical approach.

Keywords: warp knit fabrics, ontological approach, knowledge model, program-methodical package

Effect of texture on mechanical and magnetic properties of steel from the petroleum distillation column

E Dragomeretskaya

Texture, mechanical properties and coercive force of steel 09G2S from the column fragment of petroleum distillation after prolonged use studied. Anisotropy of mechanical properties and coercive force take place. Significant pair wise linear correlations and appropriate regression equations with coefficients reliability of approximation not less than 0.90 were found between magnitudes of the coercive force, tensile strength, yield strength, elongation and texture characteristics. Found correlations may be used for non-destructive mechanical properties control of investigated steel by means of monitoring of coercive force.

Keywords: Texture, anisotropy, mechanical properties, coercive force, correlation